

Studies by the U.S. Geological Survey in Alaska, 2007

Detrital Zircon Geochronology of Cretaceous and Paleogene Strata Across the South-Central Alaskan Convergent Margin

Professional Paper 1760–F



This page intentionally left blank

Studies by the U.S. Geological Survey in Alaska, 2007

Detrital Zircon Geochronology of Cretaceous and Paleogene Strata Across the South-Central Alaskan Convergent Margin

By Dwight Bradley, Peter Haeussler, Paul O'Sullivan, Rich Friedman, Alison Till, Dan Bradley,
and Jeff Trop

Professional Paper 1760–F

**U.S. Department of the Interior
U.S. Geological Survey**

U.S. Department of the Interior
KEN SALAZAR, Secretary

U.S. Geological Survey
Suzette M. Kimball, Acting Director

U.S. Geological Survey, Reston, Virginia: 2009

This report and any updates to it are available online at:
<http://pubs.usgs.gov/pp/1760/f/>

For additional information write to:
U.S. Geological Survey
Box 25046, Mail Stop 421, Denver Federal Center
Denver, CO 80225-0046

Additional USGS publications can be found at:
<http://geology.usgs.gov/index.htm>

For more information about the USGS and its products:
Telephone: 1-888-ASK-USGS (1-888-275-8747)
World Wide Web: <http://www.usgs.gov/>

Any use of trade, product, or firm names in this publication is for descriptive purposes only and does not imply endorsement by the U.S. Government.

Although this report is in the public domain, it may contain copyrighted materials that are noted in the text. Permission to reproduce those items must be secured from the individual copyright owners.

Cataloging-in-Publication data are on file with the Library of Congress

Produced in the Western Region, Menlo Park, California
Manuscript approved for publication, August 20, 2009
Text edited by Peter H. Stauffer
Layout and design by Stephen L. Scott

Suggested citation:

Bradley, D., Haeussler, P., O'Sullivan, P., Friedman, R., Till, A., Bradley, D., and Trop, J., 2009, Detrital zircon geochronology of Cretaceous and Paleogene strata across the south-central Alaskan convergent margin, in Haeussler, P.J., and Galloway, J.P., Studies by the U.S. Geological Survey in Alaska, 2007: U.S. Geological Survey Professional Paper 1760-F, 36 p.

FRONT COVER

Exposure of Upper Cretaceous sandstone of the Valdez Group on the southern Kenai Peninsula, Alaska, that was sampled for zircon geochronology studies.

Contents

Abstract	1
Introduction	2
Chugach Mountains	4
McHugh Complex	4
Geochronology of Igneous Clasts	8
Detrital Zircons	8
Valdez Group	10
Geochronology of Igneous Clasts	10
Detrital Zircons	11
Southern Talkeetna Mountains	12
Schist of Hatcher Pass	12
Arkose Ridge Formation	13
Western Alaska Range	13
Sandstone of the Canyon Creek Area—Valanginian to Hauterivian	14
Hornfels Metasandstone of the Chilligan River Headwaters—Aptian	14
Hornfels Metasandstone of the Max Lake Area—Hauterivian	15
Hornfels Metasandstone of the Crystal Creek Area—Aptian	15
Hornfels Metasandstone of the Emerald Creek Area—Copniacian	16
Hornfels Metasandstone of the Peak 6105 Area—Paleogene	16
Tectonic Implications	16
Chugach terrane	16
Talkeetna Mountains	16
Western Alaska Range	17
Implications for ca. 90-Ma Metallogeny	17
Acknowledgments	18
References Cited	18
Appendix: Analytical Methods	43
U-Pb Zircon LA-ICP-MS Techniques (University of British Columbia)	43
U-Pb Zircon SHRIMP-RG Techniques (U.S. Geological Survey-Stanford University)	43
U-Pb Zircon LA-ICP-MS Techniques (Apatite to Zircon, Inc.)	43

Figures

1. Map of Alaska showing key physiographic features	3
2. Simplified geologic map of parts of the Tyonek, Anchorage, Seward, and Kenai quadrangles	4
3. Histograms (blue boxes) and probability plots (red lines) of detrital zircon ages	6
4. Outcrop photographs of rock units sampled for geochronology	9
5. Individual $^{206}\text{Pb}/^{238}\text{U}$ ages of zircon grains from igneous clasts	10
6. Geologic map of the Nuka Bay area, Seldovia quadrangle	11

Tables

1. Analytical data and estimated resources for Cutaway Basin barite deposits	5
2. Rock density measurements from the Lakeview and Longview deposits	21

This page intentionally left blank

Detrital Zircon Geochronology of Cretaceous and Paleogene Strata Across the South-Central Alaskan Convergent Margin

By Dwight Bradley¹, Peter Haeussler¹, Paul O'Sullivan², Rich Friedman³, Alison Till¹, Dan Bradley⁴, and Jeff Trop⁵

Abstract

Ages of detrital zircons are reported from ten samples of Lower Cretaceous to Paleogene metasandstones and sandstones from the Chugach Mountains, Talkeetna Mountains, and western Alaska Range of south-central Alaska. Zircon ages are also reported from three igneous clasts from two conglomerates. The results bear on the regional geology, stratigraphy, tectonics, and mineral resource potential of the southern Alaska convergent margin.

Chugach Mountains—The first detrital zircon data are reported here from the two main components of the Chugach accretionary complex—the inboard McHugh Complex and the outboard Valdez Group. Detrital zircons from sandstone and two conglomerate clasts of diorite were dated from the McHugh Complex near Anchorage. This now stands as the youngest known part of the McHugh Complex, with an inferred Turonian (Late Cretaceous) depositional age no older than 91–93 Ma. The zircon population has probability density peaks at 93 and 104 Ma and a smattering of Early Cretaceous and Jurassic grains, with nothing older than 191 Ma. The two diorite clasts yielded Jurassic U–Pb zircon ages of 179 and 181 Ma. Together, these findings suggest a Mesozoic arc as primary zircon source, the closest and most likely candidate being the Wrangellia composite terrane. The detrital zircon sample from the Valdez Group contains zircons as young as 69 and 77 Ma, consistent with the previously assigned Maastrichtian to Campanian (Late Cretaceous) depositional age. The zircon population has peaks at 78, 91, 148, and 163 Ma, minor peaks at 129, 177, 330, and 352 Ma, and no concordant zircons older than Devonian. A granite clast from a Valdez Group conglomerate yielded a Triassic U–Pb zircon age of 221 Ma. Like the McHugh Complex, the

Valdez Group appears to have been derived almost entirely from Mesozoic arc sources, but a few Precambrian zircons are also present.

Talkeetna Mountains—Detrital zircons ages were obtained from southernmost metasedimentary rocks of the Talkeetna Mountains (schist of Hatcher Pass) and, immediately to the south, the northernmost sedimentary sequence of the Matanuska forearc basin (Arkose Ridge Formation). Detrital zircons from the Paleogene Arkose Ridge Formation are as young as 61 and 70 Ma; the population is dominated by a single Late Cretaceous peak at 76 Ma; the oldest zircon is 181 Ma. Sedimentological evidence clearly shows that the conglomeratic Arkose Ridge Formation was derived from the Talkeetna Mountains; our detrital zircon data support this inference. Zircons dated at ca. 90 Ma in the Arkose Ridge sample suggest that buried or unmapped plutons of this age may exist in the Talkeetnas. This is a particularly interesting age as it corresponds to the age of the supergiant Pebble gold-molybdenum-copper porphyry prospect near Iliamna and suggests a new area of prospectivity for Pebble-type deposits. The schist of Hatcher Pass, which was previously assigned a Jurassic depositional age, yielded surprisingly young Late Cretaceous detrital zircons, the youngest at 75 Ma. The probability density curve has four Cretaceous peaks from 76 to 102 Ma, a pair of Late Jurassic peaks at 155 and 166 Ma, three Early Jurassic to Late Triassic peaks at 186, 197, and 213 Ma, minor Carboniferous peaks at 303 and 346 Ma, and a minor Paleoproterozoic peak at 1828 Ma. The schist of Hatcher Pass was largely derived from Mesozoic arc sources, most likely the Wrangellia composite terrane, with some contribution from one or more older, inboard sources, probably including the Yukon-Tanana terrane. We postulate that the schist of Hatcher Pass represents metamorphosed rocks of the Valdez Group that were subducted and then exhumed along the Chugach terrane's "backstop" during Paleogene transtension.

Western Alaska Range—Six detrital zircon samples were collected from a little studied belt of turbidites in Tyonek quadrangle on strike with the Kahiltina assemblage of the central Alaska Range. Many of the sandstones are contact metamorphosed. On the basis of their youngest zircons, two similar samples are here assigned Early Cretaceous (Valanginian to Hauterivian and Aptian) depositional ages. Their detrital populations consist entirely of Jurassic and Early Cretaceous grains,

¹U.S. Geological Survey, 4210 University Drive, Anchorage, AK 99508 USA.

²Apatite to Zircon, Inc., 1075 Matson Rd., Viola, ID 83872 USA.

³Dept. of Earth and Ocean Sciences, University of British Columbia, Vancouver, BC V6T1Z4, Canada.

⁴Alaska Pacific University, Anchorage, AK 99508.

⁵Dept. of Geology, Bucknell University, Moore Avenue, Lewisburg, PA 17837, USA.

having peaks at 153 and 152 Ma, respectively. Two other similar samples are also assigned Early Cretaceous (Hauterivian and Aptian) depositional ages, but they differ from the first two by also containing Precambrian grains. One of these samples has probability density peaks at 149 and 181 Ma, and the other has peaks at 141, 168, and 944 Ma. The four Early Cretaceous samples appear to have been mainly derived from Jurassic to Early Cretaceous arc sources of the Wrangellia composite terrane, with minor input from older, inboard sources such as the Yukon-Tanana and Farewell terranes. These four samples can be reasonably assigned to the Kahiltna assemblage. One western Alaska Range sample is assigned a Late Cretaceous depositional age of ca. 86 Ma; it has probability density peaks at 100 and 153 Ma and contains a substantial proportion of Precambrian grains. Its zircon population appears to have been derived from Jurassic and Cretaceous arc sources as well as from older inboard rocks, such as the Yukon-Tanana terrane. The zircon age distribution is reminiscent of that of the Upper Cretaceous Kuskokwim Basin of southwest Alaska. Finally, one Alaska Range sample, for which an Early Cretaceous age was expected, instead yielded abundant Paleogene zircons, the youngest at 55 Ma. This sample has a single probability density peak at 65 Ma, reflecting derivation from an Alaska Range arc that was active during latest Cretaceous and Paleogene times. The older Alaska Range samples are believed to record deposition in an Early Cretaceous syncollisional suture, and the younger samples are interpreted to be deposits of a Late Cretaceous to Paleogene retroarc basin.

Introduction

In the rapidly advancing field of detrital zircon geochronology, a broad goal among Alaskan researchers is to obtain baseline data for each of the major bedrock units that contain sandstone or metasandstone. Such data can yield several types of information that bear on problems of regional geology and tectonic evolution. In active tectonics settings, detrital zircons commonly provide new age constraints on the depositional age of the host sandstone or metasandstone, which can be no older than the youngest concordant zircons. This is especially important in strata that are devoid of fossils, a condition linked to the age of the strata, the depositional environment, the state of deformation, the state of metamorphism, a lack of mapping, or some combination of these factors. Detrital zircon age distributions (illustrated using probability density plots, or “bar-codes”) can be used to evaluate possible connections between sandstone-bearing stratigraphic units. This information has applications in geologic mapping at the quadrangle scale, for example in assigning problematic rocks to one or another map unit, and on a regional scale in matching displaced parts of an originally continuous sedimentary or metasedimentary succession. Finally—and this is the goal that led to the worldwide explosion of detrital zircon research in the first place—detrital zircons can be linked to possible bedrock source regions by

their ages. Information of the latter type, in turn, can bear on the timing of juxtaposition of terranes and on basin evolution at an otherwise unattainable level of detail.

In this paper, we present new U-Pb detrital zircon data from a transect across the convergent margin of south-central Alaska (figs. 1 and 2; table 1). Two detrital zircon samples were collected to help constrain the depositional ages and provenance of the two main map units of the Chugach terrane (fig. 1B): the Valdez Group and McHugh Complex (Plafker and others, 1994). We also report U-Pb ages of plutonic clasts in the Valdez Group and McHugh Complex. Two other samples, from the southern Talkeetna Mountains, were collected to shed light on Paleocene evolution of the forearc basin during the time of ridge subduction (Bradley and others, 2003). Six samples are from the western Alaska Range, which during the Early Cretaceous was the site of a thickly sedimented collisional suture (Kalbas and others, 2007) and since then has been near the axis of a magmatic arc. The Alaska Range samples were collected as an aid to reconnaissance-scale geologic mapping in a seemingly monotonous expanse of deformed, fossil-poor, hornfels turbidites in the Tyonek quadrangle.

The data reported here were obtained using two techniques (LA-ICP-MS⁸ and SIMS⁹) and three different labs. Analytical methods are detailed in the appendix. For the “best age” in table 2, we have quoted the ²⁰⁶Pb/²³⁸U age for zircons younger than 1000 Ma and the ²⁰⁷Pb/²⁰⁶Pb age for older zircons; if one age is below the cutoff and the other is above, we have quoted the ²⁰⁷Pb/²⁰⁶Pb age. Except as noted, in constructing the plots in Figure 3, filters were applied to screen out results with unacceptably large analytical errors and unacceptable discordance. For all of the histograms and probability plots (fig. 3), we discounted any ages that have large errors, that is, analyses for which the 2-sigma error is >5 percent of the age. For these types of plots, most detrital zircon geochronologists also discount ages having high discordance. However, neither the way discordance is calculated nor the threshold for rejection are uniformly applied. In the data reported by University of British Columbia and Apatite to Zircon, Inc., discordance is calculated as:

$$(((^{207}\text{Pb}/^{206}\text{Pb} \text{ age}) - (^{206}\text{Pb}/^{238}\text{U} \text{ age})) / (^{207}\text{Pb}/^{206}\text{Pb} \text{ age})) * 100$$

In the data obtained on the SHRIMP-RG, discordance is calculated as:

$$(((^{207}\text{Pb}/^{206}\text{Pb} \text{ age}) - (^{206}\text{Pb}/^{238}\text{U} \text{ age})) * 100) - 100.$$

Whichever way it is calculated, discordance is expressed as a percentage. For most samples, we have rejected ages that are >10 percent normally (+) or reversely (−) discordant, a threshold

⁸Laser-ablation inductively coupled plasma mass-spectrometry.

⁹Secondary ion mass spectrometry, in this study using a SHRIMP-RG, or sensitive high resolution ion microprobe-reverse geometry.

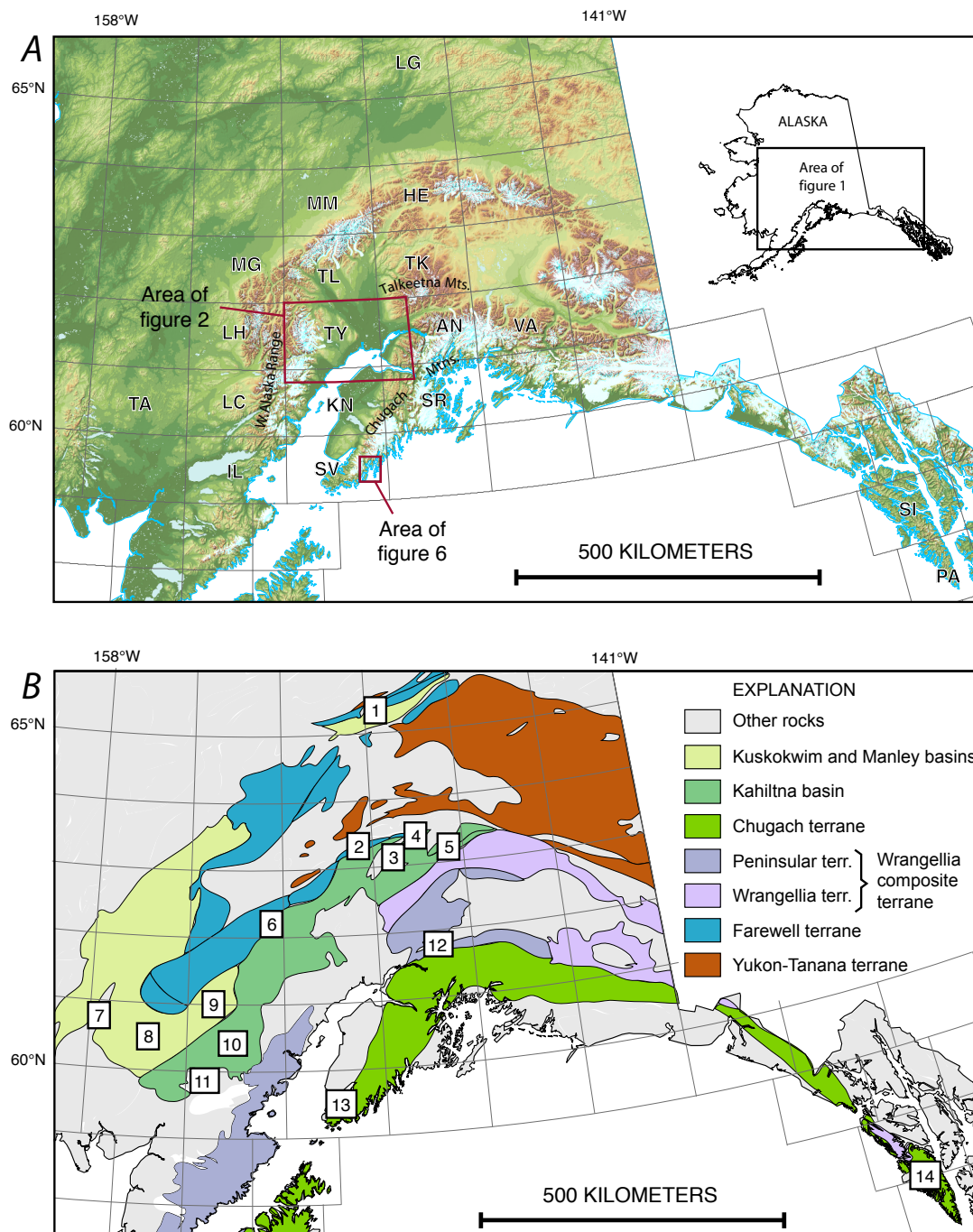


Figure 1. (A) Map of Alaska showing key physiographic features and the areas of figures 2 and 6 outlined in red. The black grid shows the outlines of 1:250,000-scale quadrangles, which are identified by the following abbreviations: AN, Anchorage; HE, Healy; IL, Iliamna; KN, Kenai; LC, Lake Clark; LG, Livengood; LH, Lime Hills; MG, McGrath; MM, Mount McKinley; PA, Port Alexander; SI, Sitka; SM, Sleetmute; SR, Seward; SV, Seldovia; TA, Taylor Mountains; TK, Talkeetna Mountains, TL, Talkeetna; VA, Valdez. (B) Generalized terrane map of the same region. Numbers in white boxes refer to localities mentioned in text, as follows: 1, Minto Unit, Livengood quadrangle; 2, Cantwell Formation, Denali area; 3, Kahiltna assemblage, Broad Pass area; 4, Caribou Pass Formation; 5, Kahiltna assemblage, Clearwater Mountains; 6, Kahiltna assemblage, Terra Cotta Mountains; 7, Gemuk Group, Cinnabar Creek area; 8, Kuskokwim Basin, Taylor Mountains quadrangle; 9, Mulchatna subbasin of Kuskokwim Basin; 10, Southern Kahiltna terrane of Wallace and others, 1989; 11, Pebble Copper prospect; 12, Matanuska Formation; 13, Seldovia area; 14, Sitka area.

that is commonly but not universally used in the detrital zircon research community. For three samples (04ATi103, 04ATi109, and 05PH104b), we did not filter for discordance. These are young samples that expose a flaw of the 10 percent discordance filter, which in some populations wrongly discredits most zircons that are younger than about 200 Ma, even though they actually overlap concordia within error.

Chugach Mountains

The Chugach Mountains of south-central Alaska are largely underlain by a Mesozoic accretionary complex, the Chugach terrane (fig. 1B). This paper reports detrital zircon data from the two main components of the Chugach terrane: the McHugh Complex on the inboard side and the Valdez Group on the outboard side (fig. 2).

McHugh Complex

The McHugh Complex (Clark, 1973) is a structural assemblage, or *mélange*, of variably deformed and disrupted

mafic volcanic rocks, gabbro, chert, graywacke, rare limestone, and rare ultramafic rocks—all in a phacoidally cleaved matrix of argillite and tuff. The McHugh Complex is characterized by moderate to intense stratal disruption, which resulted in tectonic juxtaposition of varied rock types at scales ranging from centimeters to kilometers (Bradley and Kusky, 1992). Previous age constraints on McHugh protoliths have mainly been provided by fossils and by isotope geochronology; contact relations are also locally helpful but it should be stressed that most dated rocks in the McHugh lack stratigraphic context because they are bounded by faults or shear zones. Permian fossil ages have been reported from a number of limestone bodies (Stevens and others 1997; Bradley and others, 1999) that are thought to represent decapitated seamounts. One fault-bounded gabbro body, at Halibut Cove in Seldovia quadrangle, yielded a concordant U-Pb zircon age of 227 Ma (Norian, Late Triassic; Kusky and others, 2007). None of the many basalts are directly dated, but cherts that depositionally overlie basalts range from Ladinian in the Middle Triassic to Albian-Aptian in the mid-Cretaceous (Bradley and others, 1999). At one location in the Seldovia quadrangle (locality 13 in fig. 1B), graywacke conformably overlies ribbon chert that yielded Pliensbachian (Early Juras-

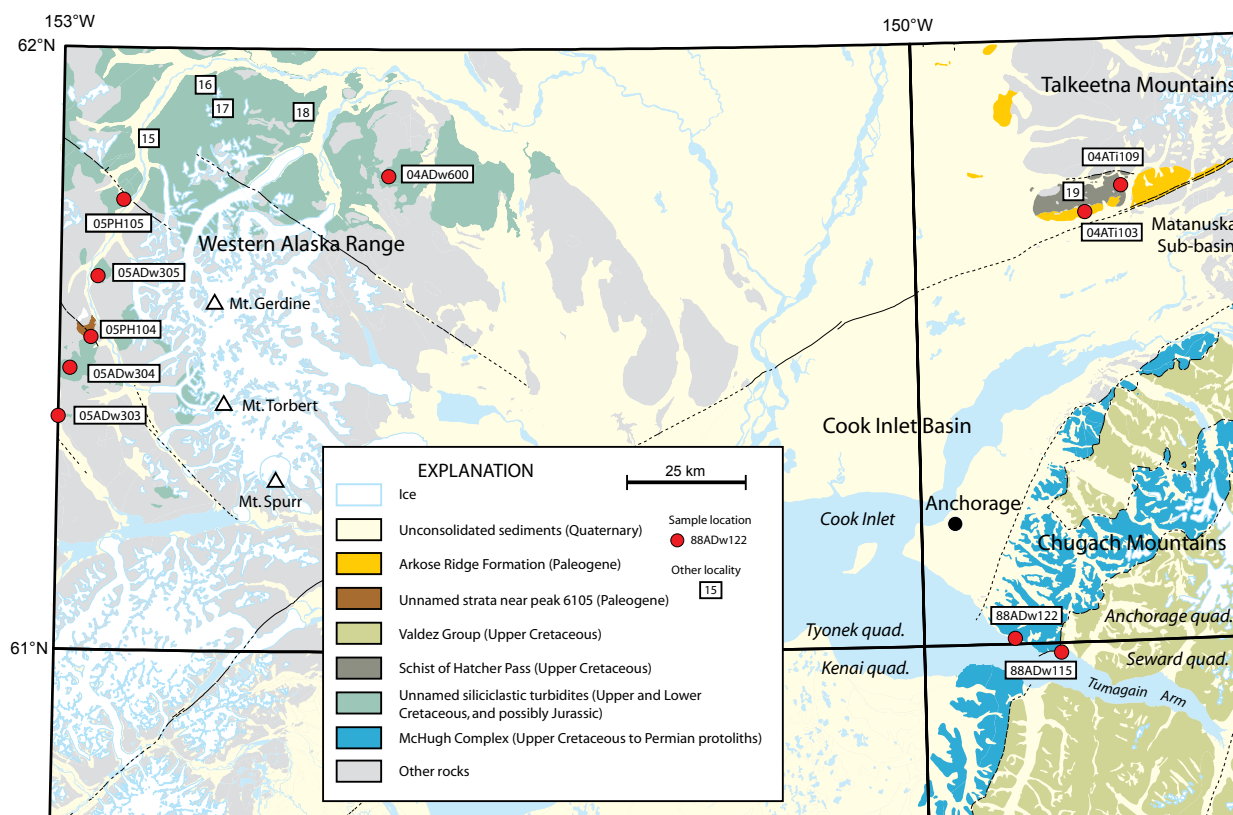


Figure 2. Simplified geologic map of parts of the Tyonek, Anchorage, Seward, and Kenai quadrangles, south-central Alaska, adapted from Wilson and others (2009). Locations of detrital zircon samples are shown by USGS sample number. Other localities mentioned in text are identified as follows: 15, Turonian bivalve occurrence; 16, Valanginian bivalve occurrence; 17, Early Jurassic to Early Cretaceous radiolarian occurrence; 18, igneous clasts dated 95-101 Ma; 19, Grubstake Gulch.

Table 1. Summary information for geochronology samples. Under Rock unit, map abbreviations correspond to those used by Wilson and others (2009).

Field number	Quadrangle	Location	Rock unit	Depositional age of DZ sample	Igneous age of clast	Latitude (decimal degrees)	Longitude (decimal degrees)
05PH104B	Tyonek C8	Near Peak 6105	Tves	Eocene	NA	61.520283	-152.896770
04ATi103	Anchorage C7	Arkose Ridge	Arkose Ridge Formation	Paleocene	NA	61.710233	-149.406416
05PH105A	Tyonek C8	Emerald Creek area	KJs	Coniacian	NA	61.746383	-152.803567
04ATi109	Anchorage D7	Hatcher Pass	Schist of Hatcher Pass	Campanian	NA	61.751316	-149.282250
88ADw122	Seward D7	Indian	Valdez Group	Campanian	NA	60.982729	-149.534971
92AKu18	Seldovia B2	McCarty Fiord	Valdez Group	NA	221±1 Ma	59.470277	-150.473611
88ADw115	Anchorage A8	Beluga Point	McHugh Complex	Turonian	179±3 & 182±2 Ma	61.006849	-149.692504
05ADW304A	Tyonek B8	N Fork Chilligan headwaters	Kes	Aptian	NA	61.461560	-152.972690
05ADw305A	Tyonek C8	Crystal Creek area	Kes	Aptian	NA	61.619910	-152.866580
05ADW303C	Tyonek B8	Near Peak 6140, Max Lake area	Kes	Hauterivian	NA	61.390360	-152.952710
04ADW600A	Tyonek D5	Canyon Creek area	Kes	Valanginian to Hauterivian	NA	61.796233	-151.833383

sic) radiolarians (Bradley and others, 1999). Regionally, graywacke has been considered to range in age from Pliensbachian through Early Cretaceous (Bradley and others, 1999; Winkler and others, 1981). Summarizing, various McHugh Complex protoliths have previously yielded reliable ages of Permian, Triassic, Jurassic, and Early Cretaceous; our results extend the age range to include the Late Cretaceous.

Along Turnagain Arm near Anchorage (fig. 2), the McHugh Complex consists of two informal subdivisions, an inboard and an outboard part. The inboard part is mainly *mélange* composed of fragments and disrupted beds of chert, mafic volcanic rocks, graywacke, and rare limestone and ultramafic rocks, set in a phacoidally cleaved matrix of argillite and tuff; this part of the McHugh Complex was not sampled for detrital zircons. The outboard part, which we sampled, is mostly siliciclastic rocks, including boulder and cobble conglomerate, graywacke, and argillite. Early in the course of regional mapping, Tysdal and Case (1977) considered the outboard part to be a separate unit from the McHugh Complex, but in a later reversal they included it as part of the McHugh Complex (Tysdal and Case, 1979).

Our samples of sandstone and igneous clasts are from a classic and much visited cliff exposure of the McHugh

Complex on the north side of the Seward Highway opposite the parking area at Beluga Point. This is Stop 3 of Bradley and Miller (2006). Most of the exposure is conglomerate (fig. 4A). Bedding is only locally observed and, even where visible, it generally cannot be traced far, because of disruption by faults and shear zones. The rocks have been metamorphosed to prehnite-pumpellyite facies, as revealed by abundant contorted prehnite veinlets; thus the rocks record temperatures far below those required to reset zircon ages. Conglomerate clasts found here include argillite, greenstone, chert, sandstone, and granitic to gabbroic plutonic rocks (Fischietto and others, 2006); these are *bonafide* clasts and *not* blocks in *mélange*. Conodonts from a limestone cobble in conglomerate 2 km southeast of Beluga Point are Meramecian to Morrowan in age (Late Mississippian to Early Pennsylvanian; Nelson and others, 1986); this clast could have been shed from the Strelina Formation of the Wrangellia terrane (Nelson and others, 1986). A plutonic clast from a nearby outcrop yielded a hornblende K/Ar age of 146±7 Ma (M.A. Lanphere, quoted in Clark, 1981). The geologic significance of this age is uncertain, owing to the very real possibilities of either excess argon or argon loss related to subduction metamorphism.

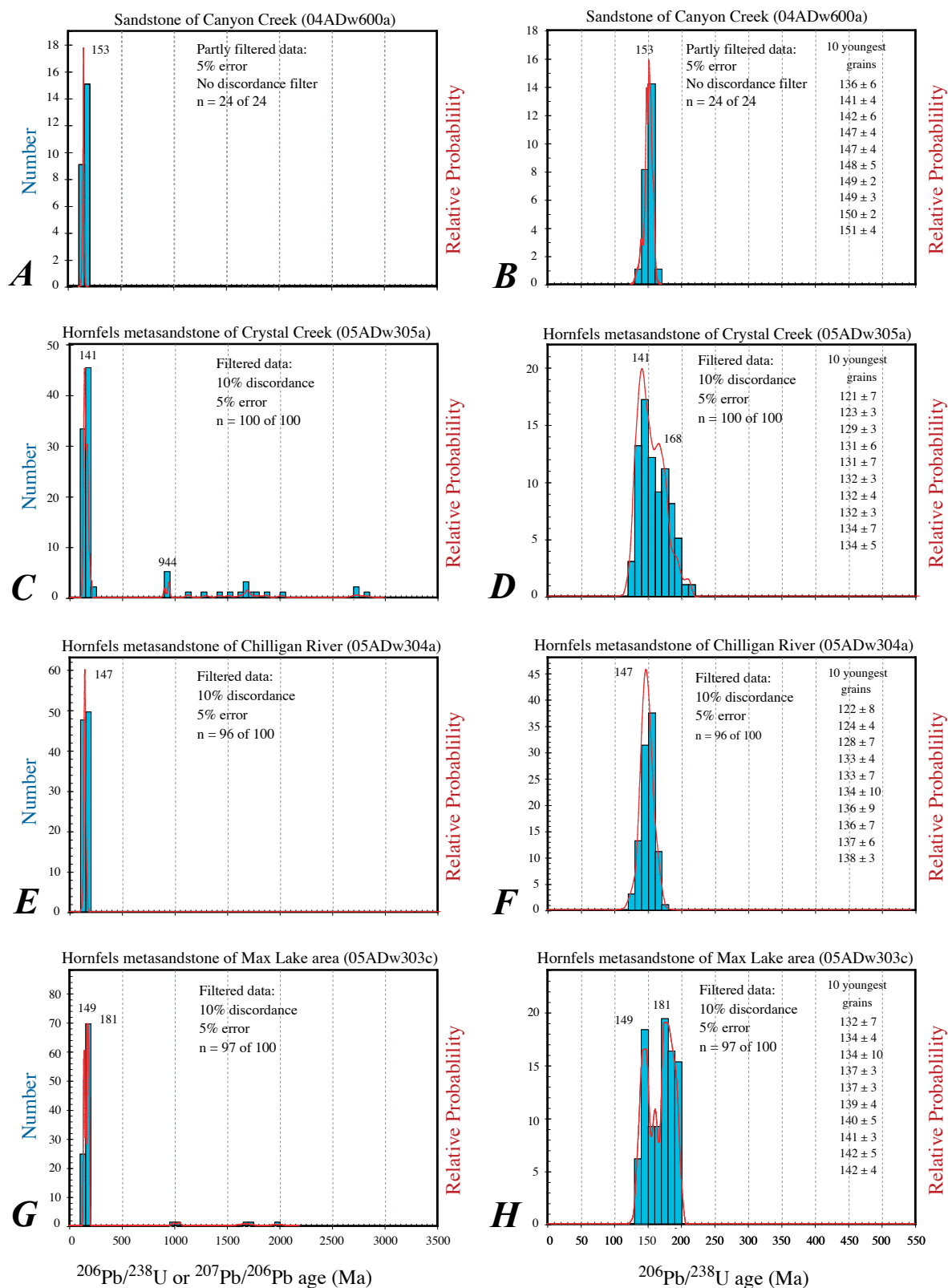
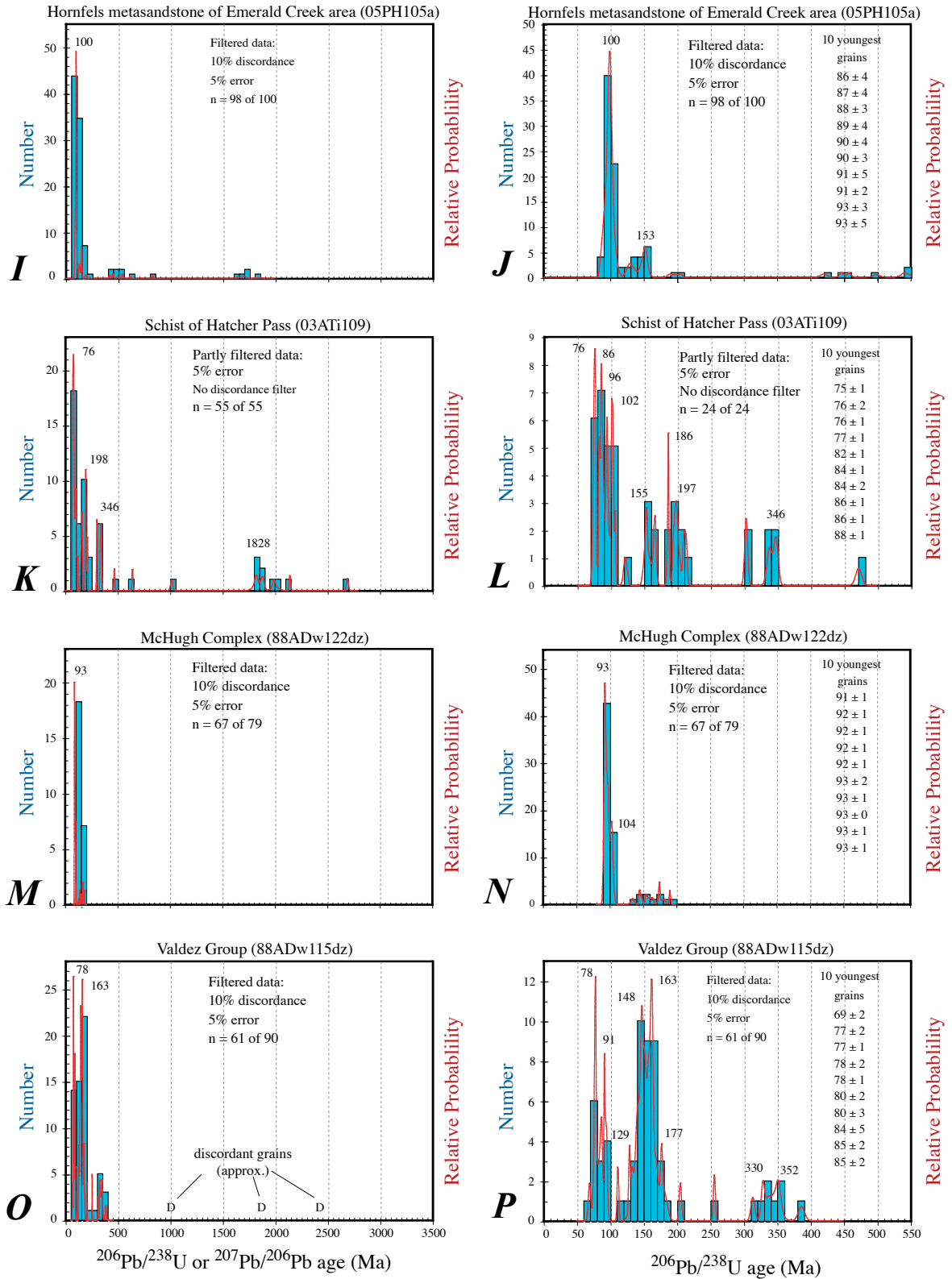


Figure 3. Histograms (blue boxes) and probability plots (red lines) of detrital zircon ages, filtered for discordance and analytical error as outlined in the text. Two plots are shown for each sample, one for 3500-0 Ma and a second one showing details for 550-0 Ma. The plots are arranged to emphasize comparisons between samples of similar age. *A* and *B*, Sample 04ADw600a, sandstone of the Canyon Creek area, western Alaska Range. *C* and *D*, Sample 05ADw305a, hornfels metasandstone of the Crystal Creek area, western Alaska Range. *E* and *F*, Sample 05ADw304a, hornfels metasandstone of the Chilligan River headwaters,



western Alaska Range. *G* and *H*, Sample 05ADw303c, hornfels metasandstone of the Max Lake area, western Alaska Range. *I* and *J*, Sample 05PH105a, hornfels metasandstone of the Emerald Creek area, western Alaska Range. *K* and *L*, Sample 04ATi109 schist of Hatcher Pass, Talkeetna Mountains. *M* and *N*, Sample 88ADw122dz, McHugh Complex, Chugach Mountains. *O* and *P*, Sample 88ADw115dz, Valdez group, Chugach Mountains. *Q* and *R*, Sample 05PH104b, hornfels metasandstone of the Peak 6105 area, western Alaska Range. *S* and *T*, Sample 04ATi103, Arkose Ridge Formation, Talkeetna Mountains.

Geochronology of Igneous Clasts

U-Pb zircon ages were obtained on two similar diorite clasts from conglomerate at Beluga Point using the U.S. Geological Survey (USGS)-Stanford SHRIMP-RG at Stanford University using methods detailed in the appendix. Both clasts are greenish gray, coarse grained diorite containing greenish altered plagioclase, hornblende, and pyroxene. The ages are almost identical, at 181.8 ± 2.1 and 179.2 ± 2.8 Ma (fig. 5A and B) (samples 88ADw122x and 88ADw122w in Table 1). The ages of these clasts match the zircon ages of arc plutons in the northern Chugach Mountains (for example, 181.4 ± 1.0 and 181.5 ± 0.3 Ma), and in the southern Talkeetna

Mountains (for example, 177.5 ± 0.8 Ma) (Rioux and others, 2007). Fischetto and others (2006) proposed a similar link between plutonic clasts from Beluga Point and Mesozoic arc rocks, on the basis of geochemistry.

Detrital Zircons

The detrital zircon sample (88ADw122dz) is from a zone of coarse sandstone within the predominantly conglomeratic outcrop at Beluga Point. U-Pb ages were obtained for 79 detrital zircon grains. The histogram and probability density curve show two peaks, one in the Late Cretaceous (93 Ma)

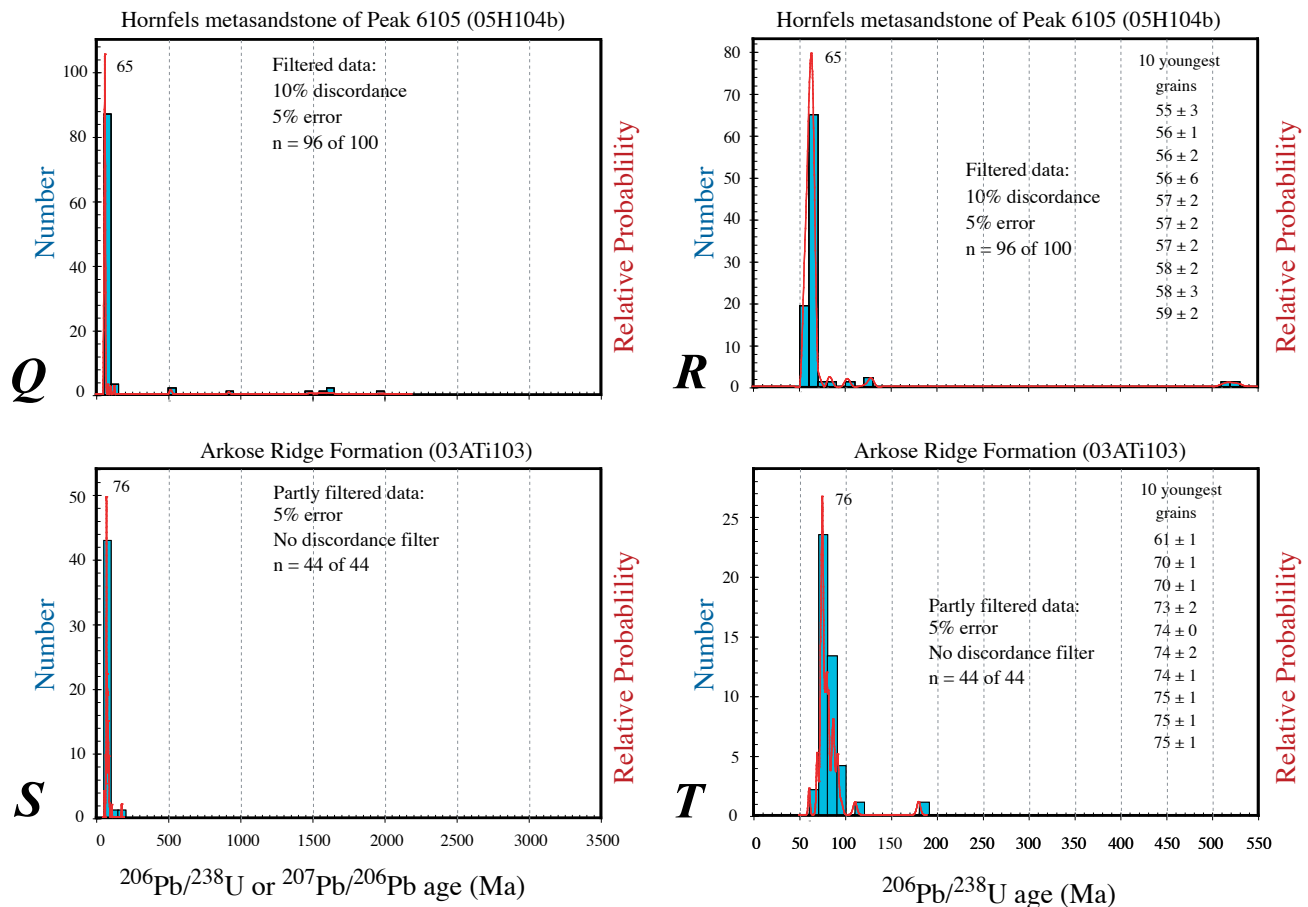


Figure 3. Histograms (blue boxes) and probability plots (red lines) of detrital zircon ages, filtered for discordance and analytical error as outlined in the text. Two plots are shown for each sample, one for 3500-0 Ma and a second one showing details for 550-0 Ma. The plots are arranged to emphasize comparisons between samples of similar age. A and B, Sample 04ADw600a, sandstone of the Canyon Creek area, western Alaska Range. C and D, Sample 05ADw305a, hornfels metasandstone of the Crystal Creek area, western Alaska Range. E and F, Sample 05ADw304a, hornfels metasandstone of the Chilligan River headwaters, western Alaska Range. G and H, Sample 05ADw303c, hornfels metasandstone of the Max Lake area, western Alaska Range. I and J, Sample 05PH105a, hornfels metasandstone of the Emerald Creek area, western Alaska Range. K and L, Sample 04ATi109 schist of Hatcher Pass, Talkeetna Mountains. M and N, Sample 88ADw122dz, McHugh Complex, Chugach Mountains. O and P, Sample 88ADw115dz, Valdez group, Chugach Mountains. Q and R, Sample 05PH104b, hornfels metasandstone of the Peak 6105 area, western Alaska Range. S and T, Sample 04ATi103, Arkose Ridge Formation, Talkeetna Mountains.—Continued.

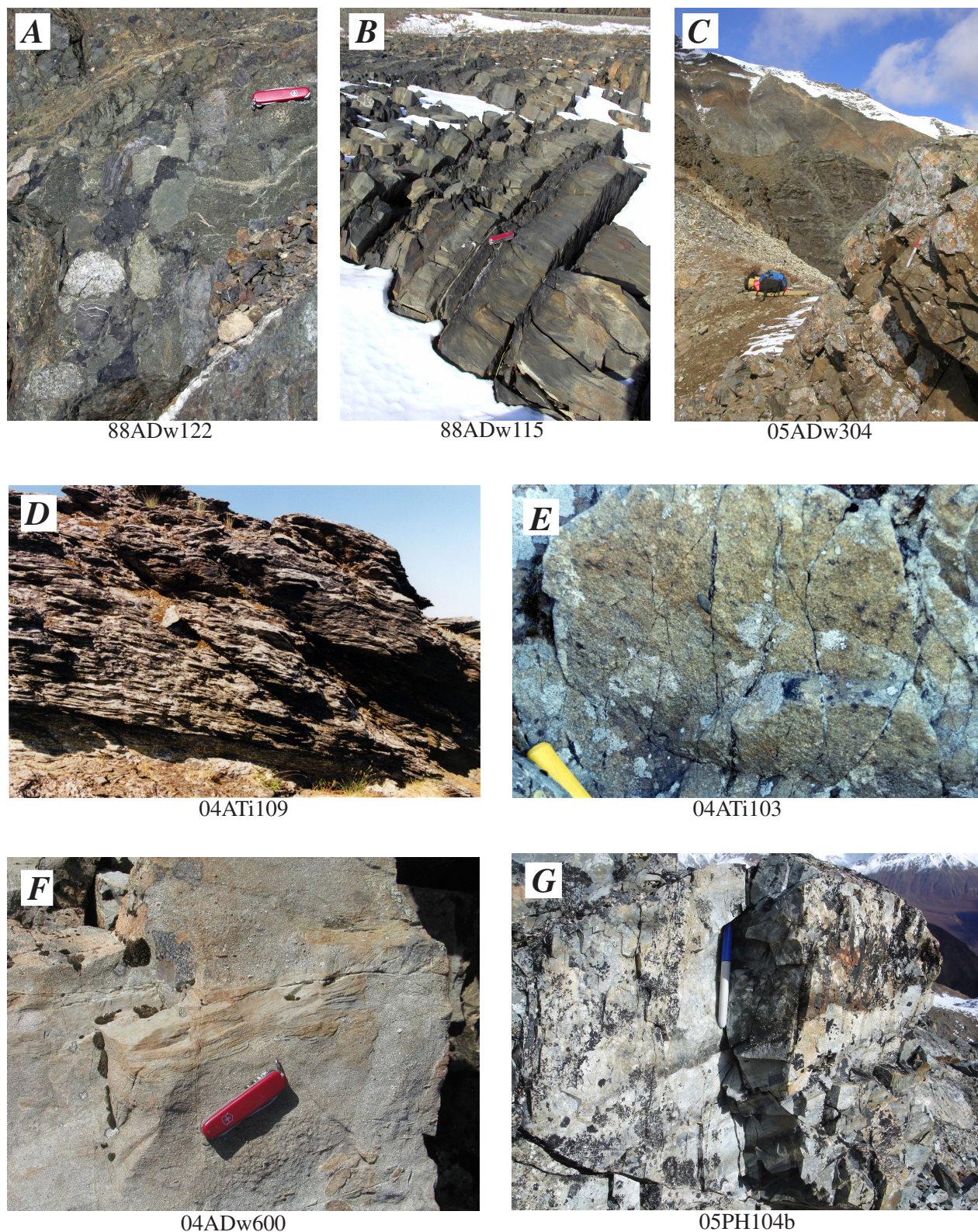


Figure 4. Outcrop photographs of rock units sampled for geochronology. *A*, 88ADw122, McHugh Complex, Upper Cretaceous conglomeratic metasandstone. *B*, 88ADw115, Valdez Group, Upper Cretaceous sandstone. *C*, 04ADw304, hornfels metasandstone of the Chilligan River headwaters, Lower Cretaceous. *D*, 04ATi109, schist of Hatcher Pass, Upper Cretaceous. *E*, 04ATi103, Arkose Ridge Formation, Paleogene. *F*, 05ADw600, sandstone of the Canyon Creek area, Lower Cretaceous. *G*, 05PH104b, hornfels metasandstone of the Peak 6105 area, Paleogene.

and one in the Late Jurassic (162 Ma) (figs. 3M and N). Of the 79 grains, 9 are Jurassic, 16 are Early Cretaceous, 42 are Late Cretaceous, and the remainder did not pass the filters. Jurassic grains at 182 and 175 are close matches for the dated igneous clasts. Older Paleozoic and Precambrian grains are completely lacking.

The probability plot is dominated by a peak at 93 Ma (fig. 3N). The 10 youngest grains are barely younger than

this, ranging from 93 ± 2 to 91 ± 2 Ma. The sandstone and conglomerate of the McHugh Complex was previously regarded as mid-Cretaceous (Winkler and others, 1981). We can now refine the age to no older than 93–91 Ma, and we suggest that it is probably about the same age as the youngest zircons, Turonian (Late Cretaceous). The McHugh sandstone appears to have been derived solely from a Mesozoic arc, one that was active during Turonian deposition and had been intermittently active at least as far back as Early Jurassic time.

The refined age assignment for this part of the McHugh Complex implies that it is the same age as much of the vast Kuskokwim Group of southwestern Alaska (Box and Elder, 1992). The detrital zircon signature of the Kuskokwim shares some common features with the detrital zircon barcode of the McHugh Complex: both contain abundant Cretaceous and Jurassic zircons (Miller and others, 2007a). The Kuskokwim differs profoundly from the McHugh, however, in containing a broad mix of Precambrian grains.

Valdez Group

The seaward part of the Chugach terrane is underlain by the Valdez Group of Campanian to Maastrichtian (Late Cretaceous) age. Age control is based on a handful of inoceramid bivalves (Tysdal and Plafker, 1978; Plafker and others, 1994). The Valdez Group includes thick-, medium-, and thin-bedded graywacke turbidites, dark gray slate, and minor pebble to cobble conglomerate. Sandstones of the Valdez Group generally are moderately well sorted and consist mostly of quartz and feldspar, some volcanic fragments, and rare chert (Dumoulin, 1987). Where no structural complications are apparent in the Seldovia quadrangle, Bradley and others (1999) estimated a minimum stratigraphic thickness of 6.5 km. Most of the Valdez Group consists of relatively coherent strata that were deformed into regional-scale tight to isoclinal folds and cut by a slaty cleavage. The Valdez Group is juxtaposed with the McHugh Complex across a regional-scale thrust fault, which in the area of Turnagain Arm is called the Eagle River Fault. Beneath the fault is a monomict mélange of partially to thoroughly disrupted Valdez Group turbidites—the informally named Iceworm mélange of Kusky and others (1997). The Valdez Group was probably deposited on the downgoing plate in a deep-sea trench (Nilsen and Zuffa, 1982) and accreted shortly thereafter.

Geochronology of an Igneous Clast

A U–Pb zircon age was obtained from a clast of granite in a Valdez Group conglomerate (92AKu18; table 1). The analysis was done on the USGS–Stanford SHRIMP–RG. The conglomerate crops out on the outer coast of the Kenai Peninsula in Seldovia quadrangle (figs. 1A, 6). A massive sandstone at this location contains isolated, matrix-supported,

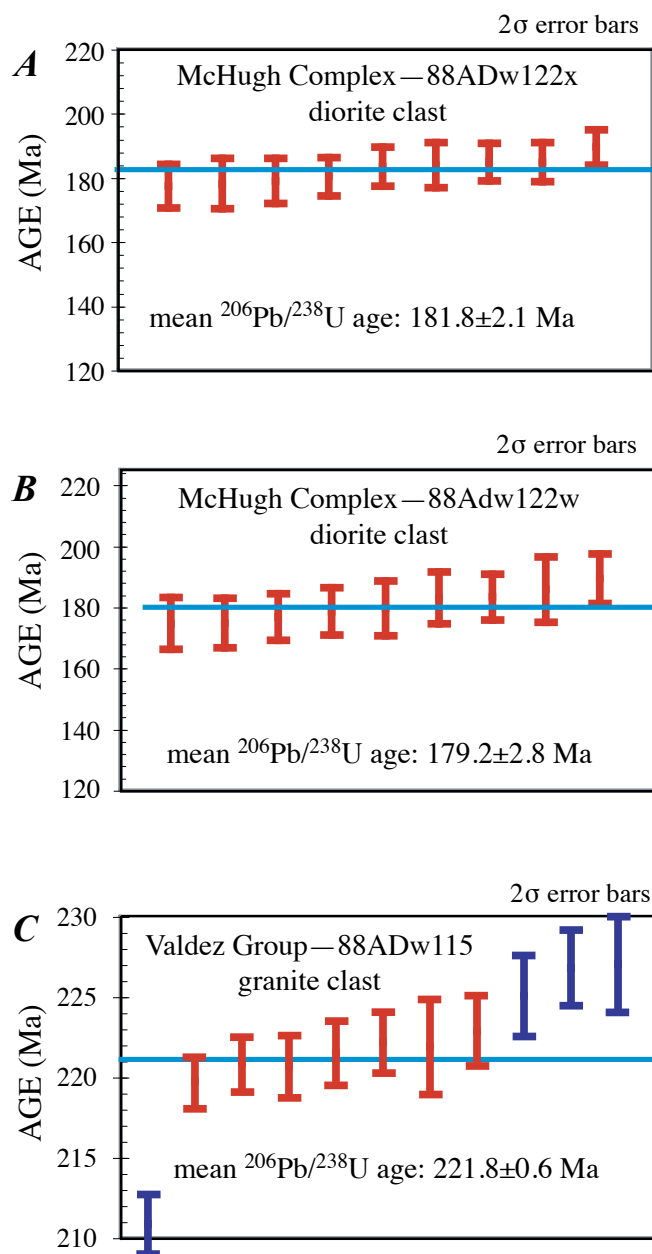


Figure 5. Individual $^{206}\text{Pb}/^{238}\text{U}$ ages of zircon grains from igneous clasts from (A, B) the McHugh Complex and (C) the Valdez Group, plotted using the TuffZirc subroutine of the Isoplot Excel macro of Ludwig (2003). Deep purple bars are analyses that were excluded from the mean calculation.

rounded granitic cobbles. The granite is fine-grained, pinkish tan, nonfoliated, leucocratic, and contains quartz, plagioclase, potassium feldspar, and rare muscovite. Single-crystal analyses of zircons from the granite clast yielded a $^{206}\text{U}/^{238}\text{Pb}$ age of 221.0 ± 1.4 Ma (fig. 5C). The age is the mean of the seven overlapping analyses that are concordant within 2 sigma. The zircons have consistently high concentrations of uranium and thorium, with mean values of 1972 and 1045 ppm, respectively.

Detrital Zircons

The detrital zircon sandstone sample was collected from the classic, wave-washed exposures of Valdez Group near Indian along Turnagain Arm (figs. 2 and 4B). This is Stop 4 of Bradley and Miller (2006). This outcrop is unusual in the clarity of the preserved sedimentary structures but is typical of Valdez Group lithologies including thin- and medium-bedded Bouma sequences of sandstone grading to slate, and medium-

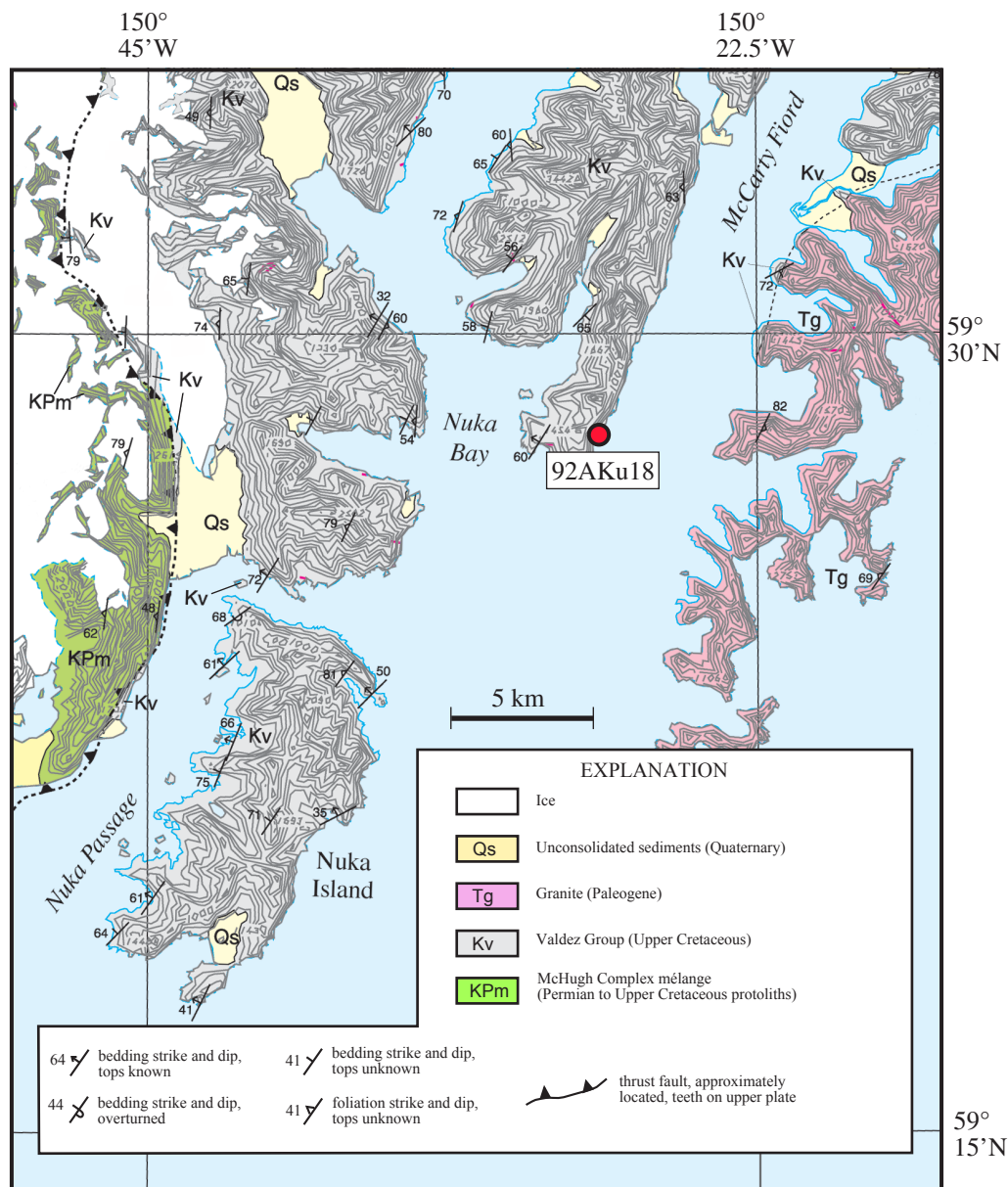


Figure 6. Geologic map of the Nuka Bay area, Seldovia quadrangle, showing the location of the igneous clast (92AKu18) from the Valdez group. From Bradley and others (1999).

to very coarse grained channel sandstones and pebble conglomerate. Paleocurrents from turbidite cross laminae at this locality are toward the southwest (Bradley and others, 2003).

U-Pb ages were obtained for 90 detrital zircon grains from sample 88ADw115dz. The histogram and probability density curve show a peak in the Late Cretaceous (78 Ma) and two peaks in the Jurassic (148 and 162 Ma) (fig. 3O and P). Of the 90 grains, 1 is Devonian, 7 are Carboniferous, 1 is Permian, 1 is Triassic, 29 are Jurassic, 8 are Early Cretaceous, and 13 are Late Cretaceous. The remaining grains did not pass the 10 percent discordance filter, but, whether they are discordant owing to lead loss or inheritance, 3 must be Precambrian, at ca. 2.4, 1.8, and 1.0 Ga (Table 2). The 10 youngest grains range from 85 ± 2 to 69 ± 2 Ma. Our detrital zircon results from the Valdez Group are consistent with the Campanian to Maastrichtian (Late Cretaceous) age suggested by sparse fossils (Plafker and others, 1994). The youngest grain, at 69 ± 2 Ma, is concordant, but it is a single grain; the next four youngest grains are 78–77 Ma.

The present results are broadly comparable with some detrital zircon results from the Sitka Graywacke of southeast Alaska (Haeussler and others, 2006), which has long been regarded as a correlative of the Valdez Group. Samples taken along an across-strike transect near Sitka (locality 14 in fig. 1B) define a younger western part of the unit, and an older eastern part. In four samples from the western part, the means of the 10 youngest grains are 72, 72, 70, and 69 Ma. If (as seems likely) the youngest grains in the western Sitka Graywacke and Valdez Group are very close to the respective depositional ages, these parts of the two rock units are close to the same age. In three samples from the eastern part of the Sitka Graywacke, the means of the 10 youngest grains are 102, 101, and 93 Ma. The eastern Sitka Graywacke thus appears to be older than our Valdez Group sample, and partly overlaps the age of our McHugh Complex sample.

Southern Talkeetna Mountains

Schist of Hatcher Pass

The informally named schist of Hatcher Pass crops out in a 6-by-16-km belt just north of the southwestern end of the Talkeetna Mountains (fig. 2). It is quite distinct from any other bedrock unit in the region, as Capps (1915) recognized nearly a century ago. Most of this belt is underlain by green-schist-facies schist (fig. 4D). The belt also includes several small, metamorphosed mafic-ultramafic slivers or lozenges that are the same metamorphic grade as the schists, and were likely tectonically interleaved with the protoliths of the schists before or during metamorphism. A metagabbro from this suite was sampled for zircon geochronology, but was barren, and the age of the mafic-ultramafic rocks remains unknown. The schist is bounded on the north by granitic rocks of the 73 to 67

Ma (Harlan and others, 2003) Willow Creek batholith across an east-west, high-angle fault. It is bounded on the south by conglomerate of the Paleocene-Eocene Arkose Ridge Formation across what has been previously mapped as an angular unconformity, but in fact is a low-angle detachment fault (A. Till and D. Bradley, unpublished mapping).

Previous assessments of the ages of the protolith and of the metamorphism have been sketchy and speculative. On the assumption that the Hatcher Pass schist shared a metamorphic history with Jurassic amphibolites to the northeast, the schist was assigned a Jurassic age of prograde metamorphism by Csejtey and others (1978), and this age assignment was adopted on the Geologic Map of the Anchorage quadrangle (Winkler, 1992, his Unit Jps). Conventional K-Ar muscovite ages of 66–55 Ma were attributed not to peak syntectonic metamorphism, but instead to the heat from Late Cretaceous plutons to the north (Csejtey and others, 1978; Winkler, 1992). Harlan and others (2003) confirmed and refined the Paleogene metamorphic ages using the $^{40}\text{Ar}/^{39}\text{Ar}$ method (61 to 57 Ma). Van Wyck and Norman (2005) reported the ages of 34 individual zircons from unconsolidated sediments at the gold placer in Grubstake Gulch (locality 19 in fig. 2), which drains an area almost entirely underlain by schist, plus minor mafic/ultramafic bodies. Van Wyck and Norman (2005) suggested that some of their zircons had been eroded out of local bedrock sources, whereas some zircons were from more distant sources. They reported age clusters at 2500–2442, 548–350, 210–160, 104–87, and 79–59 Ma. According to their interpretation, the three oldest age clusters represent detrital zircons eroded out of the schist of Hatcher Pass, to which they accordingly assigned a Late Jurassic depositional age. They interpreted the mid-Cretaceous age cluster (104–87 Ma) as having been derived from serpentinite bodies. They interpreted their youngest age cluster as having been transported (presumably by ice) into Grubstake Gulch from Late Cretaceous plutons just to the north. Our zircon data suggest a new interpretation.

U-Pb ages were obtained from 59 detrital zircons from sample 04ATi109 (Table 1) using the USGS-Stanford SHRIMP-RG (table 2). The schist has a strong, gently to moderately dipping foliation and no surviving vestige of bedding (fig. 4D). In thin section, quartz, white mica, and chlorite define foliation and deflect around porphyroblasts of garnet and albite. A mineral separate yielded abundant, 100–200 micron, rounded zircons having a variety of ages, which, together with the semipelitic to pelitic lithologies, confirm a mixed sandstone-shale protolith. The detrital zircons range in age from 2692 to 75 Ma. Of the 59 grains, 1 is Archean, 9 are Paleoproterozoic, 4 are Mesoproterozoic, 1 is Neoproterozoic, 1 is Ordovician, 6 are Carboniferous, 3 are Triassic, 10 are Jurassic, 6 are Early Cretaceous, and 18 are Late Cretaceous. The probability density curve shows four distinct Cretaceous peaks from 102 to 76 Ma, a pair of Late Jurassic peaks at 166 and 155 Ma, three Late Triassic to Early Jurassic peaks at 213, 197, and 186 Ma, and minor Carboniferous peaks at 346 and 303 Ma (figs. 3K, L).

Combining the new detrital zircon geochronology with the $^{40}\text{Ar}/^{39}\text{Ar}$ metamorphic geochronology of Harlan and others (2003), there is no question now that the sedimentary protolith of the schist of Hatcher Pass is Late Cretaceous to Paleocene in age. Specifically, it must have been deposited between ca. 61 Ma (the age of peak metamorphism) and 77–75 Ma (the age range of the four youngest zircons). We favor a depositional age close to the age of the youngest zircons, Campanian (Late Cretaceous).

The Hatcher Pass zircons have a surprisingly diverse mix of ages, reminiscent of other Upper Cretaceous strata in from at least four sedimentary sequences in Alaska. Miller et al. (2007a) reported detrital zircon data from the Kuskokwim Group of southwestern Alaska (locality 8 in fig. 1B). The main statistical peaks of a composite (multi-sample) Kuskokwim Group barcode are at 1987, 350, 187, and 93 Ma, and lesser peaks are at 1822 and 1122 Ma (Miller and others, 2007a). The Upper Cretaceous Minto Unit of the Manley Basin, Livengood quadrangle (locality 1 in fig. 1B; Weber and others, 1992), has probability peaks at 1847, 1074, 188, and 94 Ma (D. Bradley, A. Till, and R. Friedman, unpublished data, 2007). The Albian to Campanian (Upper Cretaceous) Caribou Pass Formation of the Kahiltina basin, Healy quadrangle (locality 4 in fig. 1B) has probability peaks at 353, 192, and 82 Ma, and a few Paleoproterozoic and Archean zircons (Hampton and Sunderlin, 2008). Finally, as shown in figure 3P, the Valdez Group has major probability peaks at 163, 148, 91, and 78 Ma, and lesser peaks at 352 and 330 Ma. (As noted previously, the Valdez Group sample also yielded Precambrian grains at ca. 1.0, 1.8, and 2.4 Ga, but these did not pass the 10 percent discordance filter.) This topic is developed further in the section on “Tectonic Implications.”

Arkose Ridge Formation

The Arkose Ridge Formation crops out along the northern margin of the Cook Inlet-Matanuska forearc basin (fig. 2). It has a thickness of at least 1,600 m and consists mostly of arkosic conglomerate and sandstone and subordinate mudstone, coal, tuff, and basalt (Trop and Ridgway, 2002) (fig. 4E). The age ranges from Late Paleocene to Middle Eocene (Trop and Ridgway, 2002). A tuff from the Arkose Ridge Formation yielded a late Paleocene U-Pb zircon age of 57.9 ± 0.5 Ma (2 concordant fractions; R. Friedman and D. Bradley, unpublished data).

U-Pb ages were obtained from 44 detrital zircons from sample 04ATi103 using the USGS-Stanford SHRIMP-RG. Detrital zircons were analyzed from a coarse, pebbly sandstone containing angular grains of quartz, two feldspars, and detrital biotite and hornblende. The barcode is relatively simple, with a dominant Late Cretaceous peak at 76 Ma, and minor ones at 92, 88, 80, and 70 Ma (fig. 3S). One Early Jurassic, 1 Early Cretaceous and 1 Paleocene zircon were

found in this relatively small population; all other grains are Late Cretaceous.

On geologic grounds alone, it is clear that the Arkose Ridge Formation was derived from the Talkeetna Mountains to the north (Trop and Ridgway, 2002). Our detrital zircon data show that the source area was a portion of the Talkeetnas almost entirely underlain by Late Cretaceous plutons. Four U-Pb dates are available from plutonic phases of the Willow Creek batholith a few km to the north of the Arkose Ridge sample (72.5 ± 0.4 , 71.9 ± 0.3 , 70.5 ± 0.2 , and 67.3 ± 0.2 Ma; Harlan and others, 2003)¹⁰. These plutonic ages are all younger than the 76-Ma probability peak in the detrital zircon barcode, but it should be remembered that the Willow Creek batholith is huge and many phases have yet to be sampled for modern geochronology. The Arkose Ridge detrital zircon sample probably more fully captures the complete range of Late Cretaceous plutonism in the Talkeetna Mountains. This peak is a hallmark of forearc strata in the Matanuska subbasin: the dominant peak for sandstone samples from the Upper Cretaceous Matanuska Formation, Paleocene Chickaloon Formation, and Oligocene Tsadaka Formation is 76–74 Ma (Trop, 2008; Trop and Bradley, unpublished data). Thus, Late Cretaceous arc rocks were an important sediment source throughout Cretaceous-Paleogene time for sediments exposed in both the forearc and accretionary prism.

Western Alaska Range

The western Alaska Range in the Tyonek quadrangle (fig. 2) is mainly underlain by Lower Cretaceous and younger sedimentary and volcanic rocks, including the still-active Mt. Spurr volcano, and by intrusive rocks ranging in age from 98 to 36 Ma. The 98- to 36-Ma plutons were emplaced into a belt of siliciclastic turbidites, which are little studied and not formally named. Reed and Elliott (1970) originally assigned these strata to two groups of units: Cretaceous metasedimentary rocks (their Units Km and Kw) and pre-Cretaceous metasedimentary and metavolcanic rocks (their Units Mzm, Mzv, and Mzu). On their compilation map of Alaskan terranes, Silberling and others (1994) showed the northwestern Tyonek quadrangle as being entirely underlain by their Kahiltina terrane. Later, Wilson and others (1998) assigned the same strata to Units JPzk and KJf, essentially following Reed and Elliott (1970) but with slightly different age assignments and map abbreviations. The results reported here, from samples collected between 2002 and 2005, have suggested various changes to these previous rock-unit assignments. The detrital zircon age constraints have been accounted for in the latest geological compilation of the Cook

¹⁰Note added in proof: new unpublished SHRIMP-RG U-Pb ages were obtained from plutonic rocks in the area immediately north of the Arkose Ridge Formation sample (H. Bleick and D. Bradley, unpublished data, 2009). New ages of 79.1 ± 1.0 , 76.1 ± 0.9 , and 75.8 ± 0.7 Ma were obtained from the Willow Creek batholith. In addition, an age of 90.3 ± 3 Ma was obtained from diorite in what was erroneously assigned to Unit Jma by Winkler (1992).

Inlet region by Wilson and others (2009), from which Figure 2 was simplified. The various samples are from rocks shown on that map as Units KJs, Kes, and Tves. More refinements will eventually be needed as more of these monotonous looking strata are dated and correlated using detrital zircons.

Before the present study, age control for turbidites of the northwestern Tyonek quadrangle was provided by a smattering of fossils, by intrusive relations of a few cross-cutting plutons of known age, and by ages of conglomerate clasts. The fossils include a Turonian bivalve (locality 15 in fig. 2)¹¹, a Valanginian bivalve (locality 16 in fig. 2)¹², and Early Jurassic to Early Cretaceous radiolarians (locality 17 in fig. 2)¹³. Layer (in Solie and others, 1991) obtained ⁴⁰Ar/³⁹Ar hornblende plateau ages of 101.0±0.7, 95.3±1.1, and 94.6±1.5 from individual clasts from a conglomerate (locality 18 in fig. 2), providing further evidence for the presence of strata that are younger than Early Cretaceous.

Additional age control is hinted at by extrapolation from areas to the northeast and southwest. To the immediate north in the Talkeetna quadrangle (fig. 1) is a vast area mapped by Reed and Nelson (1980) as their Unit KJs. This corresponds to the informally named Kahiltina assemblage (or Kahiltina sequence or Kahiltina terrane), which extends to the north and east into the McGrath, Mt. McKinley, Talkeetna Mountains, and Healy quadrangles (fig. 1) and ranges in age from Late Jurassic (Kimmeridgian) to Late Cretaceous (Cenomanian) (Trop and Ridgway, 2007). The Kahiltina assemblage has also been traced along strike to the south as far as the Lake Clark and Taylor Mountains quadrangles (locality 10 in fig. 1B), where Wallace and others (1989) assigned the Koksetna River sequence to what they called the southern Kahiltina terrane. These rocks have yielded Late Jurassic (Kimmeridgian) to Early Cretaceous (Valanginian) bivalves.

To the west of the Tyonek quadrangle, in the Lime Hills, Taylor Mountains, and Sleetmute quadrangles (fig. 1), lies the Kuskokwim basin of Upper Cretaceous turbidites. Strata of the eastern arm of the Kuskokwim basin (Mulchatna subbasin of Box and Elder, 1992) (locality 9 in fig. 1B) strike roughly into the Tyonek quadrangle, although intervening plutons interrupt what once might have been direct connections. The two known

fossil localities in the Mulchatna subbasin are both Cenomanian to Turonian (ca. 100 to 89 Ma) (Box and Elder, 1992).

The turbidites of the northwestern Tyonek quadrangle thus occupy a place where the Kahiltina, Kuskokwim, and Koksetna depositional basins might be expected to meet or overlap. Detrital zircon results are reported below for six samples in this area. As will be shown, depositional ages are inferred to include Early Cretaceous (4 samples), Late Cretaceous (1 sample), and—surprisingly—Paleogene (1 sample).

Sandstone of the Canyon Creek Area—Valanginian to Hauterivian

The oldest detrital zircon sample (04ADw600a) is from a chalky weathering, green, volcanoclastic sandstone that crops out in the eastern foothills of the Alaska Range (fig. 2). In the compilation of Wilson and others (1998), these rocks were assigned to Unit KJf; in light of the detrital zircon ages reported herein, Wilson et al. (2009) assigned these rocks to their Unit Kes. The sample location is at an old helicopter crash site (twisted rotor blades are all that remain) on a rounded hilltop in the upper reaches of Canyon Creek, Tyonek D-5 quadrangle. The rocks are unmetamorphosed and at the sample site dip 19° to the north. The sample location is within an intact, gently to moderately dipping stratigraphic succession of feldspathic sandstone and lesser siltstone (fig. 4F) that can be followed northward for at least 1 km and is several hundred meters thick. The detrital zircon sample is a poorly sorted, coarse sandstone containing angular clasts of quartz, plagioclase, potassium feldspar, chlorite, and intermediate volcanic rocks.

Zircons in sample 04ADw600a are generally euhedral and clear. Twenty-four grains were dated, which range in age from 160 to 136 Ma (figs. 3A, B; table 2). Paleozoic and Precambrian zircons are notably absent. The statistical peak in the probability density plot is at 153 Ma (Late Jurassic), and the depositional age must be younger still. More than half of the grains are younger than the 153-Ma peak, and the three youngest grains, dated 142±6, 141±4, and 136±6 Ma are Early Cretaceous. Accordingly, we assign an Early Cretaceous, Valanginian to Hauterivian depositional age to this sample; we reason that the depositional age is probably close to the age of the youngest zircons, as is typically the case for syntectonic sandstones deposited along convergent margins. The zircons were derived from a magmatic arc, presumably the Wrangellia composite terrane.

Hornfels Metasandstone of the Chilligan River Headwaters—Aptian

Sample 05ADw304a is from an outcrop area of hornfels in the northern headwaters of the Chilligan River in north-

¹¹During the course of mineral exploration in 1989, a coquina bed was collected in unnamed Mesozoic turbidites by Madelyn Millholland. The sample was designated F1 and the approximate location was given as 61.88333°N, 152.58333°W, lower Chickak River area. In 1989, the sample was submitted (as shipment number A-89-4M) for identification by D. Bradley to Will Elder of the U.S. Geological Survey. He identified the bivalves as *Buchia sublaevis* of Early Cretaceous, Valanginian age.

¹²During the course of mineral exploration in 1989, a bivalve was collected in unnamed Mesozoic turbidites by Madelyn Millholland. The sample was designated F2 and the approximate location was given as 61.85000°N, 152.21666°W, Skwentna River between Emerald and Muddy Creeks. In 1989, the sample was submitted (as shipment number A-89-4M) for identification by D. Bradley to Will Elder of the U.S. Geological Survey. He identified the bivalve as *Inoceramus hobetsensis* of Late Cretaceous, Middle Turonian age.

¹³The sample, number 06SWN50, is radiolarian chert, collected in 2006 by Steve Nelson. The sample was float in a cirque mainly underlain by turbidites, and is unlikely to have moved far from its original outcrop (S.W. Nelson, oral commun., 2006). Radiolarians were identified by E. Pessagno (written commun. to M.L. Miller, 2006).

western Tyonek B-8 quadrangle (fig. 2). These rocks were assigned to Unit Mzs by Reed and Elliott (1970), then to Unit JPzk in the compilation by Wilson and others (1998). In light of the detrital zircon ages reported herein, Wilson et al. (2009) assigned these rocks to their Unit Kes. The sample is from an outcrop of moderately dipping, weakly contact metamorphosed, coarse sandstone (fig. 4C) containing angular detrital grains of quartz, feldspar, chlorite, epidote, and rock fragments of chert and siltstone. At the sample site, the beds dip 55 degrees NNW and the younging direction is unknown.

Detrital zircons were analyzed by Apatite to Zircon, Inc., at Washington State University. The detrital zircons range in age from 172 to 122 Ma. Of 100 grains, 69 are Jurassic, 27 are Cretaceous, and 4 did not pass the filters. Paleozoic and Precambrian grains are absent. The probability density curve shows a lone Late Jurassic peak at 152 Ma (figs. 3E, F; table 2). The depositional age must be somewhat younger than this peak, because 66 grains are younger. The three youngest grains, dated 128 ± 7 , 124 ± 4 , and 122 ± 8 Ma, are Early Cretaceous. Accordingly, we suggest an Early Cretaceous, Aptian depositional age for this sample. The zircons were derived from a magmatic arc that had been almost continuously active between 172 and 122 Ma, with no other input.

Detrital zircon barcodes of the Canyon Creek and Chilligan River samples are remarkably similar to each other. They also resemble a detrital zircon barcode from rocks assigned to the Kahiltna assemblage in the Clearwater Mountains, about 300 km to the northeast in Healy quadrangle, east-central Alaska Range (B. Hampton, written commun., 2008) (locality 5 in fig. 1B). The probability curve of the Clearwater Mountains sample has a single peak at 156 Ma; zircons range from 176 to 139 Ma, and Paleozoic and Precambrian zircons are entirely lacking (B. Hampton, written commun., 2008). Possible zircon sources of the Clearwater Mountains sample are the Talkeetna arc (201–153 Ma) or the more distant Chitina arc (170–135 Ma)—both of the Wrangellia composite terrane (Hampton and others, 2007). Another good match is shown by a detrital zircon barcode from the restricted Gemuk Group (Miller and others, 2007b) in the Taylor Mountains quadrangle of southwest Alaska (locality 7 in fig. 1B). The probability curve of the Gemuk Group sample has closely spaced peaks at 188, 177, 167, 153, and 140 Ma; zircons range from 292 to 130 Ma, Paleozoic zircons are few (only 3 of 56 grains), and Precambrian zircons are absent.

Hornfels Metasandstone of the Max Lake Area—Hauterivian

The second-oldest detrital zircon sample (05ADw303c) is from a small outcrop area of hornfels in the watershed of the unnamed creek draining Max Lake in Tyonek B-8 quadrangle (fig. 2). These rocks were assigned to Unit Mzu by Reed and Elliott (1970), and to Unit JPzk in the compilation by Wilson and others (1998). In light of the detrital zircon ages reported herein, Wilson et al. (2009) assigned these rocks to their Unit

Kes. The sample is from an outcrop of fine-grained turbidites that have been contact metamorphosed to incipient biotite grade. At the sample site, the beds are upright and dip 82° to the northwest.

Detrital zircons were analyzed by Apatite to Zircon, Inc., at Washington State University. The detrital zircons range in age from 1985 to 132 Ma. Of 100 grains, 3 are Paleoproterozoic, 1 is Mesoproterozoic, 1 is Neoproterozoic, 78 are Jurassic, and 14 are Early Cretaceous. The probability density curve (figs. 3G–H) shows Jurassic peaks at 181 and 149 Ma. The depositional age is perhaps a bit younger than the 149-Ma peak, given that 23 grains are younger than this age. The three youngest grains, dated 134 ± 10 Ma, 134 ± 4 , and 132 ± 7 , are Early Cretaceous. Accordingly, we suggest an Early Cretaceous, Hauterivian depositional age for this sample.

Hornfels Metasandstone of the Crystal Creek Area—Aptian

Sample 05ADw305a is from an outcrop area of hornfels in the drainage of the Skwenta River, nearly opposite the mouth of Crystal Creek, Tyonek C-8 quadrangle (fig. 2). These rocks were assigned to Unit Km by Reed and Elliott (1970), and to Unit KJf in the compilation by Wilson and others (1998). In light of the detrital zircon ages reported herein, Wilson et al. (2009) assigned these rocks to their Unit Kes. At the sample site, the beds dip 81° SW and the younging direction is unknown. The detrital zircon sample is a coarse, poorly sorted sandstone containing angular clasts of quartz, plagioclase, potassium feldspar (minor), chert, and phyllite.

Detrital zircons were analyzed by Apatite to Zircon, Inc., at Washington State University. The detrital zircons range in age from 2818 to 122 Ma. Of 100 grains, 3 are Archean, 8 are Paleoproterozoic, 4 are Mesoproterozoic, 5 are Neoproterozoic, 3 are Triassic, 51 are Jurassic, and 26 are Early Cretaceous. The probability density curve (figs. 3C, D) shows a major mid-Cretaceous peak at 141 Ma, a somewhat lesser Middle Jurassic peak at 168 Ma, and a minor early Neoproterozoic peak at 944 Ma. The depositional age is perhaps a bit younger than the 141-Ma peak, because 17 grains are younger. The three youngest grains are 129 ± 3 , 123 ± 3 , and 121 ± 7 Ma. Accordingly, we suggest an Early Cretaceous, Aptian depositional age. As for the other samples, we reason that this is probably close to the age of the youngest zircons.

The detrital zircon barcodes of the samples from the Chilligan headwaters and Crystal Creek are similar to each other, being dominated by Jurassic to Early Cretaceous zircons but containing a few Precambrian grains. They differ in the latter respect from the Canyon Creek and Chilligan River samples. None of the four Lower Cretaceous samples from Tyonek quadrangle have detrital zircon barcodes that closely match barcodes from the Kahiltna assemblage to the northeast. Kalbas and others (2007) reported detrital zircon ages from a single sample from eastern McGrath quadrangle (locality 6 in

fig. 1B) that has grains as young as 109 and 106 Ma, a major peak at ca. 200 Ma, a minor peak at ca. 350 Ma, and no grains at all in the 155–140 Ma interval (in contrast, this is the dominant peak in all four Lower Cretaceous samples from Tyonek quadrangle). Hampton and others (2007) reported detrital zircon ages from four samples in southwestern Healy quadrangle (locality 3 in fig. 1B) that all feature major peaks at ca. 200 Ma, a scattering of Devonian and Mississippian zircons, and a notable paucity of grains in the 155–140 Ma interval.

Hornfels Metasandstone of the Emerald Creek Area—Coniacian

Sample 05PH105a is from the Skwentna River drainage, a few kilometers south of Emerald Creek, in northern Tyonek C-8 quadrangle (fig. 2). These rocks were assigned to Unit KM? by Reed and Elliott (1970; their query), and to Unit JPzk in the compilation by Wilson and others (1998). In light of the detrital zircon ages reported herein, Wilson et al. (2009) assigned these rocks to their Unit KJs. The sample is from an outcrop of weakly contact-metamorphosed coarse graywacke and slate. Beds dip 59° N and the younging direction is unknown. In thin section, the rock is a very coarse, poorly sorted sandstone containing euhedral crystals of plagioclase and pyroxene, as well as volcanic and siltstone rock fragments.

Detrital zircons were analyzed by Apatite to Zircon, Inc., at Washington State University. The detrital zircons range in age from 1837 to 84 Ma. Of 100 grains, 5 are Paleoproterozoic, 3 are Neoproterozoic, 2 are Cambrian, 2 are Ordovician, 1 is Silurian, 1 is Triassic, 10 are Jurassic, 36 are Early Cretaceous, and 37 are Late Cretaceous. The probability density curve (fig. 3I–J) shows a major mid-Cretaceous peak at 100 Ma and a lesser Late Jurassic peak at 153 Ma. The depositional age must be younger than the 100-Ma peak, because 42 grains are younger than this. The three youngest grains, dated 88 ± 3 , 87 ± 4 , and 86 ± 4 Ma, are Late Cretaceous. Accordingly, we suggest a Late Cretaceous, Coniacian depositional age for this sample.

Hornfels Metasandstone of the Peak 6105 Area—Paleogene

Sample 05PH104b is from an outcrop belt of contact-metamorphosed volcanic and sedimentary rocks in the Skwentna River drainage in southern Tyonek C8 quadrangle (fig. 2). These rocks were assigned to Unit Mzu by Reed and Elliott (1970) and to Unit JPzk by Wilson and others (1998). In light of the detrital zircon ages reported herein, Wilson et al. (2009) assigned these rocks to their Unit Tves. The sample is from an outcrop of volcanogenic sandstone and conglomerate (fig. 4G). At the sample site, beds are overturned and dip 83° NE. Shortening must have postdated 55 Ma. The detrital zircon

sample is a hornfels fine-grained sandstone preserving only some of the original sedimentary grains.

Detrital zircons were analyzed by Apatite to Zircon, Inc., at Washington State University. The detrital zircons range in age from 1982 to 55 Ma. Of 100 grains, 3 are Paleoproterozoic, 2 are Mesoproterozoic, 1 is Neoproterozoic, 2 are Cambrian, 3 are Early Cretaceous, 16 are Late Cretaceous, 67 are Paleocene, 2 are Eocene, and 4 did not pass the filters. The probability density curve shows a single peak at ca. 65 Ma (fig. 3Q, R). The maximum possible depositional age is certainly younger than this, because 66 grains are younger than the peak. The three youngest grains, dated 56 ± 1 , 56 ± 2 , 55 ± 1 Ma, span the Paleocene boundary at 55.8 Ma (time scale of Gradstein and Ogg, 2004). Accordingly, we suggest an earliest Eocene or latest Paleocene depositional age for this sample, following the same logic as for other samples. Most of the detrital zircons were derived from a magmatic arc that was active between approximately 73 and 55 Ma; many possible sources exist nearby in the plutons and volcanic fields of this age range in the western Alaska Range. The sparse older grains are most easily explained as third-cycle (or higher) detrital zircons derived locally from erosion of older rocks such as the Lower Cretaceous (“Kahiltna”) turbidites.

Tectonic Implications

Implications for regional geology, stratigraphy, and correlation were discussed above in the individual sections on the individual samples. Table 1 summarizes the inferred depositional ages. Here we will explore the implications for the tectonic history of south-central Alaska.

Chugach terrane

The Chugach terrane has long been regarded as an accretionary wedge that was built along the seaward margin of the Wrangellia composite terrane, which was the site of intermittent arc magmatism during the Mesozoic (Plafker and others, 1994). The age difference between sandstones of the McHugh Complex (93–91 Ma or younger) and Valdez Group (78–77 Ma or younger), while narrower than formerly suspected, is still consistent with the long-held belief that the McHugh was accreted before the Valdez. Parts of the McHugh Complex must have been accreted still earlier than the conglomerate of Beluga Point, because the McHugh Complex in northern Anchorage quadrangle was intruded by syntectonic plutons at ca. 135–125 Ma (Pavlis and others, 1988).

Talkeetna Mountains

The schist of Hatcher Pass crops out along the northern margin of the Cook Inlet-Matanuska forearc basin. It pres-

ents a problem, because its state of penetrative deformation and metamorphism stands in stark contrast to the nearby, apparently coeval, unmetamorphosed Matanuska Formation (Trop, 2008). This marine succession was deposited during the Late Cretaceous in the Matanuska basin. A recent detrital zircon study of the Matanuska Formation (from locality 12 in fig. 1B) showed that the 10 youngest grains range from 76 to 72 Ma with a mean of 74 ± 1 Ma (Trop, 2008), making it essentially the same age as the protolith of the schist of Hatcher Pass. It seems unlikely, however, that the Matanuska Formation could represent the protolith. For one thing, the Matanuska Formation entirely lacks Precambrian grains, which make up some 20 percent of the Hatcher Pass detrital zircon sample. An additional problem is the lack of any plausible mechanism for subjecting forearc basin deposits to the intense metamorphism and bedding transposition that characterizes the schist of Hatcher Pass. As noted earlier, the detrital zircon barcode of the schist of Hatcher Pass is reminiscent of barcodes from the Kuskokwim Group in Taylor Mountains quadrangle (locality 8 in fig. 1B), the Minto unit (locality 1 in fig. 1B), and the Caribou Pass Formation (locality 4 in fig. 1B). Of these, only the Caribou Pass Formation is in the right part of the world to conceivably be related to the schist of Hatcher Pass. This possibility, however, has the same problem as the Matanuska Formation: how to explain the intense deformation and metamorphism in a supra-subduction setting.

By elimination, we suggest a different scenario: that the protolith sediments of the schist of Hatcher Pass were deposited on a subducting plate in the paleo-North Pacific (presumably the Resurrection Plate; Haeussler and others, 2003). This depositional setting is also inferred for the Valdez Group (Nilsen and Zuffa, 1982). Immediately after deposition, the sedimentary package entered the subduction zone, and much of it was soon offscraped and (or) underplated, to be subsequently exposed in the Chugach terrane as the Valdez Group. The strata that were to become the schist of Hatcher Pass were carried much farther down the subduction zone. This package of rocks was eventually exhumed through transtension along the Castle Mountain Fault in the late Paleocene, during deposition of the Arkose Ridge Formation (Bradley and others, 2003). A similar chain of events has been recognized in the Mojave Desert, where the Orocochia Schist is believed to have been subducted beneath the Pacific margin and later exhumed, far inland, during Basin and Range extension (Jacobson and others, 2007). In our model, the schist of Hatcher Pass is relatively far traveled, having been deposited on a different plate a few hundred kilometers seaward of its final position. This model also accounts for the lozenges of ultramafic rock (Winkler, 1992) within the outcrop belt of the schist as fault slices of subducted oceanic lithosphere. A weakness of the Hatcher Pass schist-Valdez Group correlation is that Precambrian detrital zircons are fairly abundant in the former, and relatively scarce in the latter. More data are needed from both units.

Western Alaska Range

The Alaska Range samples were deposited over an interval of about 80 m.y. and record several stages in the regional tectonic evolution. On the basis of both age and position, the four Lower Cretaceous samples would appear to be part of the fill to the Kahiltina basin system, which has been most thoroughly studied to the north and northeast in the central Alaska Range (Kalbas and others, 2007; Hampton and others, 2007; Trop and Ridgway, 2007). The Kahiltina basin system lay between the Wrangellia composite terrane and previously tectonized terranes along the North American margin (the largest being the Yukon-Tanana and Farewell terranes) (fig. 1B). Along the basin's southeastern margin in the Healy quadrangle (localities 2 and 3 in fig. 1B), the Kahiltina was derived from the southeast, from Mesozoic arc sources in the Wrangellia composite terrane (Hampton and others, 2007) (fig. 1B). Near the opposite basin margin farther to the northwest (locality 6 in fig. 1B), the Kahiltina has been interpreted to represent the syncollisional fill of a narrowing ocean that evolved into a foredeep (Kalbas and others, 2007). In this part of the basin, the Kahiltina received clastic input not only from the Mesozoic arc sources of the Wrangellia composite terrane, but also from inboard orogenic highlands underlain by older rocks. The detrital zircon samples from the Tyonek quadrangle are broadly consistent with this framework, with the unimodal Canyon Creek and Chilligan samples having been derived from a southeasterly arc source and the Max Lake and Crystal Creek samples also including some detritus from inboard sources, perhaps the Farewell terrane (fig. 1B).

The Upper Cretaceous and Paleogene samples provide additional evidence for a polyphase depositional history in the northwestern Tyonek quadrangle, which we now know contains deformed strata as young as ca. 55 Ma. Both the Upper Cretaceous and the Paleogene strata were deposited in a retroarc setting above the ancestor to the modern subduction zone. It is not known whether the Upper Cretaceous strata of northwestern Tyonek quadrangle were deposited in the same basin as the Kuskokwim Group of southwest Alaska or in a different basin at the same time. The Paleogene strata of the Peak 6105 area appear to be broadly correlative with the upper part of the Cantwell Group of the central Alaska Range (locality 2 in fig. 1B) (Ridgway and others, 1997), though likely deposited in a different basin.

Implications for ca. 90-Ma Metallogeny

The Turonian (ca. 90 Ma) is an important but poorly documented time in the metallogenic history of south-central Alaska, being the age of the supergiant Pebble Copper porphyry system near Lake Iliamna (Bouley and others, 1995;

Schrader and others, 2001) (locality 11 in fig. 1B). Arc-related plutons of equivalent age would be prospective for porphyry-type mineralization, and such plutons are known far to the northeast of the Pebble prospect in the central Alaska Range, across an apparent 500-km magmatic gap. The question for exploration and mineral assessment in the intervening area (western Alaska Range and Talkeetna Mountains) is whether or not ca. 90-Ma plutons exist, or at least once existed.

Six detrital zircon samples in the present study are young enough that they could conceivably include ca. 90-Ma grains. Five of the six samples do, in fact, contain zircons between 93 and 87 Ma—the McHugh Complex, Valdez Group, schist of Hatcher Pass, Arkose Ridge Formation, and hornfels of the Emerald Lake area (table 2). For all of these but the Arkose Ridge, a specific sources cannot yet be identified, so little can be said about where these ca. 90-Ma zircons actually came from. The Arkose Ridge Formation, however, was clearly derived the Talkeetna Mountains, and its abundant ca. 90-Ma detrital zircons point to the presence of ca. 90-Ma plutons in that area that have not been mapped, have not been dated (see footnote 10, added in proof), have been buried, or have been eroded away.

Acknowledgments

We thank Joe Wooden and Frank Mazdab for help in the USGS-Stanford SHRIMP lab. Reviews by Heather Bleick and Ken Ridgway substantially improved the manuscript. Ric Wilson and Chad Hults provided the draft map that forms the base of Figure 2. Heather Bleick and Peter Cervelli helped with data analysis and presentation. Imagining that one day it would prove datable, Tim Kusky had the foresight to collect the small granite clast from the Valdez Group. We also thank Marti Miller, Brian Hampton, and Jay Kalbas, whose detrital zircon studies on other Cretaceous strata in the region serve as an important basis for comparison.

References Cited

- Bickford, M.E., Cullers, R.L., Shuster, R.D., Premo, W.R., and Van Schmus, W.R., 1989, U-Pb zircon geochronology of Proterozoic and Cambrian plutons in the Wet Mountains and southern Front Range, Colorado: Geological Society of America Special Paper 235, p. 49-64.
- Black, L.P., Kamo, S., Allen, C., Davis, D., Aleinikoff, J.A., Valley, J., Mundil, R., Campbell, I.H., Korsch, R., Williams, I.S. and Foudoulis, C., 2004, Improved $^{206}\text{Pb}/^{238}\text{U}$ microprobe geochronology by the monitoring of a trace-element related matrix effect; SHRIMP, ID-TIMS, ELA-ICP-MS and oxygen isotope documentation for a series of zircon standards: *Chemical Geology*, v. 205, p. 115-140.
- Bouley, B.A., St. George, P., and Wetherbee, P.K., 1995, Geology and discovery at Pebble Copper, a copper-gold porphyry system in southwest Alaska: Canadian Institute of Mining, Metallurgy, and Petroleum, Special Volume 46, p. 422-435.
- Box, S.E., and Elder, W.P., 1992, Depositional and biostratigraphic framework of the Upper Cretaceous Kuskokwim Group, southwestern Alaska: U.S. Geological Survey Bulletin 1999, p. 8-16.
- Bradley, D.C., and Kusky, T.M., 1992, Deformation history of the McHugh Complex, Seldovia quadrangle, south-central Alaska: U.S. Geological Survey Bulletin 1999, p. 17-32.
- Bradley, D., and Miller, M., 2006, Field guide to south-central Alaska's accretionary complex, Anchorage to Seward: Anchorage, Alaska, Alaska Geological Society, 32 p.
- Bradley, D.C., Kusky, T.M., Haeussler, P., Karl, S.M., and Donley, D.T., 1999, Geologic map of the Seldovia quadrangle: U.S. Geological Survey Open File Report 99-18, scale 1:250,000. [Also available online: <http://pubs.usgs.gov/of/1999/of99-018/>]
- Bradley, D., Kusky, T., Haeussler, P., Goldfarb, R., Miller, M., Dumoulin, J., Nelson, S., and Karl, S., 2003, Geologic signature of early Tertiary ridge subduction in Alaska, in Sisson, V.B., Roeske, S.M., and Pavlis, T.L., eds., *Geology of a transpressional orogen developed during ridge-trench interaction along the north Pacific margin*: Geological Society of America Special Paper 371, p. 19-49.
- Bradley, D.C., McClelland, W., Wooden, J., Till, A.B., Roeske, S., Miller, M.L., Karl, S., and Abbott, G., 2007, Detrital zircon geochronology of some Neoproterozoic to Triassic rocks in interior Alaska, in Ridgway, K.D., Trop, J.M., Glen, J.M.G., and O'Neill, J.M., eds., *Tectonic growth of a collisional continental margin, crustal evolution of southern Alaska*: Geological Society of America Special Paper 431, p. 155-180.
- Capps, S.R., 1915, The Willow Creek district, Alaska: U.S. Geological Survey Bulletin 607, 86 p.
- Clark, S.H.B., 1973, The McHugh Complex of south-central Alaska: U.S. Geological Survey Bulletin 1372-D, 11 p.
- Clark, S.H.B., 1981, Guide to bedrock geology along the Seward Highway north of Turnagain Arm: Anchorage, Alaska Geological Society, Publication no. 1, 36 p.
- Clement, S.W.J., and Compston, W., 1994, Ion probe parameters for very high resolution without loss of sensitivity: U.S. Geological Survey Circular 1107, 62 p.
- Csejtei, Bela, Jr., Nelson, W.H., Jones, D.L., Silberling, N.J., Dean, R.M., Morris, M.S., Lanphere, M.A., Smith, J.G., and Silberman, M.L., 1978, Reconnaissance geologic map and geochronology, Talkeetna Mountains Quadrangle, northern part of Anchorage Quadrangle, and southwest corner of Healy Quadrangle, Alaska: U.S. Geological Survey Open-File Report 78-558-A, 60 p., 1 sheet, scale 1:250,000.
- Dumoulin, J.A., 1987, Sandstone composition of the Valdez and Orca Groups, Prince William Sound, Alaska: U.S. Geological Survey Bulletin 1774, 37 p.

- Fischietto, N.E., Rothfuss, J.L., Flanagan, D., and Cole, R.B., 2006, Provenance of a deformed conglomerate in the Mesozoic McHugh Complex mélange, Anchorage quadrangle, Alaska: Geological Society of America Abstracts with Programs, v. 38, no. 7, p. 143.
- Gradstein, F.M., and Ogg, J.G., 2004, A geologic time scale 2004: Cambridge, Cambridge University Press, 598 p., 1 plate.
- Haeussler, P.J., Bradley, D.C., Wells, R.E., and Miller, M.L., 2003, Life and death of the Resurrection Plate; evidence for an additional plate in the northeastern Pacific in Paleocene-Eocene time: Geological Society of America Bulletin, v. 115, p. 867-880.
- Haeussler, P.J., Gehrels, G.E., and Karl, S.M., 2006, Constraints on the age and provenance of the Chugach accretionary complex from detrital zircons in the Sitka Graywacke near Sitka, Alaska: U. S. Geological Survey Professional Paper 1709-F, 24 p.
- Hampton, B.A., Ridgway, K.D., O'Neill, J.M., Gehrels, G.E., Schmidt, J., and Blodgett, R.B., 2007, Pre-, syn-, and postcollisional stratigraphic framework and provenance of Upper Triassic-Upper Cretaceous strata in the northwestern Taltetna Mountains, Alaska, *in* Ridgway, K.D., Trop, J.M., Glen, J.M.G., and O'Neill, J.M., eds., Tectonic growth of a collisional continental margin, crustal evolution of southern Alaska: Geological Society of America Special Paper 431, p. 401-438.
- Hampton, B., and Sunderlin, D., 2008, Provenance and paleoflora of the Cretaceous Caribou Pass Formation, south-central Alaska: Development of a collisional foreland in the final stages of island arc accretion: Geological Society of America Abstracts with Programs, v. 40, no. 6, p. 156.
- Harlan, S.S., Snee, L.W., Vielreicher, R.M., Goldfarb, R.G., Mortensen, J.K., and Bradley, D.C., 2003, Age and cooling history of gold deposits and host rocks in the Willow Creek mining district, Talkeetna Mountains, south-central Alaska: Geological Society of America Abstracts with Programs, v. 35, no. 6, p. 235.
- Ireland, T.R., and Williams, I.S., 2003, Considerations in zircon geochronology by SIMS: Reviews in Mineralogy and Geochemistry, v. 53, p. 215-241.
- Jacobson, C.E., Grove, M., Vucic, A., Pedrick, J.N., and Ebert, K.A., 2007, Exhumation of the Orocopia Schist and associated rocks of southeastern California; relative roles of erosion, synsubduction tectonic denudation, and middle Cenozoic extension: Geological Society of America Special Paper 419, p. 1-37.
- Kalbas, J.L., Ridgway, K.D., and Gehrels, G.E., 2007, Stratigraphy, depositional systems, and provenance of the Lower Cretaceous Kahiltina assemblage, western Alaska Range; basin development in response to oblique collision, *in* Ridgway, K.D., Trop, J.M., Glen, J.M.G., and O'Neill, J.M., eds., Tectonic growth of a collisional continental margin, crustal evolution of southern Alaska: Geological Society of America Special Paper 431, p. 307-343.
- Kusky, T.M., Bradley, D.C., Haeussler, Peter, and Karl, Susan, 1997, Controls on accretion of flysch and mélange belts at convergent margins, evidence from the Chugach Bay thrust and Iceworm mélange, Chugach Terrane, Alaska: Tectonics, v. 16, p. 855-878.
- Kusky, T.M., Glass, A., and Tucker, R., 2007, Structure, Cr-chemistry, and age of the Border Ranges Ultramafic-Mafic Complex, a suprasubduction zone ophiolite complex, *in* Ridgway, K.D., Trop, J.M., Glen, J.M.G., and O'Neill, J.M., eds., Tectonic growth of a collisional continental margin, crustal evolution of southern Alaska: Geological Society of America Special Paper 431, p. 207-226.
- Ludwig, K.R., 2001, Squid 1.00, a users manual: Berkeley Geochronology Center Special Publication No. 2, 17 pp.
- Ludwig, K.R., 2003, Isoplot 3.00, a geochronological toolkit for Microsoft Excel: Berkeley Geochronology Center, Special Publication No. 4a, Berkeley, California.
- Miller, M.L., Bradley, D.C., Kalbas, J.L., Friedman, R., and O'Sullivan, P.B., 2007a, Detrital zircon geochronology of the Upper Cretaceous Kuskokwim Group, southwestern Alaska: Geological Society of America Abstracts with Programs, v. 39, no. 6, p. 489.
- Miller, M.L., Bradley, D.C., Bundtzen, T.K., Pessagno, E.A., Jr., Blodgett, R.B., Tucker, R., and Wooden, J., 2007b, The restricted Gemuk Group—a Triassic to Early Cretaceous succession in southwest Alaska, *in* Ridgway, K.D., Trop, J.M., Glen, J.M.G., and O'Neill, J.M., eds., Tectonic growth of a collisional continental margin, crustal evolution of southern Alaska: Geological Society of America Special Paper 431, p. 273-305.
- Nelson, S.W., Blome, C.D., Harris, A.G., Reed, K.M., and Wilson, F.H., 1986, Late Paleozoic and Early Jurassic fossil ages from the McHugh Complex: U.S. Geological Survey Circular 978, p. 60-64.
- Nilsen, T.H., and Zuffa, G.G., 1982, The Chugach terrane, a Cretaceous trench-fill deposit, southern Alaska: Geological Society of London Special Publication 10, p. 213-227.
- Paces, J.B., and Miller, J.D., 1993, U-Pb ages of the Duluth Complex and related mafic intrusions, northeastern Minnesota; geochronologic insights into physical, paleomagnetic and tectonomagmatic processes associated with the 1.1 Ga mid-continent rift system: Journal Geophysical Research, v. 98, p. 13997-14013.
- Pavlis, T.L., Monteverde, D.H., Bowman, J.R., Rubenstone, J.L., and Reason, M.D., 1988, Early Cretaceous near-trench plutonism in southern Alaska: A tonalite-trondhjemite intrusive complex injected during ductile thrusting along the Border Ranges fault system: Tectonics, v. 7, p. 1179-1199.
- Plafker, G., Moore, J.C., and Winkler, G.R., 1994, Geology of the southern Alaska margin, *in* Plafker, G., and Berg, H.C., eds., The geology of Alaska: Geological Society of America, Decade of North American Geology (DNAG) Series, v. G-1, p. 389-449.
- Reed, B.L., and Elliott, R.L., 1970, Reconnaissance geologic map, analyses of bedrock and stream sediment samples, and

- aeromagnetic map of parts of the southern Alaska Range: U.S. Geological Survey Open-File Report 70-271, 145 p., scale 1:250,000.
- Reed, B.L., and Nelson, S.W., 1980, Geologic map of the Talkeetna Quadrangle, Alaska: U.S. Geological Survey Miscellaneous Investigations 1174, 15 p., 1 sheet, scale 1:250,000.
- Rioux, M., Hacker, B., Mattinson, J., Kelemen, P., Blusztajn, J., and Gehrels, G., 2007, Magmatic development of an intra-oceanic arc; high-precision U-Pb zircon and whole-rock isotopic analyses from the accreted Talkeetna arc, south-central Alaska: Geological Society of America Bulletin, v. 119, p. 1168–1184. doi: 10.1130/B25964.
- Schrader, C.M., Crowe, D., Turner, K., and Stein, H.J., 2001, $^{40}\text{Ar}/^{39}\text{Ar}$ and geochronology of the Pebble Copper Cu-Au-Mo porphyry deposit, southwest Alaska: Geological Society of America Abstracts with Programs, v.33, no. 6, p. 418.
- Solie, D.N., Gilbert, W.G., Harris, E.E., Kline, J.T., Liss, M.S., and Robinson, M.S., 1991, Preliminary geologic map of Tyonek D-6 and eastern Tyonek D-7 quadrangles, Alaska: Alaska Division of Geological and Geophysical Surveys, Public Data File 91-10, 16 p., 1 sheet, scale 1:40,000.
- Stacey, J.S., and Kramers, J.D., 1975, Approximation of terrestrial lead isotope evolution by a two-stage model: Earth and Planetary Science Letters, v. 26, p. 207–221.
- Stevens, C.H., Davydov, V.I., and Bradley, D.C., 1997, Permian Tethyan fusulinids from the Kenai Peninsula, Alaska: Journal of Paleontology, v. 71, p. 985–994.
- Trop, J.M., 2008, Latest Cretaceous forearc basin development along an accretionary convergent margin; south-central Alaska: Geological Society of America Bulletin, v. 120, p. 207–224.
- Trop, J.M., and Ridgway, K.D., 2002, Sedimentology and provenance of the Paleocene-Eocene Arkose Ridge Formation, Cook Inlet-Matanuska Valley forearc basin, southern Alaska: Alaska Division of Geological and Geophysical Surveys Professional Report 119, p. 129–144.
- Trop, J.M., and Ridgway, K.D., 2007, Mesozoic and Cenozoic tectonic growth of southern Alaska; a sedimentary basin perspective, *in* Ridgway, K.D., Trop, J.M., Glen, J.M.G., and O'Neill, J.M., eds., Tectonic growth of a collisional continental margin, crustal evolution of southern Alaska: Geological Society of America Special Paper 431, p. 55–94. doi: 10.1130/2007.2431(04).
- Tysdal, R.G., and Case, J.E., 1977, The McHugh Complex in the Seward Quadrangle, south-central Alaska: U. S. Geological Survey Circular 751-B, p. B48–B49.
- Tysdal, R.G., and Case, J.E., 1979, Geologic map of the Seward and Blying Sound quadrangles, Alaska: U.S. Geological Survey Miscellaneous Investigations 1150, 12 p., scale 1:250,000.
- Tysdal, R.G., and Plafker, G., 1978, Age and continuity of the Valdez Group, southern Alaska: U.S. Geological Survey Bulletin 1457-A, p. A120–A124.
- Van Wyck, N., and Norman, M., 2005, Detrital zircon dates as a constraint on the age of metasedimentary rocks in the Hatcher Pass area, south-central Alaska: Geological Society of America Abstracts with Programs, v. 37, no. 7, p. 82.
- Wallace, W.K., Hanks, C.L., and Rogers, J.F., 1989, The southern Kahiltna terrane; implications for the tectonic evolution of southwestern Alaska: Geological Society of America Bulletin, v. 101, p. 1389–1407.
- Weber, F.R., Wheeler, K.L., Rinehart, C.D., Chapman, R.M., and Blodgett, R.B., 1992, Geologic map of the Livengood quadrangle, Alaska: U.S. Geological Survey Open-File Report 92-562, 20 p., scale 1:250,000.
- Williams, I.S., 1997, U-Th-Pb geochronology by ion microprobe: Reviews in Economic Geology, v. 7, p. 1–35.
- Wilson, F.H., Dover, J.H., Bradley, D.C., Weber, F.R., Bundtzen, T.K., and Haeussler, P.J., 1998, Geologic map of central (interior) Alaska: U.S. Geological Survey Open-File Report 98-133, 64 p., 3 plates, scale 1:500,000.
- Wilson, F.W., Hults, C.P., Schmoll, H.R., Haeussler, P.J., Schmidt, J.M., Yehle, L.A., and Labay, K.A., 2009, Preliminary geologic map of the Cook Inlet region, Alaska: U.S. Geological Survey Open-File Report 2009-1108, 99 p., 2 plates, scale 1:250,000.
- Winkler, G.R., 1992, Geologic map and summary geochronology of the Anchorage 1° x 3° quadrangle, southern Alaska: U.S. Geological Survey Miscellaneous Investigations 2283, 1 sheet, scale 1:250,000.
- Winkler, G.R., Silberman, M.L., Grantz, Arthur, Miller, R.L., and MacKevett, E.M., Jr., 1981, Geologic map and summary geochronology of the Valdez quadrangle, southern Alaska: U.S. Geological Survey Open-File Report 80-892-A, 2 sheets, scale 1:250,000.

Table 2. U-Pb analytical data for detrital and igneous zircons, identified by sample number and lab.

[Analyses that do not pass discordance and error/age filters are shown in strike-through format. Because each lab reports its results in slightly different format, some columns are empty for some samples.]

04ATi109, detrital zircons, n = 55, SHRIMP-RG													
Spot name	207r/235	1 σ error (%)	206r/238	1 σ error (%)	Error cor- relation	207corr 206/238 age (Ma)	1 σ error (m.y.)	204corr 207/206 Age (Ma)	1 σ error (m.y.)	Best age (Ma)	1 σ error (m.y.)	Error/age	Dis- cordance (%)
04ATi109-52.1	0.07	17.9	.0114	2.2	.121	73.7	1.5	-175.6	444.3	73.7	1.5	0.021	-340
04ATi109-47.1	0.08	6.7	.0117	1.8	.262	75.1	1.3	165.9	150.7	75.1	1.3	0.018	120
04ATi109-19.1	0.08	5.3	.0118	1.4	.259	75.4	1.1	47.7	123.2	75.4	1.1	0.014	-37
04ATi109-16.1	0.07	11.6	.0119	2.9	.251	76.3	2.3	-58.5	274.0	76.3	2.3	0.030	-177
04ATi109-41.1	0.08	4.3	.0119	1.1	.261	76.4	0.9	92.3	97.2	76.4	0.9	0.011	21
04ATi109-7.1	0.06	10.1	.0119	0.8	.084	77.5	0.6	-652.1	276.1	77.5	0.6	0.008	-954
04ATi109-30.1	0.09	3.3	.0129	0.9	.262	82.4	0.7	120.2	74.2	82.4	0.7	0.009	46
04ATi109-25.1	0.10	5.7	.0132	1.5	.260	83.7	1.3	333.8	123.7	83.7	1.3	0.015	296
04ATi109-9.1	0.09	9.9	.0131	2.6	.261	84.3	2.2	47.2	229.2	84.3	2.2	0.026	-44
04ATi109-31.1	0.09	3.9	.0134	1.0	.265	85.8	0.9	154.5	87.0	85.8	0.9	0.010	80
04ATi109-1	0.10	4.3	.0135	1.2	.269	86.3	1.0	242.0	95.7	86.3	1.0	0.012	179
04ATi109-40.1	0.09	6.4	.0137	1.6	.257	87.5	1.5	56.6	146.8	87.5	1.5	0.017	-35
04ATi109-36.1	0.08	11.2	.0137	1.5	.135	88.7	1.3	-275.7	282.6	88.7	1.3	0.015	-413
04ATi109-20.1	0.09	18.8	.0141	2.3	.122	90.8	2.0	-127.1	460.8	90.8	2.0	0.022	-241
04ATi109-22.1	0.10	5.7	.0147	1.5	.264	94.1	1.4	126.4	129.8	94.1	1.4	0.015	34
04ATi109-13.1	0.09	28.2	.0146	2.2	.076	94.1	1.5	-100.2	691.3	94.1	1.5	0.016	-207
04ATi109-42.1	0.10	4.1	.0149	1.1	.263	95.0	1.0	146.9	93.1	95.0	1.0	0.011	54
04ATi109-33.1	0.10	6.5	.0153	1.7	.257	98.1	1.7	-41.8	152.0	98.1	1.7	0.017	-143
04ATi109-32.1	0.10	3.9	.0159	1.1	.267	101.9	1.1	85.8	90.2	101.9	1.1	0.011	-16
04ATi109-48.1	0.11	5.1	.0160	1.4	.267	101.9	1.4	170.4	115.3	101.9	1.4	0.014	67
04ATi109-23.1	0.10	5.1	.0159	1.1	.218	102.0	1.2	64.2	119.1	102.0	1.2	0.011	-37
04ATi109-34.1	0.11	2.7	.0162	0.7	.267	103.9	0.8	97.4	60.7	103.9	0.8	0.007	-6
04ATi109-59.1	0.11	3.5	.0167	0.9	.251	106.6	1.0	175.5	79.2	106.6	1.0	0.009	64
04ATi109-39.1	0.13	7.8	.0191	2.1	.273	122.0	2.6	211.9	173.9	122.0	2.6	0.022	73
04ATi109-53.1	0.14	9.4	.0235	1.7	.185	151.0	2.6	-169.8	231.2	151.0	2.6	0.017	-213
04ATi109-57.1	0.16	3.4	.0241	0.9	.276	153.6	1.5	144.4	76.4	153.6	1.5	0.009	-6
04ATi109-5.1	0.18	8.4	.0248	1.8	.211	157.6	2.8	288.9	188.5	157.6	2.8	0.018	83
04ATi109-37.1	0.17	6.0	.0259	1.7	.279	165.2	2.8	142.9	135.4	165.2	2.8	0.017	-13
04ATi109-28.1	0.18	5.4	.0261	1.0	.188	166.5	1.7	134.9	125.4	166.5	1.7	0.010	-19
04ATi109-45.1	0.20	3.9	.0292	0.9	.221	185.9	1.6	124.3	89.2	185.9	1.6	0.009	-33
04ATi109-46.1	0.20	1.7	.0293	0.4	.224	186.4	0.7	163.6	38.5	186.4	0.7	0.004	-12
04ATi109-11.1	0.19	6.0	.0305	1.0	.170	194.5	1.9	-14.7	142.4	194.5	1.9	0.010	-108
04ATi109-15.1	0.20	8.0	.0309	1.2	.151	197.3	2.3	15.8	190.6	197.3	2.3	0.012	-92
04ATi109-44.1	0.21	3.8	.0312	0.9	.243	198.5	1.9	139.8	87.7	198.5	1.9	0.009	-29
04ATi109-55.1	0.19	8.0	.0316	1.3	.167	202.3	2.6	-145.8	194.9	202.3	2.6	0.013	-173
04ATi109-43.1	0.23	2.5	.0331	0.7	.294	209.5	1.6	233.4	56.3	209.5	1.6	0.008	11
04ATi109-21.1	0.28	2.4	.0340	0.8	.319	213.0	1.6	605.2	48.3	213.0	1.6	0.008	181
04ATi109-56.1	0.34	4.3	.0480	0.8	.191	302.5	2.4	238.9	97.9	302.5	2.4	0.008	-21
04ATi109-2.1	0.37	2.6	.0484	0.7	.260	303.3	2.0	433.5	56.0	303.3	2.0	0.007	42
04ATi109-49.1	0.42	13.6	.0540	1.4	.104	337.8	3.6	453.1	299.7	337.8	3.6	0.011	34
04ATi109-18.1	0.37	4.8	.0537	1.3	.271	338.7	4.4	168.5	107.8	338.7	4.4	0.013	-50
04ATi109-8.1	0.40	2.0	.0551	0.8	.386	346.2	2.7	325.5	41.8	346.2	2.7	0.008	-6
04ATi109-35.1	0.41	2.5	.0557	0.8	.322	349.5	2.8	320.9	52.9	349.5	2.8	0.008	-8
04ATi109-10.1	0.61	2.7	.0761	1.0	.359	471.4	4.5	547.1	54.3	471.4	4.5	0.010	16
04ATi109-24.1	0.88	1.9	.1050	0.7	.400	644.2	4.8	621.2	37.0	644.2	4.8	0.007	-3
04ATi109-3.1	1.76	3.3	.1710	1.0	.301	1016.1	10.0	1053.4	63.0	1016.1	10.0	0.010	4
04ATi109-38.1	1.83	30.2	.1653	2.6	.086	977.0	16.2	1202.9	593.8	1202.9	593.8	0.494	22
04ATi109-12.1	1.88	9.3	.1583	1.2	.125	930.0	8.4	1344.6	178.4	1344.6	178.4	0.133	42
04ATi109-6.1	1.89	1.3	.1408	0.4	.328	819.2	3.4	1575.0	22.3	1575.0	22.3	0.014	85
04ATi109-54.1	2.65	1.0	.1899	0.4	.435	1089.7	4.6	1648.2	16.4	1648.2	16.4	0.010	47
04ATi109-17.1	4.99	1.9	.3267	0.9	.506	1823.7	17.2	1811.0	29.3	1811.0	29.3	0.016	-1
04ATi109-4.1	3.97	0.9	.2589	0.5	.567	1452.9	7.3	1821.4	13.4	1821.4	13.4	0.007	23
04ATi109-26.1	5.29	1.6	.3417	1.0	.641	1902.9	19.7	1835.8	22.5	1835.8	22.5	0.012	-3
04ATi109-27.1	5.28	1.2	.3328	0.8	.652	1848.4	13.9	1880.0	15.8	1880.0	15.8	0.008	2
04ATi109-51.1	4.13	1.1	.2597	0.7	.604	1451.0	9.7	1884.6	16.1	1884.6	16.1	0.009	27
04ATi109-29.1	6.18	1.0	.3659	0.7	.663	2012.9	13.3	1991.6	13.2	1991.6	13.2	0.007	-1
04ATi109-58.1	4.42	2.2	.2599	1.0	.463	1438.3	14.1	2004.1	34.8	2004.1	34.8	0.017	35
04ATi109-50.1	7.08	0.5	.3848	0.4	.702	2090.4	7.9	2144.1	6.6	2144.1	6.6	0.003	2
04ATi109-37.1	13.30	0.9	.5233	0.7	.776	2721.1	20.7	2691.9	8.9	2691.9	8.9	0.003	-1

Table 2. U-Pb analytical data for detrital and igneous zircons, identified by sample number and lab.—Continued

04ATi103, detrital zircons, n = 44, SHRIMP-RG													
Spot name	207r/235	1 σ error (%)	206r/238	1 σ error (%)	Error cor- relation	207corr 206/238 age (Ma)	1 σ error (m.y.)	204corr 207/206 Age (Ma)	1 σ error (m.y.)	Best age (Ma)	1 σ error (m.y.)	Error/age	Dis- cordance (%)
ATI103-41.1	0.07	5.7	.0097	1.5	.272	61.3	1.0	406.6	122.5	61.3	1.0	0.016	557
ATI103-7.1	0.04	73.5	.0106	2.9	.039	69.9	1.1			69.9	1.1	0.016	
ATI103-30.1	0.07	11.1	.0109	1.2	.110	70.1	0.8	-62.9	269.3	70.1	0.8	0.011	-190
ATI103-12.1	0.07	18.2	.0113	2.4	.131	72.8	1.7	-175.6	448.7	72.8	1.7	0.023	-343
ATI103-2.1	0.07	4.4	.0114	0.7	.153	73.6	0.5	-64.9	105.9	73.6	0.5	0.007	-188
ATI103-1	0.07	17.2	.0115	2.4	.137	74.0	1.7	-97.3	418.8	74.0	1.7	0.023	-232
ATI103-37.1	0.06	15.1	.0115	1.4	.092	74.2	0.9	-334.4	386.5	74.2	0.9	0.012	-555
ATI103-11.1	0.08	3.5	.0117	0.9	.250	74.5	0.7	178.8	79.7	74.5	0.7	0.009	139
ATI103-14.1	0.08	40.0	.0117	2.9	.072	74.9	1.3	241.7	919.2	74.9	1.3	0.017	221
ATI103-44.1	0.08	2.9	.0118	0.8	.266	75.0	0.6	263.0	63.1	75.0	0.6	0.008	249
ATI103-43.1	0.07	9.2	.0117	1.3	.142	75.4	1.0	-52.9	221.2	75.4	1.0	0.013	-170
ATI103-33.1	0.06	33.5	.0116	2.8	.083	75.5	1.9	-481.6	886.0	75.5	1.9	0.025	-746
ATI103-28.1	0.08	3.3	.0118	0.8	.231	75.6	0.6	185.1	74.4	75.6	0.6	0.008	144
ATI103-19.1	0.08	2.8	.0119	0.7	.262	75.8	0.6	192.7	62.4	75.8	0.6	0.007	154
ATI103-38.1			.0109	1.8		76.1	0.7			76.1	0.7	0.010	
ATI103-18.1	0.06	56.6	.0117	3.2	.056	76.2	1.6	-550.7	1520.5	76.2	1.6	0.021	-832
ATI103-4.1	0.06	13.2	.0118	1.1	.081	76.5	0.7	-364.2	341.2	76.5	0.7	0.009	-580
ATI103-29.1	0.07	23.4	.0119	1.9	.081	76.8	1.2	-267.5	593.3	76.8	1.2	0.016	-451
ATI103-17.1	0.10	8.9	.0122	2.5	.283	76.9	2.0	582.3	185.6	76.9	2.0	0.026	646
ATI103-32.1	0.12	7.0	.0124	2.2	.310	77.3	1.7	977.5	135.6	77.3	1.7	0.023	1127
ATI103-34.1	0.04	84.3	.0118	3.4	.041	77.9	1.9			77.9	1.9	0.024	
ATI103-3.1			.0111	5.4		78.0	2.3			78.0	2.3	0.029	
ATI103-5.1	0.10	19.7	.0124	2.8	.139	78.8	2.0	455.3	433.7	78.8	2.0	0.026	472
ATI103-31.1	0.07	31.3	.0122	2.3	.073	79.2	1.6	-424.5	819.3	79.2	1.6	0.020	-642
ATI103-40.1	0.05	39.5	.0121	2.2	.055	79.6	1.4			79.6	1.4	0.018	
ATI103-22.1	0.08	9.6	.0125	1.1	.117	80.4	0.8	-44.9	232.1	80.4	0.8	0.010	-156
ATI103-25.1	0.08	31.2	.0125	3.4	.108	80.6	2.5	-73.3	758.5	80.6	2.5	0.031	-191
ATI103-42.1	0.07	15.5	.0126	1.7	.110	81.3	1.3	-189.1	386.4	81.3	1.3	0.016	-334
ATI103-24.1	0.07	17.7	.0126	1.7	.095	81.5	1.2	-214.1	443.7	81.5	1.2	0.015	-364
ATI103-26.1			.0121	3.8		81.9	1.8			81.9	1.8	0.021	
ATI103-8.1	0.09	4.7	.0129	0.7	.143	82.5	0.6	111.4	110.3	82.5	0.6	0.007	35
ATI103-13.1	0.04	97.6	.0126	3.4	.035	83.5	2.2			83.5	2.2	0.027	
ATI103-20.1	0.11	6.5	.0135	1.9	.287	85.0	1.6	597.8	135.1	85.0	1.6	0.019	592
ATI103-27.1	0.09	4.6	.0137	1.2	.265	87.2	1.1	213.2	102.7	87.2	1.1	0.012	144
ATI103-6.1	0.08	14.7	.0136	1.6	.112	87.6	1.3	-187.7	365.9	87.6	1.3	0.015	-316
ATI103-21.1	0.07	48.9	.0135	3.1	.064	87.9	2.2	-693.7	1353.9	87.9	2.2	0.025	-902
ATI103-23.1	0.09	9.9	.0138	1.7	.173	88.1	1.5	70.6	231.7	88.1	1.5	0.017	-20
ATI103-36.1	0.05	38.5	.0134	1.9	.049	88.2	1.3			88.2	1.3	0.015	
ATI103-16.1	0.10	9.3	.0144	1.7	.182	91.9	1.5	195.8	211.5	91.9	1.5	0.017	112
ATI103-39.1			.0133	2.5		92.0	1.4			92.0	1.4	0.015	
ATI103-15.1	0.10	4.8	.0145	1.3	.263	92.6	1.2	132.8	108.1	92.6	1.2	0.013	43
ATI103-35.1	0.11	7.1	.0151	1.9	.271	96.1	1.9	342.3	155.4	96.1	1.9	0.020	254
ATI103-9.1	0.12	10.3	.0175	1.9	.183	111.3	2.1	206.0	235.3	111.3	2.1	0.019	85
ATI103-10.1	0.22	3.6	.0287	1.1	.302	180.6	2.0	467.9	75.5	180.6	2.0	0.011	157
88ADw122x, clast, SHRIMP-RG, mean 206Pb/238U age: 181.8 \pm 2.1 Ma													
Spot name	207r/235	1 σ error (%)	206r/238	1 σ error (%)	Error cor- relation	207corr 206/238 age (Ma)	1 σ error (m.y.)	204corr 207/206 Age (Ma)	1 σ error (m.y.)	Best age (Ma)	1 σ error (m.y.)	Error/age	Dis- cordance (%)
88ADw122x-1	0.15	16.1	.0274	2.1	.128	176.2	3.4	-303	408	176.2	3.4		
88ADw122x-2	0.20	6.4	.0279	2.2	.343	176.9	3.9	293	137	176.9	3.9		
88ADw122x-3	0.18	7.1	.0279	2.0	.278	177.8	3.5	54	163	177.8	3.5		
88ADw122x-4	0.17	7.1	.0280	1.7	.240	179.2	3.0	-129	169	179.2	3.0		
88ADw122x-5	0.17	8.8	.0285	1.7	.197	182.3	3.1	-151	213	182.3	3.1		
88ADw122x-6	0.21	5.1	.0288	1.9	.372	182.8	3.5	291	108	182.8	3.5		
88ADw122x-7	0.18	5.7	.0287	1.6	.279	183.7	2.9	-38	133	183.7	2.9		
88ADw122x-8	0.17	10.6	.0287	1.7	.163	183.8	3.0	-195	261	183.8	3.0		
88ADw122x-9	0.21	3.2	.0297	1.5	.462	188.3	2.7	204	65	188.3	2.7		
88ADw122w, clast, SHRIMP-RG, mean 206Pb/238U age: 179.2 \pm 2.8 Ma													
Spot name	207r/235	1 σ error (%)	206r/238	1 σ error (%)	Error cor- relation	207corr 206/238 age (Ma)	1 σ error (m.y.)	204corr 207/206 Age (Ma)	1 σ error (m.y.)	Best age (Ma)	1 σ error (m.y.)	Error/age	Dis- cordance (%)
88ADw122w-1	0.20	6.9	.0274	2.4	.349	173.5	4.2	345	146	173.5	4.2		
88ADw122w-2	0.17	10.4	.0271	2.3	.225	173.7	4.0	-79	248	173.7	4.0		
88ADw122w-3	0.12	32.7	.0270	2.5		175.5	3.8	-1013	970	175.5	3.8		
88ADw122w-4	0.19	6.2	.0279	2.2	.351	177.4	3.9	217	135	177.4	3.9		

Table 2. U-Pb analytical data for detrital and igneous zircons, identified by sample number and lab.—Continued

88ADw122w-5	0.21	7.1	.0283	2.5	.349	178.5	4.5	408	150	178.5	4.5		
88ADw122w-6	0.19	6.7	.0286	2.3	.346	181.9	4.2	141	147	181.9	4.2		
88ADw122w-7	0.18	6.2	.0285	2.1	.334	182.2	3.8	-77	142	182.2	3.8		
88ADw122w-8	0.16	17.5	.0288	3.0	.170	184.6	5.4	-258	437	184.6	5.4		
88ADw122w-9	0.18	10.2	.0294	2.2	.214	188.2	4.1	-80	243	188.2	4.1		
92AKu18, clast, SHRIMP-RG, mean 206Pb/238U age: 221.8±0.6 Ma													
Spot name	207r/235	1σ error (%)	206r/238	1σ error (%)	Error cor- relation	207corr 206/238 age (Ma)	1σ error (m.y.)	204corr 207/206 Age (Ma)	1σ error (m.y.)	Best age (Ma)	1σ error (m.y.)	Error/age	Dis- cordance (%)
92AKu18-3	0.21	2.1	.0301	0.3	.137	191.0	0.6	251.4	48.6	191.0	0.6		
92AKu18-4	0.23	2.0	.0327	0.3	.158	207.2	0.7	265.7	45.4	207.2	0.7		
92AKu18-5	0.23	3.5	.0333	0.3	.091	210.7	0.7	245.9	80.5	210.7	0.7		
92AKu18-6	0.24	1.2	.0346	0.3	.248	219.6	0.6	188.2	26.6	219.6	0.6		
92AKu18-7	0.26	2.5	.0349	0.4	.145	220.5	0.8	345.8	56.1	220.5	0.8		
92AKu18-8	0.25	1.3	.0349	0.3	.229	220.7	0.7	273.6	29.8	220.7	0.7		
92AKu18-9	0.25	1.6	.0350	0.3	.212	221.3	0.8	268.9	36.8	221.3	0.8		
92AKu18-10	0.24	2.3	.0350	0.6	.251	221.7	1.3	179.5	52.6	221.7	1.3		
92AKu18-11	0.24	1.7	.0350	0.3	.205	222.0	0.8	211.2	38.3	222.0	0.8		
92AKu18-12	0.24	1.3	.0351	0.4	.308	222.7	0.9	215.3	27.8	222.7	0.9		
92AKu18-13	0.24	2.0	.0355	0.5	.245	224.9	1.1	187.0	44.1	224.9	1.1		
92AKu18-14	0.26	1.4	.0359	0.4	.308	226.6	1.0	309.9	29.9	226.6	1.0		
92AKu18-15	0.24	3.3	.0357	0.6	.178	226.8	1.3	91.6	75.9	226.8	1.3		
88ADw115dz, detrital zircons, n = 61 of 90, Univ. of British Columbia													
Analysis #	207/235	1σ error (%)	206/238	1σ error (%)	Error cor- relation	206/238 age	1σ error (Ma)	207/206 age	1σ error (Ma)	Best age (Ma)	1σ error (Ma)	Error/age	Dis- cordance (%)
88ADw115V87	0.06713	0.00823	0.01076	0.00028	0.2123	69.0	1.8	74.6	271.7	69.0	1.8	0.026	8
88ADw115V45	0.10416	0.01093	0.01155	0.00032	0.2640	74.0	2.4	646.0	213.9	74.0	2.4	0.028	89
88ADw115V17	0.08378	0.00384	0.01176	0.00017	0.3179	75.4	1.4	463.0	405.2	75.4	1.4	0.015	54
88ADw115V47	0.08513	0.01125	0.01194	0.00035	0.2218	76.5	2.2	81.3	290.2	76.5	2.2	0.029	6
88ADw115V57	0.07835	0.00474	0.01206	0.00019	0.2604	77.3	1.2	81.0	140.4	77.3	1.2	0.016	5
88ADw115V58	0.07989	0.00737	0.01211	0.00025	0.2238	77.6	1.6	83.2	208.5	77.6	1.6	0.021	7
88ADw115V36	0.09284	0.00922	0.01244	0.00028	0.2322	77.8	1.8	356.8	212.4	77.8	1.8	0.023	78
88ADw115V11	0.07953	0.00246	0.01217	0.00011	0.2922	78.0	0.7	86.4	74.0	78.0	0.7	0.009	10
88ADw115V30	0.07796	0.00772	0.01243	0.00036	0.2925	79.6	2.3	82.8	224.3	79.6	2.3	0.029	4
88ADw115V23	0.09016	0.009	0.01245	0.00039	0.3138	79.7	2.5	79.2	226.0	79.7	2.5	0.031	-1
88ADw115V90	0.09814	0.0042	0.01262	0.00016	0.2986	80.2	1.0	523.9	92.8	80.2	1.0	0.012	85
88ADw115V71	0.08223	0.02706	0.01306	0.00074	0.1666	83.6	4.7	86.8	658.2	83.6	4.7	0.067	4
88ADw115V13	0.09324	0.00385	0.0134	0.00016	0.2958	83.9	1.0	263.4	93.6	83.9	1.0	0.012	68
88ADw115V91	0.08779	0.0069	0.01331	0.00031	0.2963	85.2	2.0	77.9	180.3	85.2	2.0	0.023	-9
88ADw115V29	0.08671	0.00852	0.01333	0.00032	0.2443	85.3	2.0	82.4	221.2	85.3	2.0	0.024	-4
88ADw115V42	0.09294	0.00406	0.01352	0.0002	0.3386	86.6	1.3	328.7	98.0	86.6	1.3	0.014	74
88ADw115V40	0.08623	0.00366	0.01364	0.00019	0.3282	87.3	1.2	89.1	100.4	87.3	1.2	0.014	2
88ADw115V79	0.09393	0.00166	0.01428	0.00009	0.3566	91.4	0.6	92.5	42.8	91.4	0.6	0.006	1
88ADw115V99	0.09529	0.01295	0.01442	0.00039	0.1990	92.3	2.5	97.5	296.5	92.3	2.5	0.027	5
88ADw115V73	0.11405	0.02054	0.01442	0.00062	0.2394	92.3	3.9	601.4	351.4	92.3	3.9	0.042	85
88ADw115V94	0.16954	0.05989	0.01442	0.00115	0.2258	92.3	7.3	4546.0	555.4	92.3	7.3	0.079	94
88ADw115V27	0.09564	0.00622	0.0145	0.00026	0.2757	92.8	1.7	84.5	150.1	92.8	1.7	0.018	-10
88ADw115V82	0.09613	0.00413	0.01479	0.00021	0.3305	94.6	1.4	91.3	101.3	94.6	1.4	0.014	-4
88ADw115V38	0.10588	0.00154	0.01594	0.00008	0.3454	101.9	0.5	201.9	33.7	101.9	0.5	0.005	59
88ADw115V97	0.11844	0.0048	0.01723	0.00024	0.2999	110.4	1.4	220.2	92.9	110.4	1.4	0.012	50
88ADw115V31	0.11052	0.00382	0.01747	0.00018	0.2981	111.7	1.2	105.7	80.5	111.7	1.2	0.010	-6
88ADw115V77	0.12525	0.00333	0.02016	0.00018	0.3358	128.7	1.1	123.2	61.7	128.7	1.1	0.009	-4
88ADw115V68	0.14307	0.02675	0.02075	0.00074	0.1907	132.4	4.7	129.4	388.4	132.4	4.7	0.035	-2
88ADw115V28	0.14227	0.00819	0.02083	0.00031	0.2585	132.9	1.9	137.1	130.0	132.9	1.9	0.015	3
88ADw115V65	0.14005	0.0093	0.02184	0.0004	0.2758	139.3	2.6	142.3	149.1	139.3	2.6	0.018	2
88ADw115V14	0.16044	0.00783	0.02187	0.00028	0.2623	139.5	1.8	247.0	408.3	139.5	1.8	0.013	44
88ADw115V84	0.15581	0.01016	0.02204	0.00038	0.2644	140.6	2.4	138.7	146.1	140.6	2.4	0.017	-1
88ADw115V74	0.14505	0.02597	0.02213	0.0007	0.1767	141.1	4.4	151.4	373.1	141.1	4.4	0.031	7
88ADw115V15	0.14746	0.01065	0.0222	0.00047	0.2931	141.6	2.9	138.3	161.3	141.6	2.9	0.021	-2
88ADw115V51	0.15649	0.01265	0.02267	0.0005	0.2728	144.5	3.2	145.2	178.8	144.5	3.2	0.022	0
88ADw115V88	0.1651	0.01131	0.0228	0.0004	0.2561	145.3	2.5	146.7	152.7	145.3	2.5	0.017	1
88ADw115V62	0.15858	0.01301	0.02299	0.00043	0.2280	146.5	2.7	156.5	180.9	146.5	2.7	0.018	6
88ADw115V19	0.15413	0.00423	0.02307	0.00021	0.3317	147.0	1.3	149.6	62.8	147.0	1.3	0.009	2
88ADw115V20	0.15203	0.00837	0.0232	0.00036	0.2819	147.8	2.3	143.5	124.1	147.8	2.3	0.015	-3
88ADw115V18	0.16061	0.00736	0.02327	0.0003	0.2813	148.3	1.9	142.9	103.8	148.3	1.9	0.013	-4
88ADw115V22	0.1738	0.01546	0.02336	0.00056	0.2695	148.8	3.5	142.7	195.0	148.8	3.5	0.024	-4
88ADw115V76	0.17954	0.02939	0.02362	0.00076	0.1974	149.9	4.8	401.4	329.7	149.9	4.8	0.032	63
88ADw115V100	0.25548	0.07905	0.02364	0.0016	0.2187	150.6	10.1	1096.9	517.8	150.6	10.1	0.067	86

Table 2. U-Pb analytical data for detrital and igneous zircons, identified by sample number and lab.—Continued

88ADw115V41	0.15636	0.00988	0.02378	0.00037	0.2462	151.5	2.3	148.6	141.4	151.5	2.3	0.015	-2
88ADw115V53	0.16839	0.0067	0.0238	0.00028	0.2957	151.7	1.8	152.5	89.9	151.7	1.8	0.012	1
88ADw115V55	0.17854	0.01542	0.02384	0.00053	0.2574	151.9	3.3	152.9	189.2	151.9	3.3	0.022	1
88ADw115V56	0.16326	0.01279	0.02401	0.00046	0.2446	153.0	2.9	149.5	173.4	153.0	2.9	0.019	-2
88ADw115V89	0.2092	0.05676	0.02406	0.00149	0.3264	153.3	9.4	1397.0	322.7	153.3	9.4	0.064	89
88ADw115V101	0.20723	0.0108	0.02413	0.00039	0.3101	153.7	2.5	608.7	407.7	153.7	2.5	0.016	75
88ADw115V60	0.16112	0.01182	0.02415	0.00044	0.2484	153.8	2.8	147.1	163.0	153.8	2.8	0.018	-5
88ADw115V49	0.17329	0.09254	0.02436	0.00193	0.1484	155.4	12.2	149.3	922.0	155.4	12.2	0.078	-4
88ADw115V81	0.17206	0.00633	0.02438	0.00028	0.3122	155.3	1.8	161.1	83.0	155.3	1.8	0.011	4
88ADw115V92	0.07334	0.34133	0.02466	0.00444	0.0392	157.4	25.9	0.4	1525.0	157.4	25.9	0.165	-157000
88ADw115V32	0.16446	0.00498	0.02474	0.00025	0.3337	157.6	1.6	163.2	68.8	157.6	1.6	0.010	3
88ADw115V75	0.15969	0.01004	0.02493	0.00036	0.2297	158.7	2.3	164.2	140.2	158.7	2.3	0.014	3
88ADw115V16	0.17339	0.00952	0.02504	0.00036	0.2619	159.4	2.3	153.1	123.0	159.4	2.3	0.014	-4
88ADw115V50	0.16502	0.00931	0.02539	0.00033	0.2304	161.6	2.1	152.8	126.5	161.6	2.1	0.013	-6
88ADw115V37	0.16931	0.00986	0.0254	0.0004	0.2704	161.7	2.5	153.4	130.3	161.7	2.5	0.016	-5
88ADw115V102	0.17341	0.01972	0.02542	0.00059	0.2041	161.8	3.7	164.2	244.9	161.8	3.7	0.023	1
88ADw115V83	0.17351	0.01317	0.02544	0.0005	0.2589	161.9	3.2	172.9	167.0	161.9	3.2	0.019	6
88ADw115V63	0.16755	0.00732	0.02549	0.00035	0.3143	162.3	2.2	158.5	98.4	162.3	2.2	0.014	-2
88ADw115V35	0.17938	0.00609	0.02553	0.00024	0.2769	162.5	1.5	172.1	76.7	162.5	1.5	0.009	6
88ADw115V85	0.16967	0.00429	0.02561	0.0002	0.3089	163.0	1.3	164.0	57.3	163.0	1.3	0.008	1
88ADw115V66	0.16599	0.02123	0.02599	0.00055	0.1655	165.4	3.5	0.4	214.4	165.4	3.5	0.021	-165300
88ADw115V26	0.20078	0.01894	0.02633	0.00058	0.2452	167.6	3.6	448.7	186.9	167.6	3.6	0.022	63
88ADw115V33	0.17383	0.01265	0.0265	0.00054	0.2800	168.6	3.4	159.7	160.9	168.6	3.4	0.020	-6
88ADw115V86	0.18554	0.01258	0.02651	0.00045	0.2504	168.7	2.9	176.2	149.4	168.7	2.9	0.017	4
88ADw115V98	0.19891	0.0296	0.02677	0.00092	0.2309	170.3	5.8	161.6	311.4	170.3	5.8	0.034	-5
88ADw115V10	0.2046	0.02054	0.027	0.00065	0.2402	171.7	4.4	425.4	207.7	171.7	4.4	0.024	60
88ADw115V39	0.18949	0.00467	0.02783	0.00023	0.3353	176.9	1.4	189.4	55.4	176.9	1.4	0.008	7
88ADw115V67	0.3024	0.06687	0.02794	0.00145	0.2347	177.4	9.4	1136.9	382.7	177.4	9.4	0.054	84
88ADw115V46	0.19792	0.01809	0.02802	0.00064	0.2499	178.2	4.0	164.2	199.1	178.2	4.0	0.022	-9
88ADw115V48	0.20423	0.01779	0.02877	0.00066	0.2634	182.9	4.1	192.6	188.2	182.9	4.1	0.023	5
88ADw115V72	0.06596	0.05004	0.0307	0.00145	0.0623	195.0	9.4	0.4	0.0	195.0	9.4	0.046	-194900
88ADw115V95	0.22188	0.00638	0.03233	0.00029	0.3120	205.1	1.8	209.3	63.6	205.1	1.8	0.009	2
88ADw115V25	0.27734	0.00454	0.04054	0.00024	0.3616	256.2	1.5	266.4	35.4	256.2	1.5	0.006	4
88ADw115V80	0.32885	0.00634	0.04539	0.00029	0.3314	286.4	1.8	338.7	40.4	286.4	1.8	0.006	46
88ADw115V21	0.38516	0.01209	0.04988	0.00048	0.3066	313.8	2.9	303.5	65.2	313.8	2.9	0.009	-3
88ADw115V12	0.38407	0.00868	0.05228	0.00038	0.3216	328.5	2.3	313.6	46.9	328.5	2.3	0.007	-5
88ADw115V69	0.15599	0.10507	0.0534	0.00223	0.0623	333.5	13.7	0.4	0.0	333.5	13.7	0.044	-333400
88ADw115V34	0.37616	0.01869	0.05328	0.00084	0.3173	334.7	5.2	327.0	101.4	334.7	5.2	0.015	-2
88ADw115V64	0.38887	0.03664	0.05397	0.00129	0.2537	338.9	7.9	317.5	191.4	338.9	7.9	0.023	-7
88ADw115V9	0.41949	0.01494	0.05433	0.00066	0.3084	341.4	3.4	404.8	67.9	341.4	3.4	0.010	46
88ADw115V44	0.39832	0.02219	0.05538	0.00092	0.2982	347.5	5.7	367.2	112.1	347.5	5.7	0.016	5
88ADw115V24	0.40674	0.03012	0.05588	0.00123	0.2972	350.5	7.5	347.6	146.4	350.5	7.5	0.021	-1
88ADw115V59	0.42836	0.01331	0.05619	0.00054	0.3093	352.4	3.3	380.9	62.6	352.4	3.3	0.009	7
88ADw115V70	0.44755	0.02053	0.06181	0.00079	0.2786	386.6	4.8	385.0	92.0	386.6	4.8	0.012	0
88ADw115V96	1.78899	0.03449	0.08707	0.0007	0.4170	538.2	4.4	2400.8	23.3	538.2	4.4	0.008	78
88ADw115V54	3.98693	0.04123	0.2544	0.00089	0.3387	1459.6	4.6	1841.3	40.3	1841.3	40.3	0.006	24
88ADw115V78	4.24177	0.09836	0.27054	0.00184	0.2933	1543.5	9.3	1902.6	20.9	1902.6	20.9	0.011	49

88ADw122dz, detrital zircons, n = 67 of 79, Univ. of British Columbia													
Analysis #	207/235	1σ error (%)	206/238	1σ error (%)	Error correlation	206/238 age	1σ error (Ma)	207/206 age	1σ error (Ma)	Best age (Ma)	1σ error (Ma)	Error/age	Discordance (%)
L28	0.09192	0.00364	0.01354	0.00017	0.3174	86.7	1.1	119.9	90.8	86.7	1.1	0.013	27.7
L29	0.09369	0.00224	0.01394	0.00011	0.3345	89.2	0.7	136.4	54.5	89.2	0.7	0.008	34.5
L22	0.09405	0.00193	0.01415	0.0001	0.3444	90.6	0.6	94.3	48.9	90.6	0.6	0.007	3.9
L24	0.09693	0.00449	0.0143	0.00021	0.3170	91.5	1.3	98.2	106.9	91.5	1.3	0.014	6.8
L36	0.09217	0.00316	0.01434	0.00016	0.3254	91.8	1.0	92.7	80.4	91.8	1.0	0.011	1.0
L14	0.09802	0.00212	0.01436	0.00011	0.3542	91.9	0.7	95.7	51.3	91.9	0.7	0.007	4.0
L45	0.09677	0.0036	0.0144	0.00016	0.2987	92.2	1.0	95.2	86.9	92.2	1.0	0.011	3.2
L10	0.0947	0.00591	0.01446	0.00027	0.2992	92.5	1.7	91.2	142.1	92.5	1.7	0.019	-1.4
L27	0.09601	0.00388	0.01449	0.00019	0.3245	92.7	1.2	97.9	93.7	92.7	1.2	0.013	5.3
L20	0.09553	0.00106	0.01449	0.00006	0.3732	92.7	0.4	101.3	26.0	92.7	0.4	0.004	8.5
L46	0.098	0.00284	0.01449	0.00014	0.3334	92.8	0.9	86.8	68.1	92.8	0.9	0.009	-6.9
L33	0.09254	0.00398	0.01452	0.00021	0.3363	92.9	1.3	101.2	98.7	92.9	1.3	0.014	8.2
L16	0.0979	0.00227	0.01454	0.00012	0.3559	93.0	0.7	95.1	54.9	93.0	0.7	0.008	2.2
L8	0.10137	0.00422	0.01455	0.0002	0.3302	93.1	1.3	100.9	94.5	93.1	1.3	0.014	7.7
L15	0.09687	0.00525	0.01456	0.00024	0.3041	93.2	1.6	95.4	124.0	93.2	1.6	0.017	2.3
L21	0.09543	0.00293	0.01457	0.00015	0.3353	93.2	1.0	98.9	72.0	93.2	1.0	0.010	5.8
L18	0.09714	0.00254	0.01461	0.00011	0.2879	93.5	0.7	95.0	61.8	93.5	0.7	0.008	1.6
L23	0.0967	0.00432	0.01461	0.00022	0.3371	93.5	1.4	95.3	103.2	93.5	1.4	0.015	1.9
L37	0.09698	0.00281	0.01461	0.00013	0.3071	93.5	0.9	101.7	67.0	93.5	0.9	0.009	8.1

Table 2. U-Pb analytical data for detrital and igneous zircons, identified by sample number and lab.—Continued

L11	0.10092	0.00478	0.01463	0.00021	0.3031	93.6	1.3	94.6	108.9	93.6	1.3	0.014	1.1
L9	0.09817	0.00238	0.01466	0.00012	0.3376	93.8	0.8	93.2	57.0	93.8	0.8	0.008	-0.6
L31	0.09783	0.00254	0.01472	0.00013	0.3402	94.2	0.8	95.9	61.3	94.2	0.8	0.008	1.8
L7	0.09585	0.00484	0.01475	0.00024	0.3222	94.4	1.6	94.2	115.8	94.4	1.6	0.016	-0.2
L53	0.09919	0.00411	0.01477	0.00019	0.3105	94.5	1.2	101.3	95.1	94.5	1.2	0.013	6.7
L52	0.09723	0.0032	0.01481	0.00016	0.3283	94.8	1.0	93.1	77.1	94.8	1.0	0.011	-1.8
L55	0.09854	0.00393	0.01484	0.00019	0.3210	95.0	1.2	90.7	92.8	95.0	1.2	0.013	-4.7
L12	0.10154	0.00359	0.01488	0.00018	0.3421	95.2	1.1	98.3	82.0	95.2	1.1	0.012	3.2
L60	0.09785	0.00349	0.01487	0.00017	0.3205	95.2	1.1	100.4	82.4	95.2	1.1	0.011	5.2
L6	0.09659	0.00394	0.0149	0.00021	0.3455	95.4	1.3	94.3	94.2	95.4	1.3	0.014	-1.2
L43	0.10165	0.00559	0.0149	0.00023	0.2807	95.4	1.5	97.2	126.3	95.4	1.5	0.015	1.9
L44	0.10114	0.00275	0.01494	0.00013	0.3200	95.6	0.8	103.1	62.9	95.6	0.8	0.009	7.3
L39	0.10384	0.00304	0.01496	0.00013	0.2997	95.7	0.8	228.0	65.5	95.7	0.8	0.009	58.0
L49	0.09793	0.00303	0.01497	0.00016	0.3454	95.8	1.0	103.8	71.5	95.8	1.0	0.010	7.7
L64	0.09987	0.00372	0.01497	0.00019	0.3407	95.8	1.2	110.8	85.7	95.8	1.2	0.012	13.5
L62	0.09795	0.00409	0.01507	0.0002	0.3178	96.5	1.3	97.1	97.3	96.5	1.3	0.013	0.6
L47	0.10153	0.00198	0.01511	0.0001	0.3394	96.7	0.6	103.4	45.2	96.7	0.6	0.007	6.5
L40	0.09978	0.00498	0.01511	0.00022	0.2917	96.7	1.4	104.2	113.8	96.7	1.4	0.014	7.2
L5	0.09996	0.00469	0.01517	0.00022	0.3091	97.1	1.4	96.3	107.9	97.1	1.4	0.014	-0.8
L72	0.09911	0.0101	0.01524	0.00042	0.2704	97.5	2.7	101.2	225.5	97.5	2.7	0.027	3.7
L48	0.10053	0.00222	0.01528	0.00012	0.3556	97.8	0.7	98.6	52.4	97.8	0.7	0.007	0.8
L58	0.10295	0.00254	0.01528	0.00013	0.3448	97.8	0.8	103.1	57.1	97.8	0.8	0.008	5.1
L2	0.1033	0.00383	0.01531	0.00018	0.3171	98.0	1.2	102.3	84.3	98.0	1.2	0.012	4.2
L57	0.10462	0.00494	0.01532	0.00024	0.2903	98.0	1.3	234.6	105.5	98.0	1.3	0.014	58.2
L68	0.11056	0.00380	0.01536	0.00018	0.3334	98.3	1.4	342.7	77.7	98.3	1.4	0.011	71.3
L41	0.10022	0.0031	0.01538	0.00014	0.2943	98.4	0.9	101.3	71.4	98.4	0.9	0.009	2.9
L1	0.10217	0.00284	0.01543	0.00014	0.3264	98.7	0.9	105.2	63.8	98.7	0.9	0.009	6.2
L70	0.10116	0.00313	0.01548	0.00015	0.3132	99.0	1.0	94.1	72.7	99.0	1.0	0.010	-5.2
L56	0.10137	0.00553	0.01551	0.00027	0.3191	99.2	1.7	103.5	124.0	99.2	1.7	0.017	4.2
L69	0.11502	0.00444	0.01560	0.0002	0.3302	100.3	1.3	284.5	85.6	100.3	1.3	0.013	64.7
L17	0.10867	0.00526	0.01573	0.00024	0.3152	100.6	1.5	105.6	109.4	100.6	1.5	0.015	4.7
L82	0.10879	0.0044	0.01576	0.0002	0.3138	100.8	1.3	106.4	92.7	100.8	1.3	0.013	5.3
L80	0.10295	0.0052	0.01589	0.00025	0.3115	101.6	1.6	101.8	115.5	101.6	1.6	0.016	0.2
L75	0.10987	0.00921	0.01589	0.00044	0.3303	101.7	2.8	97.6	188.2	101.7	2.8	0.027	-4.2
L67	0.11034	0.00220	0.01595	0.00012	0.3624	102.0	0.8	235.0	47.0	102.0	0.8	0.008	56.6
L79	0.10685	0.00382	0.01597	0.00019	0.3328	102.1	1.2	108.2	82.2	102.1	1.2	0.012	5.6
L66	0.10643	0.00425	0.01597	0.00021	0.3293	102.1	1.3	111.2	91.6	102.1	1.3	0.013	8.2
L64	0.10713	0.00579	0.01604	0.00027	0.3115	102.6	1.7	108.6	122.7	102.6	1.7	0.017	5.5
L81	0.1052	0.00942	0.01607	0.00039	0.2710	102.8	2.5	102.8	199.6	102.8	2.5	0.024	0.0
L93	0.10985	0.00608	0.01608	0.0003	0.3374	102.8	1.9	244.8	122.9	102.8	1.9	0.018	58.0
L63	0.11238	0.00672	0.0162	0.0003	0.3097	103.6	1.9	106.8	135.0	103.6	1.9	0.018	3.0
L76	0.10705	0.00359	0.01622	0.00019	0.3493	103.7	1.2	108.7	77.1	103.7	1.2	0.011	4.6
L71	0.10743	0.00339	0.01623	0.00017	0.3319	103.8	1.1	107.3	72.7	103.8	1.1	0.011	3.3
L78	0.1088	0.00532	0.01629	0.00024	0.3013	104.2	1.5	107.8	111.6	104.2	1.5	0.014	3.3
L73	0.11188	0.00428	0.01635	0.00021	0.3357	104.5	1.4	105.4	87.7	104.5	1.4	0.013	0.9
L4	0.10949	0.004	0.0165	0.00019	0.3152	105.5	1.2	110.0	82.7	105.5	1.2	0.012	4.1
L77	0.10847	0.00464	0.0165	0.00023	0.3259	105.5	1.5	164.4	97.0	105.5	1.5	0.014	35.8
L74	0.10595	0.00626	0.01651	0.00033	0.3383	105.6	2.1	113.3	133.8	105.6	2.1	0.020	6.8
L35	0.14289	0.0084	0.02112	0.00037	0.2980	134.7	2.3	145.9	129.8	134.7	2.3	0.017	7.7
L30	0.15558	0.00359	0.02275	0.00017	0.3238	145.0	1.0	147.2	51.7	145.0	1.0	0.007	1.5
L32	0.16167	0.00555	0.0232	0.00026	0.3265	147.8	1.6	157.2	75.6	147.8	1.6	0.011	6.0
L50	0.16987	0.00467	0.02436	0.00022	0.3285	155.2	1.4	163.7	60.8	155.2	1.4	0.009	5.2
L59	0.16739	0.00741	0.02501	0.00033	0.2981	159.3	2.1	169.2	97.8	159.3	2.1	0.013	5.9
L54	0.17499	0.00781	0.02582	0.00033	0.2864	164.3	2.1	176.7	98.5	164.3	2.1	0.012	7.0
L19	0.47449	0.01416	0.02626	0.00037	0.4724	167.4	2.3	2184.2	46.5	167.4	2.3	0.014	92.3
L34	0.19265	0.00784	0.02748	0.00034	0.3040	174.8	2.1	176.4	88.2	174.8	2.1	0.012	0.9
L13	0.18833	0.0024	0.0275	0.00013	0.3710	174.9	0.8	174.2	27.8	174.9	0.8	0.005	-0.4
L42	0.19707	0.01089	0.02855	0.00047	0.2979	181.5	2.9	188.1	118.6	181.5	2.9	0.016	3.5
L38	0.39477	0.01334	0.02963	0.00039	0.3904	188.2	2.4	1550.2	57.3	188.2	2.4	0.013	87.9
L65	0.20568	0.00267	0.03002	0.00015	0.3849	190.7	0.9	192.1	28.0	190.7	0.9	0.005	0.7

04ADw600a, detrital zircons, n = 24, Univ. of British Columbia

Analysis #	207/235	1 σ error (%)	206/238	1 σ error (%)	Error cor- relation	206/238 age	1 σ error (Ma)	207/206 age	1 σ error (Ma)	Best age (Ma)	1 σ error (Ma)	Error/age	Dis- cordance (%)
04ADW600A13	0.24198	0.04575	0.02127	0.00101	0.2512	136.7	6.4	1225.9	335.7	136.7	6.4	0.047	
04ADW600A19	0.15821	0.0222	0.02208	0.00058	0.1872	140.8	3.6	380.0	288.4	140.8	3.6	0.026	
04ADW600A23	0.17383	0.04017	0.02234	0.0009	0.1743	142.4	5.7	480.0	444.1	142.4	5.7	0.040	
04ADW600A2	0.10438	0.0259	0.02303	0.00065	0.1137	146.8	4.1	0.1	0.0	146.8	4.1	0.028	
04ADW600A15	0.16808	0.02797	0.02309	0.00066	0.1718	147.2	4.2	276.6	342.4	147.2	4.2	0.028	
04ADW600A12	0.14242	0.03303	0.0232	0.00074	0.1375	147.9	4.7	0.1	433.2	147.9	4.7	0.032	

Table 2. U-Pb analytical data for detrital and igneous zircons, identified by sample number and lab.—Continued

04ADW600A1	0.15508	0.00814	0.0233	0.00026	0.2126	148.5	1.7	102.5	119.4	148.5	1.7	0.011
04ADW600A10	0.14181	0.02089	0.02333	0.00054	0.1571	148.6	3.4	0.1	204.7	148.6	3.4	0.023
04ADW600A22	0.16148	0.00867	0.02347	0.00034	0.2698	149.6	2.1	240.1	116.8	149.6	2.1	0.014
04ADW600A7	0.12154	0.02699	0.02368	0.00068	0.1293	150.9	4.3	0.1	0.0	150.9	4.3	0.028
04ADW600A6	0.15166	0.01752	0.02377	0.00049	0.1784	151.4	3.1	44.6	255.7	151.4	3.1	0.020
04ADW600A18	0.15515	0.00705	0.02388	0.00026	0.2396	152.1	1.7	4.2	103.6	152.1	1.7	0.011
04ADW600A20	0.11689	0.03398	0.02391	0.00072	0.1036	152.3	4.5	0.1	0.0	152.3	4.5	0.030
04ADW600A3	0.15589	0.00946	0.02398	0.00031	0.2130	152.8	1.9	35.5	139.2	152.8	1.9	0.013
04ADW600A17	0.24599	0.02939	0.02415	0.00066	0.2287	153.8	4.2	1018.6	223.9	153.8	4.2	0.027
04ADW600A4	0.15447	0.01086	0.02424	0.00035	0.2054	154.4	2.2	71.8	159.6	154.4	2.2	0.014
04ADW600A8	0.16892	0.02324	0.02437	0.00063	0.1879	155.2	4.0	314.6	286.7	155.2	4.0	0.026
04ADW600A5	0.09203	0.06063	0.02441	0.00117	0.0728	155.4	7.4	0.1	0.0	155.4	7.4	0.047
04ADW600A14	0.16141	0.01142	0.02439	0.00038	0.2202	155.4	2.4	111.8	157.8	155.4	2.4	0.015
04ADW600A21	0.16679	0.02254	0.02441	0.00058	0.1758	155.5	3.6	133.7	289.0	155.5	3.6	0.023
04ADW600A11	0.11587	0.02384	0.02486	0.00056	0.1095	158.3	3.5	0.1	0.0	158.3	3.5	0.022
04ADW600A16	0.20379	0.05176	0.02489	0.00113	0.1787	158.5	7.4	553.9	476.4	158.5	7.4	0.045
04ADW600A9	0.16652	0.02538	0.02496	0.00066	0.1735	158.9	4.1	159.6	321.9	158.9	4.1	0.026
04ADW600A24	0.17675	0.01604	0.02513	0.00051	0.2236	160.0	3.2	222.0	195.1	160.0	3.2	0.020
05PH105a, detrital zircons, n = 98 of 100, Apatite to Zircon, Inc.												
Analysis #	207/235	2σ error (%)	206/238	2σ error (%)	206/238 age	2σ error (Ma)	207/206 age	2σ error (Ma)	Best age (Ma)	2σ error (Ma)	Error/age	Dis- cordance (%)
84905-100	0.0855	0.0251	0.0130	0.0011	83.6	7.0	75.9	23.1	83.6	7.0	0.152	-10.07%
84905-48	0.0889	0.0155	0.0135	0.0006	86.2	3.6	92.8	16.6	86.2	3.6	0.089	7.07%
84905-65	0.0902	0.0179	0.0137	0.0006	87.5	4.1	94.4	19.1	87.5	4.1	0.101	7.34%
84905-72	0.0907	0.0083	0.0137	0.0004	87.9	2.8	93.4	8.9	87.9	2.8	0.047	5.86%
84905-55	0.0922	0.0152	0.0140	0.0006	89.3	3.6	95.7	16.1	89.3	3.6	0.084	6.65%
84905-39	0.0929	0.0113	0.0141	0.0005	90.0	3.5	94.4	11.8	90.0	3.5	0.063	4.62%
84905-52	0.0933	0.0142	0.0141	0.0004	90.3	2.8	94.5	14.6	90.3	2.8	0.077	4.37%
84905-27	0.0945	0.0167	0.0143	0.0008	91.3	5.3	101.3	18.8	91.3	5.3	0.093	9.89%
84905-5	0.0944	0.0112	0.0143	0.0004	91.4	2.4	94.8	11.5	91.4	2.4	0.060	3.64%
84905-3	0.0963	0.0111	0.0146	0.0005	93.2	3.2	97.8	11.7	93.2	3.2	0.060	4.76%
84905-18	0.0966	0.0169	0.0146	0.0007	93.3	4.8	101.5	18.4	93.3	4.8	0.090	8.01%
84905-36	0.0966	0.0150	0.0146	0.0007	93.4	4.5	100.7	16.2	93.4	4.5	0.080	7.26%
84905-54	0.0968	0.0155	0.0146	0.0005	93.6	3.4	98.4	16.0	93.6	3.4	0.081	4.90%
84905-47	0.0967	0.0202	0.0147	0.0008	93.8	5.0	92.0	19.7	93.8	5.0	0.107	-1.96%
84905-7	0.0974	0.0101	0.0147	0.0005	94.1	3.1	97.5	10.3	94.1	3.1	0.053	3.47%
84905-31	0.0982	0.0132	0.0148	0.0005	94.8	3.0	100.8	13.8	94.8	3.0	0.069	5.95%
84905-97	0.0981	0.0064	0.0148	0.0004	94.9	2.2	97.2	6.5	94.9	2.2	0.033	2.41%
84905-98	0.0983	0.0106	0.0148	0.0004	95.0	2.4	99.6	10.9	95.0	2.4	0.055	4.68%
84905-88	0.0987	0.0094	0.0149	0.0005	95.4	3.0	100.6	9.8	95.4	3.0	0.049	5.16%
84905-80	0.0991	0.0084	0.0150	0.0004	95.8	2.3	97.4	8.5	95.8	2.3	0.044	1.56%
84905-14	0.0994	0.0136	0.0150	0.0008	95.9	5.2	106.0	15.2	95.9	5.2	0.072	9.54%
84905-84	0.1001	0.0090	0.0151	0.0005	96.7	2.9	101.4	9.4	96.7	2.9	0.046	4.66%
84905-62	0.1001	0.0081	0.0151	0.0004	96.7	2.2	99.5	8.3	96.7	2.2	0.042	2.80%
84905-9	0.1002	0.0132	0.0151	0.0004	96.9	2.9	100.0	13.3	96.9	2.9	0.067	3.08%
84905-96	0.1003	0.0061	0.0151	0.0003	96.9	2.0	99.2	6.2	96.9	2.0	0.031	2.32%
84905-13	0.1004	0.0068	0.0152	0.0003	97.0	2.0	99.8	6.9	97.0	2.0	0.035	2.85%
84905-56	0.1008	0.0135	0.0152	0.0008	97.2	4.9	105.9	14.9	97.2	4.9	0.070	8.22%
84905-73	0.1011	0.0234	0.0152	0.0009	97.4	5.6	107.4	25.5	97.4	5.6	0.119	9.27%
84905-16	0.1011	0.0101	0.0153	0.0005	97.6	3.0	103.2	10.6	97.6	3.0	0.051	5.39%
84905-63	0.1013	0.0182	0.0153	0.0007	97.7	4.3	103.3	18.9	97.7	4.3	0.091	5.39%
84905-78	0.1013	0.0058	0.0153	0.0003	97.8	1.9	100.8	6.0	97.8	1.9	0.030	2.95%
84905-23	0.1016	0.0134	0.0153	0.0005	98.0	3.1	101.0	13.6	98.0	3.1	0.067	2.97%
84905-24	0.1019	0.0131	0.0154	0.0005	98.3	3.1	101.9	13.4	98.3	3.1	0.066	3.59%
84905-95	0.1024	0.0070	0.0154	0.0004	98.8	2.3	100.7	7.0	98.8	2.3	0.035	1.91%
84905-12	0.1024	0.0070	0.0154	0.0004	98.8	2.3	100.7	7.0	98.8	2.3	0.035	1.91%
84905-49	0.1027	0.0144	0.0155	0.0007	98.8	4.6	107.4	15.3	98.8	4.6	0.071	7.93%
84905-8	0.1026	0.0114	0.0155	0.0004	99.0	2.5	101.3	11.4	99.0	2.5	0.056	2.31%
84905-53	0.1028	0.0074	0.0155	0.0004	99.1	2.4	103.2	7.7	99.1	2.4	0.037	3.90%
84905-61	0.1029	0.0085	0.0155	0.0003	99.3	1.9	101.9	8.6	99.3	1.9	0.042	2.59%
84905-75	0.1031	0.0096	0.0156	0.0005	99.5	3.0	102.9	10.0	99.5	3.0	0.048	3.35%
84905-11	0.1032	0.0075	0.0156	0.0003	99.7	1.8	100.6	7.4	99.7	1.8	0.037	0.88%
84905-94	0.1033	0.0063	0.0156	0.0003	99.7	2.1	102.6	6.5	99.7	2.1	0.031	2.87%
84905-85	0.1035	0.0081	0.0156	0.0003	99.9	2.2	102.5	8.3	99.9	2.2	0.040	2.62%
84905-20	0.1037	0.0155	0.0156	0.0006	99.9	4.2	107.4	16.5	99.9	4.2	0.077	7.00%
84905-64	0.1034	0.0077	0.0156	0.0003	100.0	1.9	96.2	7.3	100.0	1.9	0.038	-3.94%
84905-45	0.1038	0.0220	0.0156	0.0008	100.0	5.0	104.7	22.6	100.0	5.0	0.108	4.44%
84905-58	0.1039	0.0083	0.0157	0.0004	100.2	2.8	104.5	8.7	100.2	2.8	0.042	4.07%
84905-83	0.1042	0.0094	0.0157	0.0003	100.4	2.1	102.8	9.5	100.4	2.1	0.046	2.26%
84905-50	0.1043	0.0089	0.0157	0.0004	100.5	2.8	105.9	9.4	100.5	2.8	0.044	5.08%
84905-69	0.1045	0.0104	0.0157	0.0005	100.7	3.1	105.0	10.7	100.7	3.1	0.051	4.08%

Table 2. U-Pb analytical data for detrital and igneous zircons, identified by sample number and lab.—Continued

84905-67	0.1049	0.0104	0.0158	0.0004	101.1	2.8	104.6	10.7	101.1	2.8	0.051	3.33%
84905-93	0.1051	0.0277	0.0158	0.0005	101.2	3.2	104.9	27.8	101.2	3.2	0.132	3.53%
84905-1	0.1050	0.0090	0.0158	0.0004	101.3	2.2	104.5	9.2	101.3	2.2	0.044	3.09%
84905-79	0.1052	0.0079	0.0159	0.0004	101.4	2.8	107.0	8.3	101.4	2.8	0.039	5.23%
84905-10	0.1052	0.0121	0.0159	0.0005	101.4	3.2	106.5	12.6	101.4	3.2	0.059	4.82%
84905-25	0.1060	0.0131	0.0159	0.0006	102.0	4.0	109.9	14.0	102.0	4.0	0.064	7.25%
84905-57	0.1066	0.0091	0.0161	0.0005	102.7	2.9	105.9	9.3	102.7	2.9	0.044	3.00%
84905-74	0.1072	0.0113	0.0161	0.0004	103.3	2.4	105.3	11.3	103.3	2.4	0.054	1.92%
84905-99	0.1083	0.0285	0.0163	0.0005	104.2	3.3	110.0	29.1	104.2	3.3	0.132	5.33%
84905-81	0.1091	0.0082	0.0164	0.0004	104.9	2.3	109.0	8.4	104.9	2.3	0.039	3.78%
84905-68	0.1095	0.0121	0.0165	0.0006	105.3	3.6	110.0	12.5	105.3	3.6	0.057	4.28%
84905-70	0.1098	0.0142	0.0165	0.0005	105.7	3.3	108.2	14.2	105.7	3.3	0.066	2.28%
84905-91	0.1096	0.0076	0.0165	0.0004	105.7	2.4	101.7	7.2	105.7	2.4	0.035	-3.98%
84905-90	0.1114	0.0109	0.0167	0.0004	107.0	2.8	111.4	11.1	107.0	2.8	0.050	3.98%
84905-89	0.1115	0.0169	0.0167	0.0007	107.1	4.3	113.5	17.7	107.1	4.3	0.078	5.68%
84905-2	0.1145	0.0243	0.0172	0.0008	109.7	5.2	118.5	25.5	109.7	5.2	0.108	7.46%
84905-43	0.1146	0.0219	0.0172	0.0009	110.2	6.0	110.6	21.8	110.2	6.0	0.098	0.42%
84905-44	0.1187	0.0125	0.0178	0.0006	113.6	3.7	118.6	13.0	113.6	3.7	0.055	4.18%
84905-41	0.1199	0.0243	0.0179	0.0015	114.1	9.8	131.8	28.3	114.1	9.8	0.107	13.39%
84905-37	0.1337	0.0211	0.0199	0.0008	126.9	5.3	137.0	22.3	126.9	5.3	0.081	7.41%
84905-34	0.1337	0.0155	0.0200	0.0007	127.5	4.3	126.0	15.1	127.5	4.3	0.060	-1.14%
84905-22	0.1363	0.0348	0.0204	0.0014	130.2	8.9	120.0	31.4	130.2	8.9	0.131	-8.47%
84905-26	0.1363	0.0348	0.0204	0.0014	130.2	8.9	120.0	31.4	130.2	8.9	0.131	-8.47%
84905-86	0.1444	0.0028	0.0214	0.0003	136.6	1.9	140.1	2.6	136.6	1.9	0.009	2.47%
84905-87	0.1454	0.0030	0.0216	0.0003	137.5	2.0	141.3	2.8	137.5	2.0	0.010	2.70%
84905-30	0.1523	0.0128	0.0225	0.0006	143.5	3.7	150.5	13.1	143.5	3.7	0.044	4.65%
84905-32	0.1536	0.0153	0.0227	0.0007	144.8	4.3	150.5	15.5	144.8	4.3	0.051	3.77%
84905-28	0.1548	0.0185	0.0229	0.0006	145.7	4.1	151.5	18.4	145.7	4.1	0.061	3.87%
84905-29	0.1590	0.0146	0.0234	0.0006	149.4	3.9	156.2	14.8	149.4	3.9	0.047	4.33%
84905-40	0.1615	0.0070	0.0238	0.0005	151.7	3.3	156.7	7.1	151.7	3.3	0.023	3.21%
84905-38	0.1620	0.0192	0.0238	0.0010	151.8	6.1	162.1	19.9	151.8	6.1	0.061	6.38%
84905-4	0.1625	0.0076	0.0239	0.0004	152.5	2.7	157.1	7.5	152.5	2.7	0.024	2.93%
84905-42	0.1655	0.0096	0.0244	0.0006	155.1	4.1	162.1	9.6	155.1	4.1	0.030	4.33%
84905-6	0.1658	0.0174	0.0244	0.0007	155.3	4.3	163.0	17.6	155.3	4.3	0.054	4.78%
84905-60	0.1670	0.0176	0.0245	0.0006	156.3	4.1	162.8	17.5	156.3	4.1	0.054	3.99%
84905-17	0.2080	0.0170	0.0301	0.0008	191.1	5.1	200.7	17.0	191.1	5.1	0.042	4.78%
84905-66	0.2224	0.0119	0.0320	0.0009	203.1	5.4	212.6	11.8	203.1	5.4	0.028	4.43%
84905-21	0.5163	0.0202	0.0674	0.0011	420.4	7.1	433.3	17.4	420.4	7.1	0.020	2.99%
84905-77	0.5565	0.0148	0.0718	0.0010	447.1	6.0	458.5	12.4	447.1	6.0	0.014	2.49%
84905-71	0.5729	0.0147	0.0736	0.0010	457.8	6.3	468.4	12.2	457.8	6.3	0.013	2.28%
84905-76	0.6419	0.0214	0.0805	0.0017	499.3	10.6	520.5	18.6	499.3	10.6	0.018	4.06%
84905-59	0.7114	0.0177	0.0877	0.0015	541.9	9.3	558.8	14.9	541.9	9.3	0.013	3.02%
84905-51	0.7037	0.0227	0.0879	0.0025	543.0	15.6	532.8	17.4	543.0	15.6	0.016	-1.92%
84905-19	0.8268	0.0397	0.1002	0.0021	615.5	12.7	597.0	29.2	615.5	12.7	0.024	-3.10%
84905-46	1.2810	0.0345	0.1375	0.0020	830.4	12.0	853.8	24.0	830.4	12.0	0.014	2.74%
84905-92	3.9392	0.0604	0.2827	0.0032	1605.2	18.3	1641.7	24.7	1641.7	24.7	0.008	2.23%
84905-15	4.2811	0.0955	0.3037	0.0048	1709.5	27.1	1665.5	37.7	1665.5	37.7	0.011	-2.64%
84905-82	4.2551	0.0660	0.2952	0.0033	1667.6	18.9	1704.4	26.2	1704.4	26.2	0.008	2.16%
84905-33	4.3843	0.0776	0.3038	0.0038	1710.3	21.3	1707.8	31.1	1707.8	31.1	0.009	-0.14%
84905-35	4.9230	0.1644	0.3177	0.0068	1778.3	38.2	1837.4	60.1	1837.4	60.1	0.016	3.22%
05ADw305a, detrital zircons, n = 100 of 100, Apatite to Zircon, Inc.												
Analysis #	207/235	2σ error (%)	206/238	2σ error (%)	206/238 age	2σ error (Ma)	207/206 age	2σ error (Ma)	Best age (Ma)	2σ error (Ma)	Error/age	Dis- cordance (%)
84903-94	0.1265	0.0183	0.0189	0.0011	120.7	6.7	125.9	19.3	120.7	6.7	0.077	4.13%
84903-17	0.1292	0.0134	0.0193	0.0005	123.2	3.5	128.2	13.6	123.2	3.5	0.053	3.91%
84903-87	0.1359	0.0099	0.0202	0.0005	129.2	3.2	132.8	10.0	129.2	3.2	0.038	2.68%
84903-36	0.1380	0.0181	0.0205	0.0009	130.7	5.5	141.3	19.3	130.7	5.5	0.068	7.48%
84903-8	0.1379	0.0273	0.0205	0.0011	130.7	6.7	141.3	28.8	130.7	6.7	0.102	7.47%
84903-42	0.1390	0.0111	0.0207	0.0005	131.9	2.9	136.6	11.1	131.9	2.9	0.041	3.42%
84903-62	0.1397	0.0170	0.0208	0.0006	132.4	3.9	139.9	17.3	132.4	3.9	0.062	5.35%
84903-83	0.1396	0.0102	0.0208	0.0005	132.5	3.3	137.0	10.4	132.5	3.3	0.038	3.33%
84903-11	0.1410	0.0285	0.0210	0.0011	133.9	6.7	134.1	27.7	133.9	6.7	0.103	0.09%
84903-74	0.1419	0.0126	0.0210	0.0007	134.3	4.5	143.1	13.3	134.3	4.5	0.046	6.14%
84903-76	0.1431	0.0283	0.0212	0.0011	135.2	6.9	146.4	29.8	135.2	6.9	0.102	7.65%
84903-66	0.1440	0.0097	0.0214	0.0005	136.3	3.3	142.6	9.8	136.3	3.3	0.034	4.41%
84903-95	0.1453	0.0158	0.0217	0.0005	138.1	2.9	132.2	14.6	138.1	2.9	0.055	-4.44%
84903-90	0.1465	0.0145	0.0217	0.0006	138.5	3.7	144.8	14.7	138.5	3.7	0.051	4.35%
84903-39	0.1466	0.0127	0.0217	0.0007	138.5	4.2	145.1	12.9	138.5	4.2	0.044	4.54%
84903-16	0.1476	0.0180	0.0219	0.0007	139.4	4.6	146.9	18.4	139.4	4.6	0.063	5.14%
84903-69	0.1488	0.0074	0.0221	0.0003	140.7	2.2	144.2	7.3	140.7	2.2	0.025	2.43%
84903-1	0.1500	0.0226	0.0222	0.0010	141.3	6.5	153.1	23.9	141.3	6.5	0.078	7.73%

Table 2. U-Pb analytical data for detrital and igneous zircons, identified by sample number and lab.—Continued

84903-88	0.1497	0.0068	0.0222	0.0004	141.4	2.4	145.6	6.8	141.4	2.4	0.023	2.87%
84903-85	0.1504	0.0149	0.0223	0.0006	142.0	3.8	147.0	15.0	142.0	3.8	0.051	3.43%
84903-35	0.1517	0.0154	0.0224	0.0007	143.0	4.4	150.7	15.8	143.0	4.4	0.052	5.09%
84903-49	0.1523	0.0333	0.0225	0.0013	143.8	8.0	148.3	33.1	143.8	8.0	0.112	3.08%
84903-13	0.1529	0.0202	0.0226	0.0009	143.9	5.6	154.9	21.1	143.9	5.6	0.068	7.08%
84903-91	0.1526	0.0098	0.0226	0.0005	144.0	3.0	147.9	9.9	144.0	3.0	0.033	2.66%
84903-97	0.1531	0.0234	0.0226	0.0008	144.0	5.4	154.1	24.1	144.0	5.4	0.078	6.54%
84903-38	0.1520	0.0118	0.0226	0.0005	144.1	3.5	137.1	11.0	144.1	3.5	0.040	-5.10%
84903-65	0.1543	0.0182	0.0228	0.0007	145.2	4.7	154.4	18.7	145.2	4.7	0.060	5.99%
84903-70	0.1557	0.0109	0.0230	0.0005	146.7	3.1	152.3	11.0	146.7	3.1	0.036	3.69%
84903-24	0.1564	0.0163	0.0231	0.0008	147.1	4.9	154.7	16.8	147.1	4.9	0.054	4.92%
84903-45	0.1582	0.0128	0.0233	0.0006	148.7	4.0	156.3	13.1	148.7	4.0	0.042	4.90%
84903-52	0.1590	0.0120	0.0234	0.0007	149.4	4.2	157.5	12.2	149.4	4.2	0.039	5.12%
84903-30	0.1584	0.0156	0.0235	0.0008	149.9	4.8	140.0	14.3	149.9	4.8	0.051	-7.06%
84903-99	0.1594	0.0188	0.0235	0.0006	149.9	4.1	155.0	18.7	149.9	4.1	0.060	3.31%
84903-92	0.1599	0.0158	0.0236	0.0008	150.1	5.1	158.2	16.3	150.1	5.1	0.052	5.14%
84903-47	0.1601	0.0115	0.0236	0.0006	150.5	3.6	155.2	11.5	150.5	3.6	0.037	2.99%
84903-56	0.1625	0.0303	0.0239	0.0010	152.3	6.4	163.9	31.1	152.3	6.4	0.095	7.10%
84903-78	0.1637	0.0185	0.0241	0.0010	153.4	6.6	162.4	18.9	153.4	6.6	0.058	5.54%
84903-84	0.1632	0.0135	0.0242	0.0006	153.9	4.1	148.7	12.5	153.9	4.1	0.042	-3.47%
84903-23	0.1657	0.0229	0.0243	0.0013	154.8	8.1	169.3	24.3	154.8	8.1	0.072	8.56%
84903-25	0.1676	0.0178	0.0246	0.0008	156.9	5.0	164.2	18.0	156.9	5.0	0.055	4.44%
84903-73	0.1684	0.0145	0.0247	0.0007	157.6	4.4	166.1	14.8	157.6	4.4	0.044	5.14%
84903-50	0.1689	0.0095	0.0248	0.0006	157.9	3.9	164.3	9.6	157.9	3.9	0.029	3.87%
84903-64	0.1692	0.0124	0.0249	0.0007	158.3	4.2	165.3	12.6	158.3	4.2	0.038	4.24%
84903-3	0.1693	0.0116	0.0249	0.0006	158.4	3.6	165.0	11.6	158.4	3.6	0.035	3.94%
84903-100	0.1701	0.0272	0.0250	0.0011	158.9	7.1	168.5	27.9	158.9	7.1	0.083	5.68%
84903-67	0.1746	0.0390	0.0255	0.0014	162.4	9.0	178.5	40.7	162.4	9.0	0.114	9.06%
84903-5	0.1747	0.0610	0.0256	0.0018	163.1	11.2	169.5	60.2	163.1	11.2	0.178	3.77%
84903-86	0.1764	0.0137	0.0258	0.0007	164.5	4.5	172.1	13.7	164.5	4.5	0.040	4.45%
84903-40	0.1794	0.0193	0.0262	0.0011	166.9	6.7	178.1	19.8	166.9	6.7	0.056	6.27%
84903-22	0.1791	0.0120	0.0263	0.0005	167.1	3.1	171.5	11.8	167.1	3.1	0.034	2.60%
84903-41	0.1804	0.0203	0.0264	0.0009	168.2	5.9	171.5	19.8	168.2	5.9	0.058	1.91%
84903-51	0.1812	0.0098	0.0266	0.0005	169.0	3.0	172.3	9.5	169.0	3.0	0.028	1.91%
84903-6	0.1818	0.0074	0.0267	0.0004	169.6	2.2	171.3	7.2	169.6	2.2	0.021	1.00%
84903-82	0.1826	0.0151	0.0267	0.0008	169.7	4.8	178.7	15.0	169.7	4.8	0.042	5.01%
84903-48	0.1841	0.0203	0.0269	0.0008	171.1	5.0	179.0	20.1	171.1	5.0	0.056	4.41%
84903-57	0.1847	0.0186	0.0269	0.0009	171.3	5.9	182.4	19.1	171.3	5.9	0.052	6.08%
84903-46	0.1832	0.0176	0.0270	0.0010	171.7	6.1	159.3	15.9	171.7	6.1	0.050	-7.77%
84903-71	0.1855	0.0203	0.0271	0.0007	172.3	4.5	180.5	20.1	172.3	4.5	0.056	4.55%
84903-34	0.1854	0.0119	0.0272	0.0006	172.9	3.7	170.7	11.3	172.9	3.7	0.033	-1.30%
84903-19	0.1880	0.0141	0.0274	0.0011	174.2	6.8	185.9	14.5	174.2	6.8	0.039	6.30%
84903-37	0.1866	0.0109	0.0274	0.0006	174.3	3.6	167.1	10.1	174.3	3.6	0.030	-4.29%
84903-32	0.1884	0.0218	0.0275	0.0008	174.7	5.2	183.1	21.4	174.7	5.2	0.058	4.60%
84903-44	0.1899	0.0134	0.0277	0.0006	176.2	4.1	182.2	13.1	176.2	4.1	0.036	3.27%
84903-33	0.1914	0.0118	0.0279	0.0005	177.7	3.2	181.4	11.5	177.7	3.2	0.032	2.07%
84903-54	0.1937	0.0147	0.0282	0.0007	179.3	4.7	187.2	14.4	179.3	4.7	0.038	4.25%
84903-53	0.1957	0.0113	0.0285	0.0007	181.0	4.2	189.2	11.3	181.0	4.2	0.030	4.34%
84903-93	0.1957	0.0134	0.0285	0.0007	181.1	4.6	186.4	13.1	181.1	4.6	0.035	2.82%
84903-18	0.1966	0.0149	0.0286	0.0007	181.8	4.3	188.1	14.6	181.8	4.3	0.039	3.36%
84903-59	0.1968	0.0091	0.0287	0.0005	182.2	3.0	186.1	8.8	182.2	3.0	0.024	2.10%
84903-80	0.1970	0.0057	0.0287	0.0003	182.3	2.2	186.5	5.6	182.3	2.2	0.015	2.26%
84903-15	0.1969	0.0187	0.0287	0.0007	182.5	4.5	183.5	17.8	182.5	4.5	0.049	0.55%
84903-20	0.2036	0.0178	0.0295	0.0010	187.4	6.3	198.7	17.8	187.4	6.3	0.045	5.70%
84903-77	0.2041	0.0080	0.0297	0.0005	188.6	3.0	189.1	7.7	188.6	3.0	0.020	0.27%
84903-28	0.2074	0.0183	0.0301	0.0007	190.9	4.4	197.0	17.7	190.9	4.4	0.045	3.09%
84903-72	0.2087	0.0348	0.0301	0.0017	191.0	10.6	211.5	35.5	191.0	10.6	0.084	9.70%
84903-61	0.2084	0.0099	0.0302	0.0006	191.9	3.6	197.0	9.6	191.9	3.6	0.024	2.59%
84903-4	0.2156	0.0347	0.0311	0.0014	197.5	9.1	206.7	34.4	197.5	9.1	0.083	4.43%
84903-26	0.2182	0.0209	0.0315	0.0007	199.8	4.3	208.0	20.3	199.8	4.3	0.049	3.93%
84903-29	0.2179	0.0042	0.0315	0.0004	200.1	2.6	202.3	4.0	200.1	2.6	0.010	1.10%
84903-31	0.2330	0.0205	0.0334	0.0009	211.9	5.8	221.0	20.1	211.9	5.8	0.045	4.08%
84903-98	1.4581	0.0468	0.1498	0.0038	900.1	22.9	945.5	32.5	900.1	22.9	0.017	4.80%
84903-55	1.4414	0.0367	0.1509	0.0027	905.9	16.3	908.1	23.6	905.9	16.3	0.013	0.24%
84903-75	1.5419	0.0934	0.1570	0.0048	940.0	28.7	964.4	58.2	940.0	28.7	0.030	2.54%
84903-58	1.5377	0.0353	0.1572	0.0027	941.0	15.9	957.0	22.2	941.0	15.9	0.012	1.67%
84903-96	1.5617	0.0347	0.1582	0.0024	946.8	14.4	974.7	21.9	946.8	14.4	0.011	2.87%
84903-43	2.1170	0.0708	0.1989	0.0036	1169.4	21.4	1126.4	40.1	1126.4	40.1	0.018	-3.81%
84903-21	2.6951	0.1177	0.2321	0.0062	1345.3	35.7	1298.9	56.5	1298.9	56.5	0.022	-3.57%
84903-10	2.9883	0.1033	0.2409	0.0053	1391.2	30.4	1425.3	51.1	1425.3	51.1	0.018	2.39%
84903-14	3.3614	0.1344	0.2593	0.0087	1486.5	49.6	1509.5	50.9	1509.5	50.9	0.017	1.53%
84903-63	4.0674	0.1802	0.2961	0.0064	1672.0	36.3	1617.2	74.0	1617.2	74.0	0.023	-3.39%

Table 2. U-Pb analytical data for detrital and igneous zircons, identified by sample number and lab.—Continued

84903-81	4.1522	0.1393	0.2949	0.0089	1665.9	50.4	1663.2	58.0	1663.2	58.0	0.017	-0.16%
84903-12	4.1464	0.0848	0.2911	0.0042	1647.2	23.7	1685.3	37.1	1685.3	37.1	0.011	2.26%
84903-2	4.3989	0.0858	0.3065	0.0042	1723.6	23.4	1699.3	35.1	1699.3	35.1	0.010	-1.43%
84903-79	4.3285	0.1549	0.2982	0.0089	1682.6	50.2	1719.2	64.5	1719.2	64.5	0.019	2.13%
84903-60	4.6775	0.1529	0.3092	0.0053	1736.7	29.9	1795.5	60.9	1795.5	60.9	0.017	3.27%
84903-7	5.2508	0.1337	0.3338	0.0059	1857.0	32.9	1865.4	48.3	1865.4	48.3	0.013	0.45%
84903-68	6.0701	0.1570	0.3557	0.0062	1961.8	33.9	2011.4	52.7	2011.4	52.7	0.013	2.47%
84903-27	13.3195	0.3980	0.5137	0.0097	2672.3	50.6	2725.5	86.1	2725.5	86.1	0.016	1.95%
84903-89	13.3195	0.3980	0.5137	0.0097	2672.3	50.6	2725.5	86.1	2725.5	86.1	0.016	1.95%
84903-9	14.7223	0.3808	0.5367	0.0095	2769.8	48.9	2817.7	75.6	2817.7	75.6	0.013	1.70%
05ADw303c, detrital zircons, n = 97 of 100, Apatite to Zircon, Inc.												
Analysis #	207/235	2 σ error (%)	206/238	2 σ error (%)	206/238 age	2 σ error (Ma)	207/206 age	2 σ error (Ma)	Best age (Ma)	2 σ error (Ma)	Error/age	Dis- cordance (%)
84901-71	0.1396	0.0200	0.0207	0.0011	132.1	7.2	144.0	21.8	132.1	7.2	0.076	8.22%
84901-82	0.1413	0.0307	0.0210	0.0006	134.0	3.8	138.7	30.3	134.0	3.8	0.109	3.38%
84901-73	0.1423	0.0311	0.0210	0.0015	134.2	9.9	151.3	34.5	134.2	9.9	0.114	11.27%
84901-3	0.1444	0.0116	0.0215	0.0004	136.8	2.8	140.1	11.6	136.8	2.8	0.041	2.32%
84901-55	0.1446	0.0089	0.0215	0.0005	137.0	3.3	139.2	8.9	137.0	3.3	0.032	1.52%
84901-34	0.1470	0.0357	0.0218	0.0006	138.9	4.0	146.7	35.8	138.9	4.0	0.122	5.35%
84901-33	0.1481	0.0158	0.0219	0.0008	139.7	5.0	149.2	16.6	139.7	5.0	0.056	6.36%
84901-48	0.1498	0.0112	0.0222	0.0005	141.5	3.4	147.9	11.4	141.5	3.4	0.039	4.38%
84901-27	0.1501	0.0178	0.0222	0.0008	141.7	5.0	149.9	18.5	141.7	5.0	0.062	5.51%
84901-38	0.1501	0.0101	0.0222	0.0007	141.7	4.2	148.0	10.1	141.7	4.2	0.034	4.23%
84901-94	0.1508	0.0166	0.0223	0.0008	142.1	5.4	152.1	17.5	142.1	5.4	0.058	6.57%
84901-85	0.1516	0.0109	0.0224	0.0007	142.9	4.2	150.2	11.0	142.9	4.2	0.037	4.87%
84901-57	0.1526	0.0174	0.0226	0.0008	143.8	5.3	152.1	18.0	143.8	5.3	0.059	5.41%
84901-46	0.1525	0.0098	0.0226	0.0005	144.0	3.0	147.7	9.8	144.0	3.0	0.033	2.52%
84901-45	0.1525	0.0103	0.0226	0.0004	144.0	2.9	147.8	10.3	144.0	2.9	0.035	2.54%
84901-35	0.1532	0.0089	0.0227	0.0005	144.6	3.0	148.2	8.9	144.6	3.0	0.030	2.39%
84901-83	0.1544	0.0090	0.0228	0.0004	145.6	2.7	150.8	9.1	145.6	2.7	0.030	3.44%
84901-100	0.1549	0.0201	0.0229	0.0007	145.8	4.3	152.7	20.2	145.8	4.3	0.066	4.52%
84901-22	0.1551	0.0161	0.0229	0.0007	145.9	4.6	154.7	16.5	145.9	4.6	0.053	5.68%
84901-69	0.1554	0.0089	0.0230	0.0004	146.5	2.8	150.2	8.8	146.5	2.8	0.029	2.45%
84901-11	0.1571	0.0158	0.0232	0.0005	147.9	3.3	153.2	15.6	147.9	3.3	0.051	3.45%
84901-31	0.1577	0.0117	0.0233	0.0005	148.5	3.2	153.0	11.7	148.5	3.2	0.038	2.89%
84901-87	0.1581	0.0121	0.0233	0.0006	148.6	3.7	155.6	12.4	148.6	3.7	0.040	4.48%
84901-1	0.1601	0.0216	0.0234	0.0025	149.0	15.7	178.2	24.6	149.0	15.7	0.069	16.39%
84901-51	0.1587	0.0116	0.0234	0.0006	149.3	3.9	156.4	11.7	149.3	3.9	0.037	4.56%
84901-91	0.1592	0.0131	0.0235	0.0007	149.7	4.3	155.6	13.2	149.7	4.3	0.042	3.82%
84901-47	0.1595	0.0090	0.0235	0.0004	150.0	2.7	155.0	9.0	150.0	2.7	0.029	3.23%
84901-24	0.1627	0.0137	0.0240	0.0006	152.9	3.9	157.9	13.6	152.9	3.9	0.043	3.16%
84901-78	0.1633	0.0159	0.0240	0.0007	153.1	4.6	161.5	15.9	153.1	4.6	0.049	5.23%
84901-53	0.1636	0.0148	0.0241	0.0007	153.4	4.3	161.1	14.8	153.4	4.3	0.046	4.82%
84901-42	0.1638	0.0163	0.0241	0.0009	153.6	5.5	163.3	16.9	153.6	5.5	0.052	5.99%
84901-21	0.1663	0.0205	0.0244	0.0011	155.5	7.3	167.9	22.0	155.5	7.3	0.065	7.40%
84901-15	0.1674	0.0155	0.0246	0.0007	156.6	4.8	165.7	15.9	156.6	4.8	0.048	5.50%
84901-6	0.1681	0.0169	0.0247	0.0005	157.4	3.3	164.0	16.8	157.4	3.3	0.051	3.98%
84901-92	0.1710	0.0110	0.0251	0.0008	159.8	4.9	167.4	10.8	159.8	4.9	0.032	4.53%
84901-25	0.1720	0.0084	0.0253	0.0006	160.9	3.8	166.9	8.3	160.9	3.8	0.025	3.64%
84901-67	0.1721	0.0101	0.0253	0.0005	161.1	3.4	165.1	10.0	161.1	3.4	0.030	2.41%
84901-97	0.1735	0.0120	0.0255	0.0006	162.0	3.7	168.7	11.9	162.0	3.7	0.035	3.94%
84901-93	0.1748	0.0088	0.0256	0.0007	163.1	4.5	171.1	8.7	163.1	4.5	0.025	4.67%
84901-26	0.1772	0.0112	0.0260	0.0008	165.2	4.9	172.4	10.9	165.2	4.9	0.032	4.13%
84901-29	0.1783	0.0099	0.0261	0.0007	166.1	4.5	174.7	9.9	166.1	4.5	0.028	4.93%
84901-58	0.1789	0.0178	0.0262	0.0011	166.5	6.7	177.9	18.3	166.5	6.7	0.052	6.43%
84901-8	0.1787	0.0151	0.0262	0.0006	167.0	4.1	166.8	14.3	167.0	4.1	0.043	-0.14%
84901-30	0.1804	0.0298	0.0263	0.0017	167.2	10.6	186.8	31.9	167.2	10.6	0.085	10.53%
84901-63	0.1821	0.0142	0.0266	0.0007	169.4	4.6	177.3	14.2	169.4	4.6	0.040	4.46%
84901-79	0.1844	0.0314	0.0269	0.0013	170.8	8.4	185.6	32.1	170.8	8.4	0.086	7.93%
84901-7	0.1849	0.0176	0.0270	0.0006	171.8	3.9	179.7	17.5	171.8	3.9	0.049	4.39%
84901-88	0.1866	0.0092	0.0272	0.0007	173.3	4.2	181.4	9.2	173.3	4.2	0.025	4.43%
84901-19	0.1877	0.0161	0.0274	0.0009	174.0	5.6	183.6	16.0	174.0	5.6	0.044	5.23%
84901-43	0.1879	0.0197	0.0274	0.0008	174.2	5.0	183.9	19.9	174.2	5.0	0.054	5.26%
84901-65	0.1886	0.0148	0.0275	0.0007	174.9	4.6	183.3	14.8	174.9	4.6	0.040	4.61%
84901-44	0.1886	0.0095	0.0275	0.0007	175.1	4.2	182.1	9.4	175.1	4.2	0.026	3.87%
84901-49	0.1891	0.0078	0.0276	0.0005	175.6	2.9	180.2	7.7	175.6	2.9	0.021	2.53%
84901-12	0.1896	0.0095	0.0277	0.0005	176.0	3.1	180.4	9.3	176.0	3.1	0.026	2.42%
84901-61	0.1900	0.0061	0.0277	0.0006	176.4	3.9	181.8	6.0	176.4	3.9	0.017	2.97%
84901-96	0.1911	0.0326	0.0278	0.0014	176.6	8.7	191.7	33.1	176.6	8.7	0.086	7.88%
84901-70	0.1916	0.0128	0.0279	0.0008	177.6	4.9	185.8	12.8	177.6	4.9	0.034	4.41%
84901-56	0.1913	0.0059	0.0279	0.0004	177.6	2.5	181.9	5.6	177.6	2.5	0.015	2.35%

Table 2. U-Pb analytical data for detrital and igneous zircons, identified by sample number and lab.—Continued

84901-99	0.1922	0.0176	0.0280	0.0006	178.1	4.0	184.9	17.3	178.1	4.0	0.047	3.66%
84901-17	0.1926	0.0141	0.0280	0.0007	178.3	4.2	185.7	14.0	178.3	4.2	0.038	3.98%
84901-9	0.1909	0.0119	0.0281	0.0011	178.4	7.3	165.1	10.8	178.4	7.3	0.033	-8.05%
84901-20	0.1938	0.0129	0.0282	0.0007	179.5	4.2	186.5	12.9	179.5	4.2	0.034	3.79%
84901-37	0.1937	0.0099	0.0282	0.0006	179.5	3.8	185.1	9.9	179.5	3.8	0.027	3.00%
84901-64	0.1944	0.0083	0.0283	0.0008	180.0	4.8	186.0	8.1	180.0	4.8	0.022	3.23%
84901-98	0.1956	0.0087	0.0285	0.0005	181.1	3.5	185.7	8.5	181.1	3.5	0.023	2.49%
84901-59	0.1961	0.0180	0.0285	0.0009	181.2	5.7	191.1	18.2	181.2	5.7	0.048	5.20%
84901-28	0.1970	0.0069	0.0287	0.0005	182.5	2.9	184.6	6.6	182.5	2.9	0.018	1.18%
84901-32	0.1974	0.0117	0.0287	0.0009	182.5	5.7	188.4	11.8	182.5	5.7	0.031	3.13%
84901-36	0.1985	0.0090	0.0289	0.0007	183.4	4.6	192.1	9.3	183.4	4.6	0.024	4.54%
84901-2	0.1989	0.0161	0.0289	0.0009	183.5	5.5	193.9	16.1	183.5	5.5	0.042	5.37%
84901-90	0.1990	0.0093	0.0289	0.0006	183.9	3.7	190.0	9.3	183.9	3.7	0.024	3.17%
84901-4	0.1998	0.0111	0.0291	0.0007	184.7	4.2	190.6	10.8	184.7	4.2	0.028	3.10%
84901-54	0.2006	0.0084	0.0292	0.0005	185.6	3.1	186.6	8.1	185.6	3.1	0.022	0.55%
84901-14	0.2018	0.0328	0.0292	0.0014	185.7	8.8	200.6	33.3	185.7	8.8	0.083	7.44%
84901-62	0.2015	0.0239	0.0294	0.0009	186.5	6.0	184.8	22.4	186.5	6.0	0.061	-0.92%
84901-13	0.2020	0.0087	0.0294	0.0005	186.5	3.1	192.2	8.5	186.5	3.1	0.022	2.95%
84901-81	0.2044	0.0176	0.0296	0.0009	188.1	5.9	199.1	17.4	188.1	5.9	0.044	5.53%
84901-74	0.2041	0.0170	0.0296	0.0007	188.2	4.7	195.3	16.7	188.2	4.7	0.043	3.63%
84901-23	0.2055	0.0143	0.0298	0.0007	189.4	4.7	196.2	13.9	189.4	4.7	0.035	3.50%
84901-18	0.2055	0.0149	0.0298	0.0008	189.4	5.0	196.5	14.5	189.4	5.0	0.037	3.64%
84901-76	0.2066	0.0218	0.0299	0.0010	190.1	6.4	200.1	21.7	190.1	6.4	0.054	5.02%
84901-72	0.2067	0.0084	0.0300	0.0006	190.5	4.1	196.2	8.2	190.5	4.1	0.021	2.91%
84901-40	0.2071	0.0107	0.0300	0.0007	190.7	4.3	198.5	10.4	190.7	4.3	0.026	3.96%
84901-39	0.2085	0.0136	0.0302	0.0008	191.7	5.3	199.4	13.0	191.7	5.3	0.033	3.86%
84901-75	0.2088	0.0111	0.0302	0.0009	191.9	5.8	202.3	10.4	191.9	5.8	0.026	5.14%
84901-60	0.2097	0.0104	0.0304	0.0006	193.0	3.9	199.2	10.2	193.0	3.9	0.026	3.13%
84901-86	0.2119	0.0163	0.0306	0.0010	194.3	6.4	204.8	15.9	194.3	6.4	0.039	5.11%
84901-10	0.2109	0.0299	0.0306	0.0013	194.3	8.5	193.5	28.0	194.3	8.5	0.072	-0.44%
84901-5	0.2126	0.0055	0.0308	0.0005	195.4	3.0	200.4	5.3	195.4	3.0	0.013	2.48%
84901-66	0.2133	0.0094	0.0309	0.0006	196.1	3.7	200.8	9.2	196.1	3.7	0.023	2.34%
84901-77	0.2146	0.0052	0.0311	0.0004	197.3	2.7	200.4	5.0	197.3	2.7	0.012	1.58%
84901-50	0.2157	0.0177	0.0311	0.0009	197.6	5.6	208.6	17.5	197.6	5.6	0.042	5.25%
84901-84	0.2160	0.0099	0.0312	0.0007	198.1	4.2	206.2	9.8	198.1	4.2	0.024	3.90%
84901-52	0.2167	0.0191	0.0312	0.0011	198.2	6.9	210.6	19.0	198.2	6.9	0.045	5.89%
84901-68	0.2168	0.0101	0.0313	0.0008	198.8	4.8	206.1	9.8	198.8	4.8	0.024	3.54%
84901-41	1.6895	0.0607	0.1692	0.0035	1007.7	20.7	997.8	37.2	997.8	37.2	0.019	-1.00%
84901-89	1.7393	0.0510	0.1699	0.0033	1011.5	19.8	1049.7	32.6	1049.7	32.6	0.016	3.64%
84901-95	4.5608	0.2751	0.3250	0.0173	1814.3	96.3	1656.7	99.4	1656.7	99.4	0.030	-9.51%
84901-80	4.7740	0.2665	0.3312	0.0170	1844.3	94.8	1706.2	96.3	1706.2	96.3	0.028	-8.09%
84901-16	5.7733	0.2775	0.3435	0.0155	1903.4	85.8	1985.3	94.8	1985.3	94.8	0.024	4.13%

05ADw304a, detrital zircons, n = 96 of 100, Apatite to Zircon, Inc.

Analysis #	207/235	2σ error (%)	206/238	2σ error (%)	206/238 age	2σ error (Ma)	207/206 age	2σ error (Ma)	Best age (Ma)	2σ error (Ma)	Error/age	Dis- cordance (%)
84902-9	0.1279	0.0232	0.0190	0.0012	121.6	8.0	134.9	25.4	121.6	8.0	0.094	9.85%
84902-20	0.1303	0.0135	0.0194	0.0006	124.0	3.8	130.8	13.9	124.0	3.8	0.053	5.21%
84902-42	0.1348	0.0201	0.0201	0.0010	128.3	6.6	131.0	20.1	128.3	6.6	0.077	2.08%
84902-26	0.1400	0.0145	0.0208	0.0006	132.6	4.0	140.7	15.0	132.6	4.0	0.053	5.72%
84902-82	0.1405	0.0219	0.0208	0.0012	132.8	7.4	146.9	23.6	132.8	7.4	0.080	9.59%
84902-35	0.1423	0.0302	0.0210	0.0016	134.1	10.4	153.7	33.8	134.1	10.4	0.110	12.73%
84902-64	0.1424	0.0394	0.0212	0.0015	135.5	9.4	129.1	36.7	135.5	9.4	0.142	-4.97%
84902-91	0.1438	0.0287	0.0213	0.0010	135.8	6.6	147.8	30.3	135.8	6.6	0.102	8.12%
84902-94	0.1456	0.0255	0.0216	0.0010	137.4	6.3	149.2	26.8	137.4	6.3	0.090	7.90%
84902-87	0.1460	0.0077	0.0217	0.0004	138.3	2.6	141.1	7.6	138.3	2.6	0.027	1.94%
84902-88	0.1462	0.0084	0.0217	0.0005	138.4	3.0	142.7	8.4	138.4	3.0	0.029	3.04%
84902-92	0.1466	0.0143	0.0217	0.0007	138.5	4.6	145.7	14.8	138.5	4.6	0.051	4.94%
84902-81	0.1469	0.0129	0.0218	0.0005	138.9	3.5	145.3	13.0	138.9	3.5	0.045	4.43%
84902-57	0.1474	0.0154	0.0218	0.0007	139.2	4.2	146.2	15.7	139.2	4.2	0.054	4.75%
84902-95	0.1472	0.0142	0.0219	0.0005	139.4	3.5	140.4	13.7	139.4	3.5	0.049	0.73%
84902-58	0.1480	0.0217	0.0219	0.0008	139.8	4.8	147.9	22.2	139.8	4.8	0.075	5.43%
84902-37	0.1495	0.0239	0.0221	0.0009	141.0	6.0	150.8	24.8	141.0	6.0	0.082	6.51%
84902-48	0.1496	0.0244	0.0221	0.0012	141.0	7.4	152.4	25.7	141.0	7.4	0.084	7.53%
84902-4	0.1495	0.0232	0.0221	0.0010	141.0	6.1	151.1	23.8	141.0	6.1	0.079	6.65%
84902-96	0.1486	0.0289	0.0222	0.0013	141.2	8.0	130.8	26.4	141.2	8.0	0.101	-7.95%
84902-8	0.1505	0.0227	0.0222	0.0009	141.9	5.9	152.3	23.4	141.9	5.9	0.077	6.85%
84902-16	0.1511	0.0147	0.0224	0.0005	142.7	3.5	148.2	14.8	142.7	3.5	0.050	3.71%
84902-14	0.1513	0.0175	0.0224	0.0010	142.9	6.6	146.9	17.2	142.9	6.6	0.059	2.72%
84902-49	0.1520	0.0147	0.0225	0.0007	143.3	4.6	152.5	15.3	143.3	4.6	0.050	6.05%

Table 2. U-Pb analytical data for detrital and igneous zircons, identified by sample number and lab.—Continued

84902-31	0.1520	0.0108	0.0225	0.0004	143.4	2.8	147.6	10.7	143.4	2.8	0.036	2.86%
84902-86	0.1521	0.0168	0.0226	0.0006	143.9	4.0	140.7	15.8	143.9	4.0	0.056	-2.30%
84902-90	0.1531	0.0128	0.0226	0.0006	144.3	3.6	150.5	13.0	144.3	3.6	0.043	4.09%
84902-84	0.1538	0.0077	0.0228	0.0005	145.2	3.4	149.3	7.7	145.2	3.4	0.026	2.78%
84902-7	0.1543	0.0168	0.0228	0.0009	145.3	5.6	154.2	17.3	145.3	5.6	0.056	5.80%
84902-17	0.1542	0.0169	0.0228	0.0007	145.3	4.4	151.8	17.2	145.3	4.4	0.057	4.29%
84902-76	0.1542	0.0068	0.0228	0.0004	145.5	2.8	149.3	6.8	145.5	2.8	0.023	2.54%
84902-25	0.1549	0.0155	0.0229	0.0009	145.7	6.0	155.5	16.4	145.7	6.0	0.053	6.31%
84902-78	0.1548	0.0107	0.0229	0.0005	145.9	3.2	151.7	10.8	145.9	3.2	0.036	3.84%
84902-72	0.1552	0.0145	0.0230	0.0005	146.4	3.4	150.9	14.4	146.4	3.4	0.048	3.00%
84902-66	0.1562	0.0456	0.0230	0.0015	146.4	9.4	164.6	49.0	146.4 146.4	9.4 9.4	0.149	11.04% 11.04%
84902-85	0.1560	0.0143	0.0231	0.0005	147.0	3.3	153.1	14.3	147.0	3.3	0.047	3.98%
84902-5	0.1567	0.0159	0.0231	0.0009	147.2	5.8	157.6	16.5	147.2	5.8	0.052	6.63%
84902-83	0.1573	0.0205	0.0232	0.0009	147.8	5.8	157.3	21.1	147.8	5.8	0.067	6.06%
84902-6	0.1574	0.0179	0.0232	0.0008	148.0	5.4	156.8	18.5	148.0	5.4	0.059	5.61%
84902-34	0.1575	0.0124	0.0233	0.0005	148.4	3.4	152.6	12.3	148.4	3.4	0.040	2.74%
84902-69	0.1568	0.0159	0.0233	0.0007	148.5	4.3	139.9	14.6	148.5	4.3	0.052	-6.16%
84902-21	0.1586	0.0316	0.0234	0.0011	148.9	7.2	160.5	32.7	148.9	7.2	0.102	7.26%
84902-71	0.1583	0.0163	0.0234	0.0007	148.9	4.4	155.6	16.5	148.9	4.4	0.053	4.30%
84902-24	0.1588	0.0276	0.0234	0.0009	149.1	5.9	160.4	28.4	149.1	5.9	0.088	7.03%
84902-68	0.1589	0.0217	0.0235	0.0008	149.4	5.0	156.3	21.8	149.4	5.0	0.070	4.40%
84902-3	0.1590	0.0129	0.0235	0.0007	149.5	4.7	156.5	13.1	149.5	4.7	0.042	4.47%
84902-73	0.1591	0.0138	0.0235	0.0005	149.7	3.5	155.3	13.8	149.7	3.5	0.045	3.60%
84902-80	0.1588	0.0409	0.0235	0.0017	150.0	10.9	145.1	38.5	150.0	10.9	0.133	-3.35%
84902-11	0.1599	0.0135	0.0236	0.0008	150.1	5.3	158.2	13.8	150.1	5.3	0.043	5.14%
84902-52	0.1595	0.0118	0.0236	0.0005	150.1	3.0	154.9	11.7	150.1	3.0	0.038	3.08%
84902-43	0.1599	0.0250	0.0236	0.0009	150.3	5.6	158.7	25.3	150.3	5.6	0.080	5.32%
84902-32	0.1600	0.0162	0.0236	0.0006	150.3	3.8	156.6	16.2	150.3	3.8	0.052	4.03%
84902-74	0.1605	0.0104	0.0237	0.0004	151.0	2.8	154.9	10.3	151.0	2.8	0.033	2.49%
84902-59	0.1604	0.0078	0.0237	0.0004	151.0	2.7	153.5	7.7	151.0	2.7	0.025	1.60%
84902-23	0.1617	0.0435	0.0237	0.0014	151.1	9.1	169.2	46.3	151.1 151.1	9.1 9.1	0.137	10.71% 10.71%
84902-12	0.1605	0.0142	0.0237	0.0007	151.2	4.5	152.1	13.7	151.2	4.5	0.045	0.60%
84902-30	0.1614	0.0147	0.0238	0.0007	151.5	4.6	159.0	15.0	151.5	4.6	0.047	4.71%
84902-50	0.1622	0.0232	0.0239	0.0010	152.1	6.1	161.7	23.8	152.1	6.1	0.074	5.95%
84902-98	0.1619	0.0111	0.0239	0.0005	152.2	3.2	156.6	11.1	152.2	3.2	0.035	2.81%
84902-54	0.1611	0.0231	0.0239	0.0009	152.2	5.9	142.9	21.0	152.2	5.9	0.073	-6.52%
84902-2	0.1629	0.0187	0.0240	0.0011	152.6	6.8	164.2	19.5	152.6	6.8	0.059	7.07%
84902-61	0.1623	0.0072	0.0240	0.0004	152.7	2.5	155.3	7.1	152.7	2.5	0.023	1.66%
84902-89	0.1624	0.0114	0.0240	0.0004	152.8	2.9	153.2	11.0	152.8	2.9	0.036	0.26%
84902-36	0.1637	0.0394	0.0240	0.0015	152.8	9.8	170.9	42.2	152.8 152.8	9.8 9.8	0.123	10.56% 10.56%
84902-18	0.1627	0.0128	0.0240	0.0006	152.9	3.6	158.1	12.9	152.9	3.6	0.041	3.31%
84902-47	0.1632	0.0150	0.0240	0.0007	153.0	4.6	162.1	15.5	153.0	4.6	0.048	5.61%
84902-13	0.1624	0.0207	0.0240	0.0008	153.0	5.2	149.2	19.3	153.0	5.2	0.065	-2.55%
84902-41	0.1635	0.0104	0.0241	0.0005	153.6	3.3	157.8	10.4	153.6	3.3	0.033	2.68%
84902-62	0.1640	0.0181	0.0241	0.0008	153.6	5.2	163.8	18.8	153.6	5.2	0.057	6.23%
84902-27	0.1639	0.0213	0.0241	0.0007	153.7	4.4	161.1	21.3	153.7	4.4	0.066	4.62%
84902-40	0.1642	0.0145	0.0241	0.0008	153.8	5.1	162.8	14.8	153.8	5.1	0.045	5.54%
84902-60	0.1645	0.0187	0.0242	0.0009	154.0	5.6	165.1	19.4	154.0	5.6	0.059	6.71%
84902-97	0.1633	0.0157	0.0242	0.0007	154.2	4.7	144.5	14.3	154.2	4.7	0.049	-6.68%
84902-56	0.1655	0.0147	0.0244	0.0006	155.1	3.5	162.1	14.7	155.1	3.5	0.045	4.29%
84902-45	0.1657	0.0156	0.0244	0.0007	155.3	4.4	163.4	15.9	155.3	4.4	0.048	4.99%
84902-29	0.1647	0.0133	0.0244	0.0006	155.3	3.8	147.6	12.3	155.3	3.8	0.042	-5.19%
84902-38	0.1659	0.0134	0.0244	0.0006	155.5	3.9	162.4	13.5	155.5	3.9	0.041	4.23%
84902-44	0.1663	0.0157	0.0244	0.0008	155.6	5.3	166.1	16.2	155.6	5.3	0.049	6.30%
84902-10	0.1672	0.0135	0.0245	0.0011	156.2	7.2	169.3	14.1	156.2	7.2	0.042	7.76%
84902-22	0.1667	0.0168	0.0245	0.0007	156.3	4.2	162.6	16.7	156.3	4.2	0.051	3.85%
84902-1	0.1674	0.0105	0.0246	0.0010	156.5	6.2	167.0	10.9	156.5	6.2	0.033	6.27%
84902-70	0.1678	0.0125	0.0247	0.0006	157.2	3.6	163.1	12.4	157.2	3.6	0.038	3.62%
84902-46	0.1682	0.0074	0.0248	0.0004	157.7	2.4	162.3	7.3	157.7	2.4	0.022	2.84%
84902-28	0.1686	0.0136	0.0248	0.0007	157.8	4.5	165.6	13.8	157.8	4.5	0.042	4.71%
84902-15	0.1687	0.0151	0.0248	0.0006	158.0	3.7	164.3	14.9	158.0	3.7	0.045	3.79%
84902-79	0.1701	0.0299	0.0249	0.0014	158.6	8.8	175.6	32.1	158.6	8.8	0.091	9.72%
84902-53	0.1699	0.0194	0.0250	0.0007	158.9	4.7	165.9	19.4	158.9	4.7	0.059	4.24%
84902-51	0.1710	0.0081	0.0252	0.0005	160.3	2.9	163.0	7.8	160.3	2.9	0.024	1.70%
84902-75	0.1717	0.0176	0.0252	0.0008	160.4	5.2	168.4	17.7	160.4	5.2	0.053	4.72%
84902-100	0.1723	0.0425	0.0252	0.0017	160.6	10.5	173.4	43.8	160.6	10.5	0.126	7.41%
84902-77	0.1728	0.0232	0.0253	0.0010	161.3	6.2	171.1	23.4	161.3	6.2	0.069	5.68%
84902-67	0.1719	0.0454	0.0254	0.0017	161.4	10.9	155.5	42.2	161.4	10.9	0.136	-3.82%
84902-19	0.1731	0.0162	0.0254	0.0009	161.5	5.6	171.4	16.7	161.5	5.6	0.049	5.78%
84902-65	0.1745	0.0289	0.0255	0.0014	162.2	9.2	179.7	30.8	162.2	9.2	0.086	9.74%
84902-99	0.1773	0.0158	0.0260	0.0008	165.2	5.0	173.0	16.1	165.2	5.0	0.046	4.51%
84902-39	0.1790	0.0444	0.0261	0.0018	165.9	11.1	186.0	47.3	165.9 165.9	11.1 11.1	0.127	10.81% 10.81%

Table 2. U-Pb analytical data for detrital and igneous zircons, identified by sample number and lab.—Continued

84902-93	0.1790	0.0143	0.0262	0.0007	166.7	4.7	174.5	14.6	166.7	4.7	0.042	4.47%
84902-33	0.1800	0.0229	0.0263	0.0013	167.5	8.4	177.6	23.2	167.5	8.4	0.065	5.69%
84902-63	0.1821	0.0202	0.0266	0.0009	169.2	5.8	180.7	20.6	169.2	5.8	0.057	6.40%
84902-55	0.1858	0.0356	0.0270	0.0015	171.9	9.4	190.1	37.6	171.9	9.4	0.099	9.56%
05PH104b, detrital zircons, n = 96 of 100, Apatite to Zircon, Inc.												
Analysis #	207/235	2 σ error (%)	206/238	2 σ error (%)	206/238 age	2 σ error (Ma)	207/206 age	2 σ error (Ma)	Best age (Ma)	2 σ error (Ma)	Error/age	Dis- cordance (%)
84904-74	0.0558	0.0088	0.0086	0.0004	55.2	2.8	54.8	9.0	55.2	2.8	0.025	-0.72%
84904-11	0.0565	0.0050	0.0087	0.0002	55.8	1.3	57.5	5.3	55.8	1.3	0.012	3.08%
84904-10	0.0569	0.0093	0.0087	0.0003	56.1	1.9	59.7	9.9	56.1	1.9	0.017	5.97%
84904-65	0.0572	0.0217	0.0088	0.0010	56.3	6.1	66.0	26.0	56.3	6.1	0.054	44.73%
84904-55	0.0576	0.0053	0.0089	0.0003	56.8	1.8	57.4	5.5	56.8	1.8	0.016	0.92%
84904-19	0.0579	0.0083	0.0089	0.0003	57.1	2.0	59.1	8.7	57.1	2.0	0.017	3.37%
84904-94	0.0580	0.0062	0.0089	0.0003	57.2	1.8	59.5	6.5	57.2	1.8	0.016	3.89%
84904-53	0.0585	0.0066	0.0090	0.0003	57.7	2.1	57.1	6.7	57.7	2.1	0.018	-1.01%
84904-14	0.0589	0.0037	0.0090	0.0004	58.0	2.8	61.6	4.2	58.0	2.8	0.024	5.80%
84904-89	0.0593	0.0063	0.0091	0.0003	58.4	1.8	61.7	6.8	58.4	1.8	0.016	5.39%
84904-54	0.0594	0.0068	0.0091	0.0003	58.5	2.1	61.0	7.2	58.5	2.1	0.018	4.08%
84904-44	0.0599	0.0035	0.0092	0.0002	59.1	1.1	58.4	3.5	59.1	1.1	0.009	-1.09%
84904-71	0.0601	0.0098	0.0092	0.0004	59.2	2.8	63.2	10.6	59.2	2.8	0.023	6.45%
84904-24	0.0600	0.0046	0.0092	0.0002	59.2	1.3	59.1	4.7	59.2	1.3	0.011	-0.21%
84904-12	0.0603	0.0038	0.0092	0.0005	59.3	2.9	62.6	4.3	59.3	2.9	0.024	5.15%
84904-64	0.0603	0.0101	0.0092	0.0004	59.3	2.6	62.1	10.7	59.3	2.6	0.022	4.45%
84904-93	0.0606	0.0052	0.0093	0.0002	59.7	1.6	61.3	5.4	59.7	1.6	0.013	2.54%
84904-67	0.0607	0.0062	0.0093	0.0003	59.7	2.1	62.7	6.7	59.7	2.1	0.018	4.79%
84904-15	0.0607	0.0052	0.0093	0.0002	59.8	1.4	60.8	5.4	59.8	1.4	0.012	1.70%
84904-43	0.0610	0.0056	0.0093	0.0003	60.0	1.9	63.6	6.0	60.0	1.9	0.016	5.72%
84904-28	0.0609	0.0048	0.0094	0.0002	60.0	1.5	61.3	4.9	60.0	1.5	0.013	2.07%
84904-68	0.0610	0.0074	0.0094	0.0003	60.1	2.1	58.9	7.3	60.1	2.1	0.018	-2.08%
84904-8	0.0613	0.0112	0.0094	0.0004	60.3	2.6	65.0	12.2	60.3	2.6	0.022	7.19%
84904-61	0.0614	0.0100	0.0094	0.0004	60.4	2.8	63.9	10.7	60.4	2.8	0.023	5.41%
84904-96	0.0616	0.0126	0.0094	0.0004	60.6	2.8	64.9	13.6	60.6	2.8	0.023	6.57%
84904-29	0.0617	0.0118	0.0094	0.0006	60.6	3.7	66.9	13.4	60.6	3.7	0.031	9.40%
84904-20	0.0616	0.0088	0.0094	0.0005	60.6	2.9	65.2	9.7	60.6	2.9	0.024	7.05%
84904-37	0.0618	0.0048	0.0095	0.0002	60.9	1.3	63.2	5.0	60.9	1.3	0.011	3.65%
84904-56	0.0618	0.0060	0.0095	0.0003	60.9	1.8	62.4	6.2	60.9	1.8	0.014	2.46%
84904-50	0.0619	0.0089	0.0095	0.0004	60.9	2.5	63.2	9.3	60.9	2.5	0.021	3.60%
84904-22	0.0620	0.0072	0.0095	0.0003	61.0	1.9	64.5	7.7	61.0	1.9	0.015	5.47%
84904-36	0.0620	0.0037	0.0095	0.0002	61.0	1.3	62.7	3.9	61.0	1.3	0.011	2.69%
84904-45	0.0623	0.0083	0.0095	0.0005	61.2	3.1	67.0	9.4	61.2	3.1	0.026	8.60%
84904-41	0.0626	0.0041	0.0096	0.0002	61.5	1.5	63.9	4.4	61.5	1.5	0.012	3.75%
84904-76	0.0626	0.0046	0.0096	0.0003	61.6	1.6	62.4	4.8	61.6	1.6	0.013	1.32%
84904-17	0.0633	0.0048	0.0097	0.0002	62.4	1.2	61.8	4.8	62.4	1.2	0.010	-0.89%
84904-34	0.0634	0.0065	0.0097	0.0003	62.4	1.9	63.6	6.8	62.4	1.9	0.015	1.94%
84904-73	0.0635	0.0080	0.0097	0.0004	62.5	2.3	63.9	8.3	62.5	2.3	0.019	2.29%
84904-85	0.0636	0.0063	0.0098	0.0003	62.6	2.1	63.9	6.5	62.6	2.1	0.016	2.13%
84904-32	0.0637	0.0087	0.0098	0.0004	62.6	2.6	65.8	9.3	62.6	2.6	0.021	4.81%
84904-30	0.0637	0.0039	0.0098	0.0002	62.7	1.5	64.1	4.1	62.7	1.5	0.012	2.15%
84904-13	0.0638	0.0031	0.0098	0.0003	62.8	2.1	63.9	3.3	62.8	2.1	0.017	1.74%
84904-91	0.0639	0.0046	0.0098	0.0003	62.8	1.8	64.2	4.9	62.8	1.8	0.014	2.26%
84904-23	0.0638	0.0064	0.0098	0.0003	62.8	1.6	62.9	6.4	62.8	1.6	0.013	0.07%
84904-25	0.0639	0.0046	0.0098	0.0002	62.9	1.4	61.3	4.5	62.9	1.4	0.011	-2.66%
84904-38	0.0640	0.0073	0.0098	0.0003	62.9	2.0	64.9	7.6	62.9	2.0	0.015	3.10%
84904-77	0.0640	0.0054	0.0098	0.0003	63.0	2.0	66.5	5.7	63.0	2.0	0.016	5.27%
84904-52	0.0640	0.0083	0.0098	0.0004	63.0	2.4	65.5	8.7	63.0	2.4	0.019	3.81%
84904-75	0.0642	0.0069	0.0098	0.0003	63.0	2.0	66.5	7.3	63.0	2.0	0.016	5.14%
84904-27	0.0642	0.0041	0.0098	0.0002	63.1	1.4	64.9	4.3	63.1	1.4	0.011	2.65%
84904-5	0.0642	0.0093	0.0098	0.0003	63.2	2.1	65.2	9.6	63.2	2.1	0.017	3.05%
84904-72	0.0644	0.0067	0.0099	0.0003	63.3	2.0	64.5	6.8	63.3	2.0	0.016	1.87%
84904-26	0.0647	0.0050	0.0099	0.0002	63.6	1.2	65.2	5.2	63.6	1.2	0.010	2.37%
84904-40	0.0648	0.0098	0.0099	0.0004	63.7	2.6	68.3	10.6	63.7	2.6	0.020	6.75%
84904-97	0.0649	0.0129	0.0099	0.0006	63.7	4.1	71.7	14.9	63.7	4.1	0.032	44.22%
84904-46	0.0649	0.0057	0.0099	0.0003	63.8	1.7	66.5	6.0	63.8	1.7	0.014	4.16%
84904-51	0.0651	0.0051	0.0100	0.0003	63.9	1.6	66.4	5.3	63.9	1.6	0.013	3.71%
84904-7	0.0650	0.0062	0.0100	0.0003	64.0	1.8	64.9	6.3	64.0	1.8	0.014	1.39%
84904-2	0.0651	0.0074	0.0100	0.0004	64.0	2.5	66.1	7.6	64.0	2.5	0.019	3.13%
84904-80	0.0652	0.0047	0.0100	0.0003	64.1	1.8	65.6	5.0	64.1	1.8	0.014	2.31%
84904-66	0.0654	0.0137	0.0100	0.0005	64.1	3.2	70.2	15.0	64.1	3.2	0.025	8.63%
84904-58	0.0655	0.0057	0.0100	0.0003	64.4	2.1	65.9	6.0	64.4	2.1	0.016	2.38%
84904-78	0.0655	0.0048	0.0100	0.0002	64.4	1.5	66.3	5.0	64.4	1.5	0.012	2.91%

Table 2. U-Pb analytical data for detrital and igneous zircons, identified by sample number and lab.—Continued

84904-4	0.0655	0.0074	0.0100	0.0003	64.4	2.0	65.8	7.7	64.4	2.0	0.015	2.17%
84904-82	0.0658	0.0088	0.0101	0.0003	64.6	1.9	67.0	9.1	64.6	1.9	0.015	3.55%
84904-48	0.0658	0.0069	0.0101	0.0003	64.6	2.0	68.4	7.4	64.6	2.0	0.015	5.44%
84904-31	0.0660	0.0069	0.0101	0.0003	64.8	2.1	68.8	7.5	64.8	2.1	0.016	5.91%
84904-57	0.0661	0.0101	0.0101	0.0004	64.9	2.8	67.9	10.7	64.9	2.8	0.022	4.48%
84904-59	0.0662	0.0047	0.0101	0.0003	65.0	1.7	65.0	4.9	65.0	1.7	0.013	-0.03%
84904-90	0.0664	0.0170	0.0101	0.0009	65.0	5.6	73.8	19.8	65.0 65.6	5.6 5.6	0.043	41.84%
84904-16	0.0663	0.0097	0.0102	0.0004	65.1	2.4	67.1	10.0	65.1	2.4	0.018	3.01%
84904-49	0.0664	0.0052	0.0102	0.0003	65.3	1.7	65.9	5.3	65.3	1.7	0.013	0.98%
84904-63	0.0670	0.0095	0.0102	0.0005	65.7	2.9	70.1	10.3	65.7	2.9	0.022	6.32%
84904-21	0.0669	0.0053	0.0103	0.0003	65.9	1.6	62.6	5.1	65.9	1.6	0.012	-5.20%
84904-42	0.0671	0.0024	0.0103	0.0002	65.9	1.1	67.7	2.5	65.9	1.1	0.008	2.57%
84904-84	0.0672	0.0090	0.0103	0.0003	66.0	2.0	69.8	9.5	66.0	2.0	0.015	5.52%
84904-81	0.0671	0.0044	0.0103	0.0002	66.1	1.5	63.0	4.2	66.1	1.5	0.012	-4.84%
84904-79	0.0676	0.0038	0.0104	0.0002	66.4	1.2	67.4	3.9	66.4	1.2	0.009	1.57%
84904-70	0.0681	0.0111	0.0104	0.0004	66.8	2.6	69.7	11.6	66.8	2.6	0.019	4.18%
84904-86	0.0688	0.0058	0.0105	0.0003	67.5	2.2	69.7	6.1	67.5	2.2	0.016	3.19%
84904-87	0.0692	0.0077	0.0106	0.0004	67.8	2.5	71.3	8.2	67.8	2.5	0.018	4.82%
84904-69	0.0694	0.0099	0.0106	0.0005	68.0	3.0	71.6	10.6	68.0	3.0	0.022	4.93%
84904-3	0.0700	0.0067	0.0107	0.0003	68.6	2.0	71.4	7.1	68.6	2.0	0.015	3.97%
84904-1	0.0703	0.0115	0.0107	0.0007	68.8	4.2	74.5	12.4	68.8	4.2	0.030	7.58%
84904-9	0.0704	0.0109	0.0108	0.0005	69.0	3.3	73.4	11.8	69.0	3.3	0.024	6.04%
84904-39	0.0705	0.0103	0.0108	0.0005	69.1	3.0	73.3	11.1	69.1	3.0	0.022	5.82%
84904-98	0.0722	0.0186	0.0110	0.0007	70.5	4.3	79.0	20.9	70.5 70.5	4.3 4.3	0.031	40.77%
84904-92	0.0746	0.0129	0.0114	0.0005	72.9	3.2	78.6	14.0	72.9	3.2	0.022	7.25%
84904-60	0.0856	0.0091	0.0130	0.0005	83.2	2.9	88.2	9.7	83.2	2.9	0.017	5.66%
84904-47	0.1079	0.0168	0.0162	0.0007	103.8	4.3	109.9	17.6	103.8	4.3	0.021	5.61%
84904-88	0.1318	0.0087	0.0197	0.0004	125.5	2.8	128.6	8.7	125.5	2.8	0.011	2.41%
84904-83	0.1349	0.0089	0.0201	0.0005	128.2	2.9	133.7	9.1	128.2	2.9	0.011	4.11%
84904-100	0.6675	0.0238	0.0833	0.0014	516.0	8.6	531.7	19.6	516.0	8.6	0.008	2.95%
84904-95	0.6854	0.0251	0.0852	0.0014	526.9	8.8	542.1	20.4	526.9	8.8	0.008	2.81%
84904-99	1.4632	0.0561	0.1543	0.0028	925.1	17.0	890.6	35.0	925.1	17.0	0.009	-3.87%
84904-33	3.2836	0.0963	0.2559	0.0061	1468.9	34.8	1489.2	46.2	1489.2	46.2	0.016	1.36%
84904-35	3.6760	0.1112	0.2762	0.0062	1572.0	35.5	1558.6	48.6	1558.6	48.6	0.016	-0.86%
84904-6	4.0685	0.1239	0.2975	0.0081	1678.9	45.7	1608.2	52.3	1608.2	52.3	0.016	-4.40%
84904-62	4.0953	0.0868	0.2952	0.0053	1667.4	29.9	1635.8	35.5	1635.8	35.5	0.011	-1.93%

This page intentionally left blank

Appendix: Analytical Methods

U-Pb Zircon LA-ICP-MS Techniques (University of British Columbia)

Zircons are separated from their host rocks using conventional mineral separation methods and sectioned in an epoxy grain mount along with grains of internationally accepted standard zircon (FC-1, a ~1100-Ma zircon standard), and brought to a very high polish. The grains are examined using a stage-mounted cathodoluminescence imaging setup that makes it possible to detect the presence of altered zones or inherited cores within the zircon. The highest quality portions of each grain, free of alteration, inclusion, or cores, are selected for analysis. The surface of the mount is then washed for ~10 minutes with dilute nitric acid and rinsed in ultraclean water. Analyses are carried out using a New Wave 213nm Nd-YAG laser coupled to a Thermo Finnigan Element2 high resolution ICP-MS (inductively coupled plasma mass spectrometer). Ablation takes place within a New Wave “Supercell” ablation chamber, which is designed to achieve very high efficiency entrainment of aerosols into the carrier gas. Helium is used as the carrier gas for all experiments, and gas flow rates, together with other parameters such as torch position, are optimized before beginning a series of analyses. We typically use a 25-micron spot with 60 percent laser power and do line scans rather than spot analyses in order to avoid within-run elemental fractions. Each analysis consists of a 7-second background measurement (laser off) followed by a ~28-second data acquisition period with the laser firing. A typical analytical session consists of four analyses of the standard zircon, followed by four analyses of unknown zircons, two standards, four unknowns, and so forth, and finally four standard analyses. Data are reduced using the GLITTER software package developed by the GEMOC group at Macquarrie University, which subtracts background measurements, propagates analytical errors, and calculates isotopic ratios and ages. This application generates a time-resolved record of each laser shot. For detrital zircon samples, 60-100 grains are analysed and displayed on concordia and probability plots. Plotting of the analytical results employs ISOPLOT 3.00 software (Ludwig, 2003).

U-Pb Zircon SHRIMP-RG Techniques (U.S. Geological Survey-Stanford University)

Zircon separations were done at the U.S. Geological Survey in Anchorage using standard density and magnetic separation techniques. At the jointly operated USGS-Stanford SHRIMP-RG lab at Stanford, zircons were hand picked for final purity, mounted on double-stick tape on glass slides in 1x6-mm rows, cast in epoxy, ground and polished to a 1-micron finish on a disc 25 mm in diameter by 4 mm thick. All grains were imaged with transmitted light and reflected light (and incident light if needed) on a petrographic microscope, and with cathodoluminescence

and back scattered electrons as needed on a JEOL 5600 SEM to identify internal structure, inclusions, and physical defects. The mounted grains were washed with 1N HCl or EDTA solution (if acid soluble) and distilled water, dried in a vacuum oven, and coated with Au. Mounts typically sit in a loading chamber at high pressure (10^{-7} torr) for several hours before being moved into the source chamber of the SHRIMP-RG. Secondary ions are generated from the target spot with an O_2^- primary ion beam varying from 4 to 6 nA. The primary ion beam typically produces a spot with a diameter of 20-40 microns and a depth of 1-2 microns for an analysis time of 9-12 minutes. Nine peaks are measured sequentially for zircons (the SHRIMP-RG is limited to a single collector, usually an EDP electron multiplier): $^{90}Zr^{16}O$, ^{204}Pb , Bgd (0.050 mass units above ^{204}Pb), ^{206}Pb , ^{207}Pb , ^{208}Pb , ^{238}U , $^{248}Th^{16}O$, and $^{254}U^{16}O$. Autocentering on selected peaks and guide peaks for low or variable abundance peaks (that is, $^{96}Zr^{16}O$, 0.165 mass unit below ^{204}Pb) are used to improve the reliability of locating peak centers. The number of scans through the mass sequence and counting times on each peak are varied according to sample age and U and Th concentrations to improve counting statistics and age precision. Measurements are made at mass resolutions of 6,000-8,000 (10 percent peak height), which eliminates all interfering atomic species. The SHRIMP-RG was designed to provide higher mass resolution than the standard forward geometry of the SHRIMP I and II (Clement and Compston, 1994). This design also provides very clean backgrounds and, combined with the high mass resolution, the acid washing of the mount, and rastering the primary beam for 90-120 seconds over the area to be analyzed before data are collected, assures that any counts found at mass of ^{204}Pb are actually Pb from the zircon and not surface contamination. In practice, greater than 95 percent of the spots analyzed have no common Pb. Concentration data for zircons are standardized against zircon standard SL-13 (238 ppm U) or CZ3 (550 ppm U) and age data against AS3 and AS57 zircons (1098 Ma) from the Duluth Gabbro (Paces and Miller, 1993), RG-6 (1440 Ma, granite of Oak Creek stock; Bickford and others, 1989), or R33 (419 Ma, quartz diorite of Braintree complex, Vermont; Black and others, 2004), which are analyzed repeatedly throughout the duration of the analytical session. Data reduction follows the methods described by Williams (1998) and Ireland and Williams (2003) and use the Squid and Isoplot programs of Ludwig (2001, 2003).

U-Pb zircon LA-ICP-MS Techniques (Apatite to Zircon, Inc.)

Mineral separates were obtained at the laboratories of Apatite to Zircon, Inc., in Viola, Idaho. Lithium polytungstate and a centrifuge were used in place of the conventional Wilfley table, thus guarding against loss of zircon grains that might inadvertently be washed away, undetected, in the conventional method. Zircons (both standards and unknowns) were then mounted in 1-cm² epoxy wafers and ground down to expose internal grain surfaces before final polishing. Grains, and the locations for

laser spots on these grains, were selected for analysis from all sizes and morphologies present using transmitted light with an optical microscope at a magnification of $\times 2000$. This approach is used instead of cathodoluminescence 2-D imaging because it allows the recognition and characterization of features below the surface of individual grains, including the presence of inclusions and the orientation of cracks, which could otherwise result in spurious isotopic counts.

Isotopic analyses were performed with a New Wave UP-213 laser ablation system in conjunction with a Thermo-Finnigan Element2 single collector double-focusing magnetic sector inductively coupled plasma-mass spectrometer (LA-ICP-MS) in the GeoAnalytical Lab at Washington State University. In comparison to a quadropole ICP-MS, the Element2 has flat-top peaks and higher sensitivity, resulting in larger Pb signals, better counting statistics, and more precise and accurate measurement of isotopic ratios. For all analyses (both standard and unknown), the diameter of the laser beam was set at 20 μm and the laser frequency was set at 5 Hz, yielding ablation pits $\sim 10\text{--}15\ \mu\text{m}$ deep. He and Ar gas were used to deliver the ablated material into the plasma source of the mass spectrometer. Each analysis of 250 cycles took approximately 30 seconds to com-

plete and consisted of a 6-second integration on peaks with the laser turned off (for background measurements) followed by a 25-second integration with the laser firing. A delay of as much as 30 seconds occurred between analyses in order to purge the previous analysis and prepare for the next. The isotopes measured included ^{202}Hg , $^{204}(\text{Hg} + \text{Pb})$, ^{206}Pb , ^{207}Pb , ^{208}Pb , ^{232}Th , ^{235}U , and ^{238}U . The Element2 detector was set at analog mode for ^{232}Th and ^{238}U and at pulse counting mode for all other isotopes. Common Pb correction was made by using the measured ^{204}Pb content and assuming an initial Pb composition from Stacey and Kramers (1975).

Interelement fractionation of Pb/U is generally <20 percent, whereas fractionation of Pb isotopes is generally <5 percent. At the beginning of each LA-ICP-MS session, zircon standards (Peixe and FC1) were analyzed until fractionation was stable and the variance in the measured $^{206}\text{Pb}/^{238}\text{U}$ and $^{207}\text{Pb}/^{206}\text{Pb}$ ratios was at or near 1 percent. In order to correct for interelement fractionation during the session, these standards were generally reanalyzed after each 15–25 unknowns. Fractionation also increases with depth into the laser pit. The accepted isotopic ratios were accordingly determined by least-squares projection through the measured values back to the initial determination.

This page intentionally left blank



Haeussler and Galloway, editors—**Studies by the U.S. Geological Survey in Alaska, 2007**—Professional Paper 1760—F